1966

Field model tests for the prediction of foundation settlement

Nathaniel Sill Fox
Iowa State University

FIELD MODEL TESTS FOR THE PREDICTION OF FOUNDATION SETTLEMENT

by

Nathaniel Sill Fox

A Dissertation Submitted to the
Graduate Faculty in Partial Fulfillment of
The Requirements for the Degree of
DOCTOR OF PHILOSOPHY

Major Subject: Soil Engineering

Approved:

Signature was redacted for privacy.

In Charge of Major Work

Signature was redacted for privacy.

Head of Major Department

Signature was redacted for privacy.

Dean of Graduate College

Iowa State University
Of Science and Technology
Ames, Iowa

1966

TABLE OF CONTENTS

I. INTRODUCTION

Settlement prediction is one of the major tasks of the soil engineer today. Most structures are ultimately supported by soil, and soil, being a deformable material, compresses upon application of a load. This compression causes a vertical downward displacement of the structure and its lowest extremity, the foundation. This displacement is called settlement.

The general mechanisms of soil deformation are quite well established. Terzaghi's classical one-dimensional consolidation theory explains settlement due to consolidation, i.e., the settlement accompanying one-dimensional compression of soil voids simultaneous to expulsion of soil water from these voids. Improvements in the consolidation theory to include two and three-dimensional consolidation have been proposed, but are not in common use.

Terzaghi's consolidation theory is commonly used in conjunction with laboratory consolidation tests. Soil samples are restricted from undergoing lateral displacement, thus maintaining one dimensional consolidation within the sample. Vertical deformation measurements of the consolidation sample with corresponding time and load increment are recorded and interpreted.

The laboratory consolidation test and one-dimensional consolidation theory form the basis of most settlement predictions

today. Although this technique appears to yield better results than other techniques, numerous cases can be found in which inaccurate predictions have resulted from its use. Several important limitations of the consolidation method of settlement prediction include: One-dimensional consolidation is seldom approximated in the actual foundation soil; soil samples are disturbed in handling, and the amount of disturbance is difficult to evaluate; consolidation is only one of at least three mechanisms involved in settlement; consolidation testing does not allow for evaluation of the effect of the size, shape, and rigidity of the foundation on the amount of settlement.

Settlement is known to result from other mechanisms than consolidation. Immediate settlement, sometimes called elastic settlement, is caused by deformation of the soil mass by compression of void spaces at the time of load application. This phenomenon occurs almost immediately after application of load.

Another mechanism of settlement, known as secondary compression, secondary consolidation, or plastic lag, is also observed to occur. Soil will often continue to deform after immediate settlement and consolidation have ceased. This long term deformation involves practically no volume change within the soil mass. It may occur so slowly that in some situations it could be disregarded for the lifetime of the structure, whereas in other situations, secondary compression can cause excessive settlements.

The phenomenon of settlement is complicated by the observation that settlement is not only a function of the soil, the load, and the time of loading, but also is influenced by the size, shape, rigidity, and roughness of the foundation itself.

A complete settlement analysis should include all three settlement components, and furthermore, should consider the soil and the foundation together rather than the soil alone. This approach involves too many variables for mathematical solution and lends itself to solution by means of model foundation tests to predict prototype foundation settlement.

Model foundation tests, often called model load tests, are not new, but they have been performed with limited success from 1930 to the present. An extensive literature review of model footing studies in the period from 1930 to 1960 concluded that every attempt to use small scale footing experiments to verify quantitative relationships for full-scale footing performance had been unsuccessful (45), due to difficulty in evaluating size effects of the footings.

In addition to the problem of size effects, a second problem is recognized to exist with model load tests. The zone of influence of stresses induced in the soil beneath a loaded foundation is commonly approximated as extending 1.5 times the width of the least dimension of the foundation. Thus settlement of a full-scale foundation is influenced by the soil at a greater depth than in the case of the model

foundation, and buried soft soil layers can influence the full-scale foundation without influencing the model foundation. Model load tests normally have been conducted at or near the ground surface.

The objectives of this research are to seek ways to overcome these two difficulties which exist in model load testing. More specifically, it is proposed to (1) employ theories of similitude in order to develop test devices and procedures which will give meaningful results and information for settlement prediction, and (2) conduct tests utilizing the new devices or procedures.

II. REVIEW OF LITERATURE

A. Dimensional Analysis and Similitude Theory

Dimensional analysis is based on the principle of dimensional homogeneity between the physical quantities appearing in an equation connecting these quantities. The term "dimension" is applied to the power to which a quantity occurs (29). For example, area is dimensionally equal to L^2 and is said to have a dimension of 2 in length.

Length in the above example is said to be a primary or fundamental quantity. A fundamental quantity is one that apparantly can neither be derived from another, nor can it be resolved into anything more fundamental (27). In the science of mechanics two common fundamental quantity systems exist, the length-force-time system and the length-mass-time system.

A quantity which is not a primary quantity is called a secondary quantity, and can be expressed in terms of fundamental quantities as the product of the fundamental quantities raised to appropriate powers (39). For example, $A \doteq F^a L^b T^c$, where A represents any secondary quantity, the symbol $\doteq$ means "is dimensionally equal to", F, L, T are the primary quantities force, length, and time, respectively, and a, b, c represent appropriate powers. The validity of this dimensional equation may be proven mathematically utilizing the following two axioms (39):

Axiom 1: Absolute numerical equality of quantities may

exist only when the quantities are similar qualitatively.

Axiom 2: The ratio of the magnitudes of two like quantities is independent of the units used in their measurement, provided that the same units are used for measuring each of the two quantities.

The first axiom implies dimensional homogeneity, and means, for example, that apples cannot equal oranges. An example of the second axiom is that the ratio of the length to the width of an object is the same regardless of whether the object is measured in feet, inches, centimeters, etc.

The general form of the equation for a secondary quantity is exponential: $A \triangleq F^a L^b T^c$; therefore the general form of an equation to describe any phenomenon can be made exponential. By utilizing the two axioms above, one can often determine the values of the exponents or dimensions involved in a physical problem.

Dimensional analysis is thus seen to be a method for investigating the nature of the solution of physical problems. The end result of dimensional analysis is to reduce the number of variables which must be investigated in solving, or partially solving, any physical problem (8).

The basic ideas underlying the field of dimensional analysis can be traced back to several ancient Greek philosophers, but modern development in this field is generally considered to have begun with Rayleigh in 1915 (44).

The mathematical relationship which forms the essence of

dimensional analysis is known as the "Pi Theorem" and is ascribed to E. Buckingham (9). The name Pi is derived from the Greek letter π, which is often used in mathematics to indicate that the product of a set of numbers is to be taken (29). The Buckingham Pi Theorem is derived from the two basic axioms, and essentially states that the number of dimensionless and independent groups of variables required to express a relationship among the pertinent variables in a given phenomenon is equal to the number of variables involved minus the number of fundamental quantities in which these variables may be measured (39).

Let S = the number of dimensionless and independent groups of variables, the groups being called "pi terms".

N = the total number of variables involved in the phenomenon

B = the number of fundamental quantities involved.

Then the Buckingham Pi Theorem states that $S = N - B$.

A direct result of the above theorem is to reduce the number of functionally related quantities to a number below the total number of variables involved in a phenomenon. This reduction of variables will facilitate the design, construction, and analysis of models and prototypes of systems which may be too complex for solution by the usual methods of problem solving.

In engineering practice models are often constructed and tested in order to predict the behavior of full-size proto-

type structures, vehicles, machines, or other systems. The principles underlying the construction of models and the interpretation of model test results to predict prototype performances, comprises the theory of similitude. The theory of similitude is developed from dimensional analysis, and dimensional analysis may be considered to be the basic tool of similitude theory.

Similitude theory and model studies have been useful in many branches of engineering (33, 39), particularly the branches of hydraulic engineering, mechanical engineering, aeronautical engineering, and structural (civil) engineering. Less work has been accomplished with similitude studies in the field of soil engineering, although recent publications indicate a rapid increase in its use in solving and investigating soil problems. Only a few examples have been found in which similitude theory has been used in model foundation or footing investigations (14, 22, 32). None of these investigators attempted to employ distorted model theory, nor did they attempt to reduce the amount of distortion involved in the foundation-soil system, although the presence of a distortion was recognized.

B. Model Foundation Tests

1. General

A model foundation test, also referred to as model load test, or model footing test, may be considered to be any test

in which a small-scale model is used to determine full-scale prototype foundation behavior. Such tests have been used to accomplish one or more of 3 basic objectives:

1) Model foundation tests have been used to predict the bearing capacity of full-scale foundation-soil systems. Bearing capacity is defined as the largest intensity of pressure which may be applied by a foundation to the soil which supports it without causing excessive settlement or shear failure (53).

2) Model foundation tests have been used to predict settlement under the full-scale prototype foundation.

3) Model foundation tests have been used for specialized objectives such as finding the extent of elastic deformation in soil, or the modes of deformation and patterns of soil behavior during settlement or shear rupture.

The first detailed study of model foundations was probably performed by W. Fellenius in 1930. He studied footings of various dimensions in order to determine the effect of size and shape on the bearing capacity of footings in sand. He compared his model results with theoretical analyses using the "Fellenius circular arc" failure surface method. A major conclusion reached by Fellenius was that the bearing capacity of elliptical and rectangular footings on sand is proportional to the least width of the footings (45).

2. Bearing capacity in sand

Numerous model foundation investigations on bearing capacity in sand have been performed since Fellenius' work (45). Between 1931 and 1933 A. Pandya performed a series of tests at Massachusetts Institute of Technology, and found that the bearing capacity of surface footings on sand was a function of the least width of the footing, and was essentially independent of footing shape (45).

In a later study, published in 1941, H. Q. Golder performed a series of experiments with rectangular model footings of varying length and breadth dimensions on sand. He also found that the bearing capacity of sand was a function of the footing width, but not its shape (21).

In 1948, H. Peynircioglu studied the mechanism of shear failure in sand by taking time exposure photographs of soil-footing behavior during loading. He found that the curved portion of the shear rupture surface in the soil closely approximated a logarithmic spiral. In addition, he found that failure occurred in all tests by the tipping of the footing to one side or the other.

G. G. Meyerhof conducted an extensive series of experiments in sand from 1948 to 1955. He listed the most important factors in determining bearing capacity in sand to be:

1) Foundation: size, shape, depth, roughness, and method of placement.

2) Soil: stress prior to loading, and strength and deformation characteristics.

Meyerhof also found satisfactory agreement between experiment and theory for the bearing capacity of surface footings on sand when the friction angle was determined and the average pressure acting normal to the failure surface was used in computation (36).

V. G. Berezantzeu and V. A. Yaroshenko using photographs and movies, performed experiments in Russia in 1957 to study the character of deformation and stability of loose and dense sands. They described the soil deformation process essentially as follows: The soil particles under the foundation initially move vertically downward until a compacted core is formed. Upon increased settlement this core displaces soil laterally along slip surfaces which reach the ground surface with shallow footings, and terminate within the soil mass with deep footings and loose sand (5).

G. F. Sowers made load tests on sand with plates 1 square foot to 3 square feet in area. He found that the computed bearing capacity using Terzaghi's bearing capacity formula was approximately 30% greater than the measured value (50).

A. S. Vesic, D. C. Banks, and J. M. Woodard studied the effects of loading rate on bearing capacity of footings on sand. They found a decrease in bearing capacity of dry or submerged sand with an increase in load rate for slow load rates, then an increase in bearing capacity with higher load rates (59).

J. Feda studied the bearing capacity of loose sandy subsoil and he reported two types of failure, local and complete. He described local failure as that in which the subsoil becomes compacted during failure, whereas in complete failure, the soil becomes loosened during failure. Furthermore, Feda stated that the type of subsoil failure depends upon the size of the base of the foundation, the depth of the foundation, and the relative density of the loose soil (15).

E. E. DeBeer reported that a different bearing capacity factor, N_γ for large and small footings is a possible explanation for the size effect problem with model footings due to the fact that the progressive rupture phenomenon cannot be reproduced to scale (14).

Results of these and other investigations on bearing capacity of model footings on sand were often conflicting. In particular, the effects of size on bearing capacity was in disagreement. Some investigators found that plate roughness was important to the bearing capacity, others found it less important. Possible causes for different test results include the following factors: varied load rates among different investigations; different densities, moisture contents, and other soil properties of the sand tested; and varied sizes of soil tanks in which the soil was enclosed. In general, the following conclusions have been reached in regard to the investigation of bearing capacity in sand:

(1) The bearing capacity of sand is a function of the

size and shape of the model foundation, and generally increases with increased area of the foundation.

(2) The bearing capacities of foundations with smooth contact surfaces are less than those with rough surfaces.

(3) The bearing capacity of the foundation-soil system increases with increased foundation depth.

(4) The bearing capacity of a foundation-soil system in sand is proportional to the density or unit weight of the sand, and is influenced by ground water conditions as they affect the effective unit weight of the sand.

(5) The bearing capacity of sand is decreased with an increase in load rate for slow load rates, and then increased with higher load rates.

3. Bearing capacity in clay

Far less work appears to have been done with model foundation tests to study the bearing capacity in clay than in sand. In 1941 H. Q. Golder tested 3 inch by 3 inch square footings and 3 inch by 18 inch strip footings in a remolded London clay. He found the mean bearing capacity to be 5.1 times the cohesive shear strength of the clay for the strip footing, and approximately 6.6 times the cohesive shear strength for the square footing (21).

A. W. Skempton wrote about model footing studies conducted at Imperial College on undisturbed and remolded clays. Skempton pointed out the necessity of making corrections for

consolidation during loading. He also indicated that when the load settlement curves were plotted in a dimensionless form, they were about the same for all footings (49).

G. G. Meyerhof developed theoretical solutions for bearing capacity in cohesive soils. He also established semi-empirical design curves for any shape footing at any depth of embedment in a cohesive soil (38).

In 1956, A. Bergfelt performed a series of tests with various sizes and shapes of loading plates in clay. His results agreed well with those of Meyerhof regarding the relation between failure load and shear strength and between bearing capacity and shape of the loaded area. Bergfelt also studied the deformation which occurred within a clay mass by placing lead shot in the clay and taking X-ray photographs of the deformation process. No slip planes were observed, even though settlement reached 10% of the plate width (6).

The following general conclusions have been reached concerning the bearing capacity of footings on clay:

(1) Test results have quite reliably established the effect of foundation shape on bearing capacity, but the effect of size has been less well-established, and is in dispute.

(2) Different modes of failure are reported. For stiff clays in which stress-strain relationships approximate those assumed in plastic behavior, failure surfaces are similar to those presented by Terzaghi (56) and Meyerhof (38), in which noticeable shear rupture surfaces develop. In soft clay

local shear failure with incomplete rupture surfaces occurs.

(3) Roughness of the foundation contact surface is less important in clay than in sand, and in the case of a saturated clay, roughness may have no effect whatsoever.

4. Settlement prediction

The use of model foundation tests to predict settlement has been quite limited. In 1933 G. Gilboy performed tests on dry sand in 3 states of compaction: dense, medium and loose. He used 3 different sized but similarly shaped footings of 1, 3, and 6 square feet. His test results showed that at pressures significantly less than ultimate pressure, the stress required to produce a given settlement was almost independent of footing size (31).

Kogler conducted a series of tests with circular model footings ranging in size from about 3 inches in diameter to 25 inches in diameter. He concluded that the settlement of a loaded plate in sand increases with increasing diameter of the plate, although not in direct proportion to the diameter (45). Kogler also discovered that plate size below a certain critical size will produce increased settlements with decreased size. He presents an empirical equation to correct for size effects of settlement in sand (57) $S = S_1\left(\frac{2B}{B+1}\right)^2$, where S is the settlement of a footing B feet in width, S_1 is the settlement of a model footing one foot wide.

Pandya found that increasing the depth of a foundation

greatly reduced the amount of settlement under a given load, but found that in sand, for a given load intensity the settlement was practically independent of size of footing (45).

Bond attempted to predict the settlement of prototype footings on sand in 1956. He was able to predict settlements satisfactorily for dense sands, but not loose sands. He explained that loose sand was so compressible that the assumed shear surface did not develop. Bond found that more accurate results were obtained for low load intensities by assuming vertical compression with no lateral deformation (7).

W. G. Holtz and H. J. Gibbs reported load tests on loess soil with square plates 1 x 1 feet, 3 x 3 feet, and 5 x 5 feet. The tests were conducted in holes 5 feet deep, the holes and the plates having the same cross-sectional dimensions (24).

The results of these tests were that the larger plates produced greater settlements than did the smaller plates. Since all plates were placed at the same depth, the surcharge confining pressure was equal in all tests. The settlement of the larger plates was assumed to be greater because their effective bulbs of pressure were larger, i.e., the stressed volume of soil went to greater depths beneath the larger plates than under the smaller plates.

M. Rocha and J. Folque described two cases in which model studies were used to estimate full-scale foundation settlement. The soil tested was sandy clay and clay, and model studies were performed in the laboratory with undis-

turbed samples. The surcharge weight of the soil above the foundation was reproduced by applying a stress to the surface of the model soil. The predictions were reported to be reasonably good, and considerably better than predictions made for the same prototypes based on results of consolidation tests on undisturbed samples (46).

K. Terzaghi presents a graph which shows size effects generally observed with sands and with soft clays subjected to footing loads. This graph is shown in Figure 1. (57). The large amounts of settlement at plate widths less than one foot have been attributed to excessive shear strains that occur with small model footings (11). J. O. Osterberg presents graphs of unit applied stress versus the ratio of settlement to footing size on a logarithmic scale for several cohesive soils. These plots were designed so that one might directly observe any size effects and thereby predict settlements of any size and shape of footing on these soils. Overestimates of settlements by as much as 500% from the use of these graphs has been reported (41).

Several investigators have used a surcharge pressure to approximate the stress from the dead weight of the soil above the level of an embedded footing. Burmister applied a surcharge confining pressure by vacuum within an enclosed container, with a rubber membrane placed on top of the footing and sealed to the top of the container. He found that the load intensity for a constant settlement increased consistently

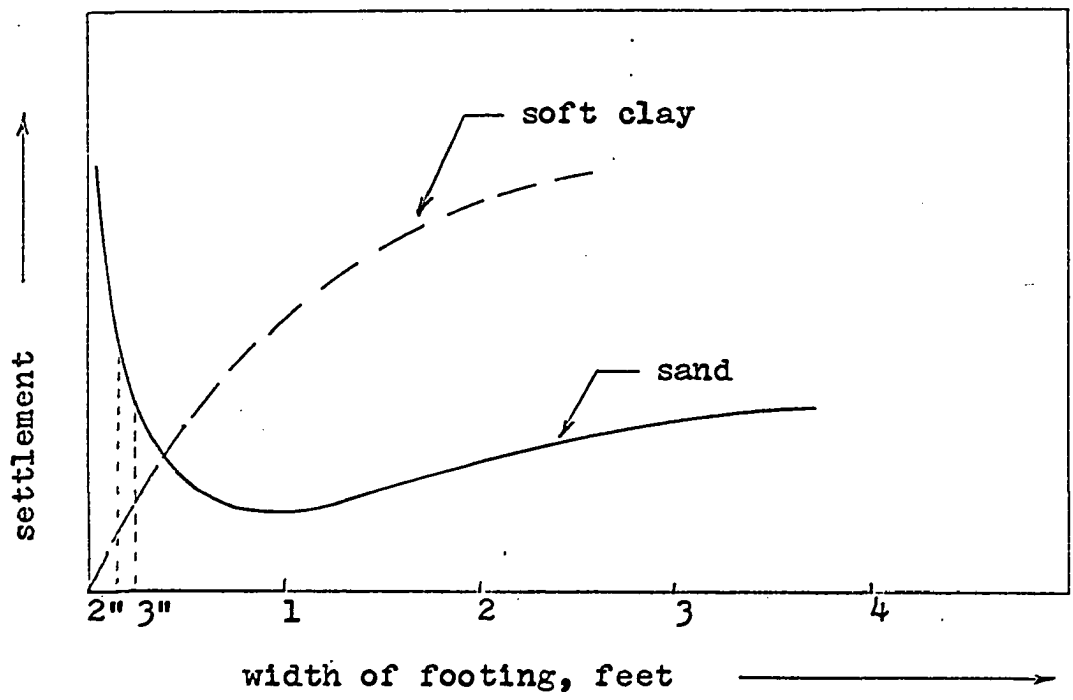

Figure 1. Relationship between footing size and settlement on sands and soft clays, according to Terzaghi (56)

with an increase in confining stress level. The amount of increase varied with the relative density of the soil.

The general conclusions reached by investigators on model load tests to predict settlement of prototype foundations have often been conflicting. For instance, Gilboy and Pandya agree that settlement of a footing in sand is practically independent of the size of the footing. Kogler and Bond however, found that the settlement of a footing on sand increased with increasing footing size, although not necessarily in proportion to the footing size.

In summarizing the performance of model load tests to predict prototype settlement, the presidential address given by Terzaghi at the 1st International Conference on Soil Mechanics and Foundation Engineering in 1936 may still be appropriate: "Grossly unbalanced is also the evidence offered in support of the claim that the settlement of a building can be predicted from the results of one or of several small-scale loading tests performed at the level of the base of the future foundation. For each case of evidence for this claim which has thus far come to my attention, I can quote at least two cases out of my own experience which contradicts it. Considering these facts, the academic merits of the underlying theory are utterly irrelevant, because the empirical arguments suffice to invalidate the claim." (55).

5. Similitude theory in model foundation tests

The use of dimensional analysis and similitude theory in analyzing model foundation tests has been extremely limited. Many examples can be found of a partial similitude treatment to the settlement problem, particularly in plotting test results as dimensionless quantities. For example, a dimensionless ratio of applied pressure to strength may be plotted against settlement divided by foundation width. However, few investigators have employed extensive similitude analysis to the study. R. L. Kondner has done much work in load-settlement testing and analysis using the principles of similitude. In his lists of variables, Kondner does not include unit weight of the soil as a pertinent soil variable. He attributes distortion which is seen to exist from experiments to viscous effects which cannot be modeled (32). L. J. Goodman, E. Hegedus and R. A. Liston, in a recent publication (22) applied similitude analysis to plate settlement tests. They include unit weight as a pertinent variable, and point out that a distortion exists in satisfying the similitude requirements for a model and prototype study involving a cohesive soil. They furthermore isolate this distortion to being in the unit weight of the model and prototype soils. Neither Goodman nor Kondner attempt to apply distorted model theory to analyze the distortion, nor do they present suggestions on how to reduce or eliminate this distortion.

III. ANALYTICAL INVESTIGATION

A. Application of Similitude Theory and Dimensional Analysis to Settlement Prediction

The method used herein to determine the model design equations follows the general procedure as outlined by Murphy (39). This procedure involves (a) identification of variables pertinent to the studied phenomenon, (b) formation of a set of dimensionless and independent pi terms composed of these variables, and (c) the determination of the design equations and prediction equation.

The most difficult step in model theory is to identify all variables which significantly affect the behavior of the system. The variables in the foundation-soil problem will be categorized as geometry variables, material variables, and load variables.

The dependent variable which is the quantity to be predicted, is the vertical displacement of the foundation under application of load. The independent variables associated with geometry are b, which represents a specific length of the foundation such as foundation width, and λ, which represents any other characteristic length of the foundation, such as radius of curvature.

The material properties of the footing have been limited to E for modulus of elasticity and G, for modulus of rigidity. The yield strength will not be considered an important vari-

able since it is assumed that the stresses imposed by the weight of the structure and the reaction of the soil, will remain considerably below the yield strength of the foundation material, normally concrete or reinforced concrete in the prototype and steel or aluminum in the models.

The pertinent material properties of the soil are considered to be their engineering properties. C and ϕ are the soil shear strength parameters defining the Coulomb failure envelope. K designates soil compressibility and may be defined as the change in soil void ratio per change in applied pressure. γ designates soil unit weight, defined as the weight of the soil and soil water divided by the volume of soil.

Other soil properties such as grain size, Atterberg limits, moisture content, amount of clay, and so forth are considered to be important only as they influence the above three engineering properties. This approach, emphasizing the engineering characteristics of a material rather than its index characteristics has been used successfully in model concrete systems, where the textural gradation and water-cement ratio was considered important only as they influence the engineering properties of the concrete.

The engineering properties of shear strength, compressibility and unit weight of the soil were chosen after consideration of the foundation settlement process. Since settlement beneath a foundation may involve shear strains and compression of soil voids, shear strength and compressibility character-

istics have been included. Since the unit weight of the soil will affect the force required to move the soil against the force of gravity, such as occurs when the soil ruptures with resulting shear displacements upward and outward, the unit weight has been included. The shear strength of the soil is most often expressed in terms of the shear parameters C and ϕ, where C is called the cohesive shear strength or cohesion, and is the stress independent portion of the soil shear strength. ϕ is called the angle of internal friction and is the stress dependent portion of the soil shear strength.

The viscosity and surface tension of the soil water are considered to be soil-related material properties.

The load variables include the applied force, R, on the foundation, which may comprise the weight of the structure and the dead weight of the foundation; the "surcharge" load, P, of the soil, which is the pressure of the soil adjacent to the foundation above an imaginary plane parallel to the bottom of the foundation. Another load-related variable is g, gravitational acceleration. Weight by definition is a gravitational force due to the existence of gravitational acceleration, and may be expressed by Newton's law $F = Ma$: force equals mass times acceleration. In this case the force is weight and the acceleration is g, gravitational acceleration. Three other load-related variables are the number of load applications, N, the velocity of penetration or velocity of settlement, V, and the time of load duration, t.

A list of the variables assumed to be pertinent to the foundation-soil settlement phenomenon, including their dimensions is shown below:

Symbol	Variable	Dimension
y	settlement of foundation	L
b	length of least width of foundation	L
λ	any other characteristic length of the foundation	L
E	modulus of elasticity of the foundation	FL^{-2}
G	modulus of rigidity of the foundation	FL^{-2}
C	cohesive shear strength of the soil	FL^{-2}
ϕ	angle of internal friction of the soil	dimensionless
K	coefficient of compressibility of the soil	$F^{-1} L^{2}$
γ	unit weight of the soil	FL^{-3}
ρ	density of the soil fluid (soil water)	$FL^{-4} T^{2}$
μ	viscosity of the soil fluid	FTL^{-2}
σ	surface tension of the soil fluid	FL^{-1}
R	force or load on the foundation	F
P	surcharge load per unit area above the horizontal base of the foundation	FL^{-2}
N	number of load applications	dimensionless
V	velocity of settlement	LT^{-1}
g	acceleration of gravity	LT^{-2}
t	duration of load applications	T

There are 18 variables, therefore from the Buckingham

Pi Theorem 15 dimensionless and independent pi terms may be selected which will describe the phenomenon. The following pi terms were chosen:

y/b; λ/b; R/b^2E; G/E; R/b^2C; ϕ; RK/b^2; $R/b^3\gamma$; R/b^2P; N; V^2/gb; $\rho Vb/\mu$; $\rho V^2b/\sigma$; $\gamma V^2K/g$; b/Vt.

The dependent pi term is y/b. Therefore the chosen set of pi terms leads to the following general equation:

$$y/b = f(\lambda/b,\ R/b^2E,\ G/E,\ R/b^2C,\ \phi,\ RK/b^2,\ R/b^3\gamma,\ R/b^2P,\ N,\ V^2/gb,\ \rho Vb/\mu,\ \rho V^2b/\sigma,\ \gamma V^2K/g,\ b/Vt).$$

A similar equation may be written for the model system, using the subscript m to designate model system variables:

$$y_m/b_m = f(\lambda_m/b_m,\ R_m/b^2{}_mE_m,\ R_m/b^2{}_mC_m,\ \phi_m,\ R_mK_m/b^2{}_m,\ R_m/b^3{}_m\gamma_m,\ R_m/b^2{}_m{}_m,\ N_m,\ V^2{}_m/g_mb_m,\ \rho_mV_mb_m/\mu_m,\ \rho_mV^2{}_mb_m/\sigma_m,\ \gamma_mV^2{}_mK_m/g_m,\ b_m/V_mt_m).$$

Each of these two general equations is assumed to refer to the same type of system, therefore the functions are identical in form. The design equations which must be satisfied in order for the model to be a true model are given below:

a) $\lambda_m/b_m = \lambda/b$

b) $R_m/b^2{}_mE_m = R/b^2E$

c) $G_m/E_m = G/E$

d) $R_m/b^2{}_mC_m = R/b^2C$

e) $\phi_m = \phi$

f) $R_m K_m / b^2_m = RK/b^2$

g) $R_m / b^2_m P_m = R/b^2 P$

h) $R_m / b^3_m \gamma_m = R/b^3 \gamma$

i) $N_m = N$

j) $V^2_m / g_m b_m = V^2/gb$

k) $\rho_m V_m b_m / \mu_m = \rho Vb/\mu$

l) $\rho_m V^2_m b_m / \sigma_m = \rho V^2 b/\sigma$

m) $\gamma_m V^2_m K_m / g_m = \gamma V^2 K/g$

n) $b_m / V_m t_m = b/Vt$

If these design equations are all satisfied, the prediction equation becomes $y/b = y_m/b_m$. Since the model and prototype foundations are assumed to be geometrically similar, b/b_m is equal to the linear scale ratio of prototype to model which will be designated n. Thus $y = n \cdot y_m$ if all design equations are satisfied.

Design condition (a) indicates that the model is to be geometrically similar to the prototype. Once this condition is met all geometrical properties such as area and moment of inertia are modeled.

Design condition (b) indicates that if $E_m = E$, then R_m/b^2_m must $= R/b^2$. This will be considered a requirement of loading, where the model load per model area must be equal to the prototype load per prototype area. With this load restric-

tion imposed, design condition (b) is satisfied.

Design condition (c) indicates that if $E_m = E$, G_m must = G. If the same material is used for model and prototype foundation, this design condition will be satisfied.

Design condition (d) indicates a relationship between applied load per area and the cohesive shear strength of the soil. With the loading restriction imposed that R/b^2 be equal in model and prototype, $C_m = C$. C_m is assumed to equal C, since the same soil is to be used in model and prototype, and C by definition is stress independent. Therefore, this design condition is satisfied.

Design condition (e) indicates that the angle of internal friction in the model soil must be equal to that in the prototype soil. This is assumed to be satisfied, since the same soil will be used in both systems.

Design condition (f) is similar to design condition (d), except that a soil property, 1/K is involved rather than C. 1/K is assumed to equal $1/K_m$, since the same soil is involved. $R_m/b^2_m = R/b^2$ from the loading restriction, therefore this design condition is satisfied.

Design condition (g) indicates a relationship between the applied load per area and the surcharge load per area. With the loading restriction imposed, P_m must = P for this design condition to be satisfied.

Design condition (h) indicates a relationship between the applied load per area and the unit weight of the soil.

With the loading restriction imposed, $1/b_m\gamma_m = 1/b\gamma$. Thus, $\gamma_m/\gamma = b/b_m$ or n if this design condition is to be satisfied. If $\gamma = \gamma_m$, since the same soil is to be used, $b/b_m = 1$, and the size of the model is restricted to being equal to the size of the prototype foundation. For practical reasons the model must be smaller than the prototype foundation, therefore this design condition cannot be satisfied and a distortion is introduced into the problem.

Design condition (i) indicates that the number of load repetitions must be the same in the model as in the prototype system.

Design condition (j) involves pi terms which are analogous to the Froude number in fluid mechanics. Dimensionally the Froude number is equivalent to the ratio of inertial force to gravitational force (39). It can also be seen that the pi terms indicate a relationship between the velocity of settlement and the length ratio and gravitational acceleration. If $g_m = g$, then V_m must equal $\sqrt{b_m/b}$ times V, or $V_m = V/\sqrt{n}$ for this condition to be satisfied.

Design condition (k) involves pi terms which are analogous to the Reynold's number, which is dimensionally equivalent to the ratio of inertial forces to viscous forces. If $\mu_m = \mu$ and $\rho_m = \rho$, then it is seen that V_m must = $V\, b/b_m$ or Vn, in order that this design condition be satisfied. This requirement violates the requirement for model velocity in design condition (j). Thus a second distortion is introduced into

the problem.

Design condition (l) involves pi terms which are analogous to the Weber number, which is dimensionally equivalent to the ratio of the inertial force to the surface tension force. If $\sigma_m = \sigma$ and $\rho_m = \rho$, V_m must equal $\sqrt{b/b_m}\ V$ or $V\sqrt{n}$, which violates the requirement for velocity in design conditions (j) and (k). A third distortion is therefore introduced.

Design condition (m) indicates that if $K_m = K$, $g_m = g$, and $\gamma_m = \gamma$, then V_m must = $\overline{V}$. This requirment also violates the requirement for velocity in design conditions (j), (k), and (l).

Design condition (n) stipulates a time-velocity relationship. If the velocity is assumed to be equal in the model and prototype, then $t_m = b_m t/b$, or t/n. Thus the time of load application for the model is 1/n th that of the prototype if the velocities are assumed equal.

In review it is seen that four design conditions require different velocity relationships (design conditions (j), (k), (l) and (m)). The pi terms in design conditions (k) and (l) will be ignored, since it has been proposed that the Reynold's number pi term and the Weber number pi term are considerably less important in soil systems than the Froude number pi term (26, 52). In addition, design condition (h) restricted the size of the model to being equal to the size of the prototype is a "true" model were to be constructed. Since this restriction is impractical, a "distorted" model

must be considered. A distorted model may be defined as a model in which at least one design condition is violated.

At this point in the analysis two approaches to the problem are possible. The first approach is to accept the design conditions as they are and apply distorted model theory (39). A coefficient known as a "distortion factor" is assigned to each unsatisfied design condition. For example, design condition (h) becomes $R_m/b^3{}_m\gamma_m = \alpha\ R/b^3\gamma$, where α is the distortion factor. Since $R_m/b^2{}_m = R/b^2$, $1/b_m\gamma_m = \alpha\ 1/b\gamma$, or $\alpha = n\ \gamma/\gamma_m$. Since the same soil is involved in model and prototype systems, $\gamma = \gamma_m$, and $\alpha = n$. Thus if the model is 1/10th the linear dimensions of the prototype, the distortion factor is 10.

Distorted design conditions will result in modified prediction equations. In this problem the prediction equation $y = n\ y_m$ becomes $y = \delta n\ y_m$, where δ is called the prediction factor. δ normally must be determined experimentally. If δ is determined experimentally, then the distorted model-prototype problem should yield a meaningful solution. This distorted model theory approach will be attempted with the experimental results obtained in the investigation.

A second possible approach to the distorted similitude problem is to reduce or eliminate the distortion involved. In this way the distorted model system can be made to approach or become a true model system. This second approach, attempting to reduce or remove the distortion, is emphasized in this

study, and will be investigated at this time.

γ, the unit weight of the soil, is included in the unsatisfied design condition (h), and for reasons which will become more obvious, is replaced by its equivalent $\rho' g$ where ρ' is the mass density of the soil in mass units per length units cubed, such as slugs per cubic foot. g, as already stated, is the acceleration of gravity. Design condition (h) now becomes $R_m/b^3{}_m \rho'_m g_m = R/b^3 \rho' g$. Since $\rho'_m = \rho'$, and $R_m/b^2{}_m = R/b^2$, this design condition reduces to $1/g_m b_m = 1/gb$, or $g/g_m = 1/n$. From this equation it is seen that if the model is to be made smaller than the prototype, that is, n is greater than 1, then g_m must be made greater than g by the ratio b/b_m, or n.

An examination of the original design conditions reveals that γ appears in two other design conditions in addition to (h). Upon substitution of ρg for γ, design condition (m) becomes $\rho_m g_m V^2{}_m K_m/g_m = \rho g V^2 K/g$. The g's will cancel out, and since $\rho_m = \rho$, and $K_m = K$, the velocity in the model, V_m, must equal the velocity in the prototype, V.

g also appears in design condition (j), $V^2{}_m/g_m b_m = V^2/gb$. If $g_m/g = n$, then $V^2{}_m = V^2$, or $V_m = V$. This is in agreement with the velocity relationship established in design condition (m), and since design conditions (k) and (l) have been assumed to be relatively unimportant, and have been discarded, there is no longer an inconsistency in the velocity requirements.

At this point it appears that all design conditions may

be satisfied and a true model can be constructed if g_m can be made equal to n times g. If this can be accomplished without distorting any of the variables, then the distortion has been removed from the problem and the model system becomes a true model system. In this case the prediction equation will be $y/b = y_m/b_m$, or the settlement in the prototype will equal n times the settlement in the model.

Since design conditions (k) and (l) were discarded, and several simplifying assumptions have been made, such as the soil properties being exactly equal for model and prototype, and since it will be shown to be impossible to make $g_m = ng$ without introducing some disturbance into the soil system, a true model system can only be approximated. How close the approximation will be to the true model system can be determined from the experimental results obtained in tests conducted with model and prototype systems in the same soil.

B. Settlement Prediction Assuming Similar Model and Prototype Systems

The following analyses re-explore the prediction equation in the light of traditional analytic mechanics treatments. The prediction equation which resulted from the similitude analysis was that $y = ny_m$. This conclusion is valid only if true similarity exists between the prototype and model systems. For the following analyses, the assumption is made that a true similarity does in fact exist between the prototype and

the model systems. That is, that all the design conditions can be satisfied. It is pointed out that the linear scale ratio, n, is equal to $\sqrt{A/A_m}$ as well as being equal to b/b_m, where A refers to the area of the foundations.

1. Theory of elasticity

Settlement under a rigid foundation employing the theory of elasticity, has been described by the following equation (56): $y' = \frac{w\, p \sqrt{A}}{C}$, where y' is the elastic settlement, where w is a shape factor, A is the size of the loaded area, p is the load pressure, or load R divided by loaded area, A, and C are the soil properties. To determine the ratio of settlement, prototype to model, one has only to divide the prototype equation by the model equation. Thus, $y'/y_m = \frac{w\, p \sqrt{A}\, A_m}{w_m p_m \sqrt{A_m}\, C}$. The load per area, or p's are equal according to the loading restriction previously specified. Also $w_m = w$, since the two foundations are assumed to be geometrically similar. $C_m = C$, since the same soil is used for model and prototype. Thus the equation reduces to $y/y_m = \sqrt{A/A_m}$, or $y' = ny'_m$.

2. Consolidation

The equation widely used for prediction of settlement from consolidation testing is $y'' = d \frac{e_1 - e_2}{1 \quad e_1}$, where y'' is the consolidation settlement, d is the depth or extent of the compressible layer of soil, e_1 is the initial void ratio of the soil, and e_2 is the final void ratio of the soil. Since the model and prototype systems are assumed to be similar, and

the loading restriction has been made that applied load intensities will be equal in model and prototype, the stress distribution within the soil should be similar in the model and prototype systems as depicted in Figure 2a. If e_1 is the initial void ratio of the soil at a particular depth, H, in the prototype system and e_{1m} is the initial void ratio of the model soil at a corresponding depth H_m (equal to H/n), then e_1 is assumed to be equal to e_{1m} since the model and prototype soils were assumed to be identical. The stress distributions are similar in the two systems, therefore e_2 should equal e_{2m} since the compression of the soil mass and reduction of void ratio is a function of the soil and the stresses imposed on the soil mass. Thus $y'/y'_m =$

$$d/d_m \; \frac{\frac{e_1 - e_2}{1 + e_1}}{\frac{e_{1m} - e_{2m}}{1 + e_{1m}}}$$ becomes $y'/y'_m = d/d_m$, upon substitution of

equal corresponding void ratios. Since the model and prototype systems were assumed to be similar in all respects, they must be similar geometrically, and the ratio d/d_m must be equal to the linear scale ratio, n. Therefore, $y'' = ny'_m$.

In actuality, e_1 will not be exactly equal to e_{1m}, since the soil at a depth H in the prototype system will be n times deeper than the soil at a depth H_m, and is therefore under a greater surcharge confining stress intensity. Thus e_1 can be expected to be smaller than e_{1m}. Also the danger of encount-

ering a different soil layer, as shown in Figure 2b is apparent in which case the bulb of pressure may affect the lower layer of soil beneath the prototype but not beneath the model.

3. Shear rupture

The equation to be investigated is the Prandtl punch theory equation for ultimate pressure, as modified by Terzaghi (56). The formula as given by Terzaghi is: $p_u = \gamma t[\tan^2 (45 + \phi/2)\, e^{\pi \tan \phi} - 1]$. The t is a ratio of the area of wedges and sector from the assumed failure geometry of Prandtl, divided by the length of the log spiral failure surface abc, or 1/2 area I + area II + area III, divided by abc, as shown in Figure 3. p_u is the ultimate pressure, defined as the pressure on the loaded surface which, if exceeded, will result in a shear rupture along the shear surface. Since the investigation is specifically interested in settlement, and not in ultimate pressure, an assumption is introduced. Since one mechanism of settlement is shear rupture resulting from shear strains in the stressed soil, settlement resulting from shear rupture, y''', may also be a function of the ultimate pressure.

Thus $y''' = f(\gamma t[\tan^2(45 + \phi/2\, e^{\pi \tan \phi} - 1])$ and $y'''_m = f(\gamma_m t_m[\tan^2(45 + \phi_m/2\, e^{\pi \tan \phi_m} - 1])$, where f is read "is a function of". All the soil properties are equal for the two systems. Furthermore, since the two systems are assumed to be similar, the functions, although not specified, must be

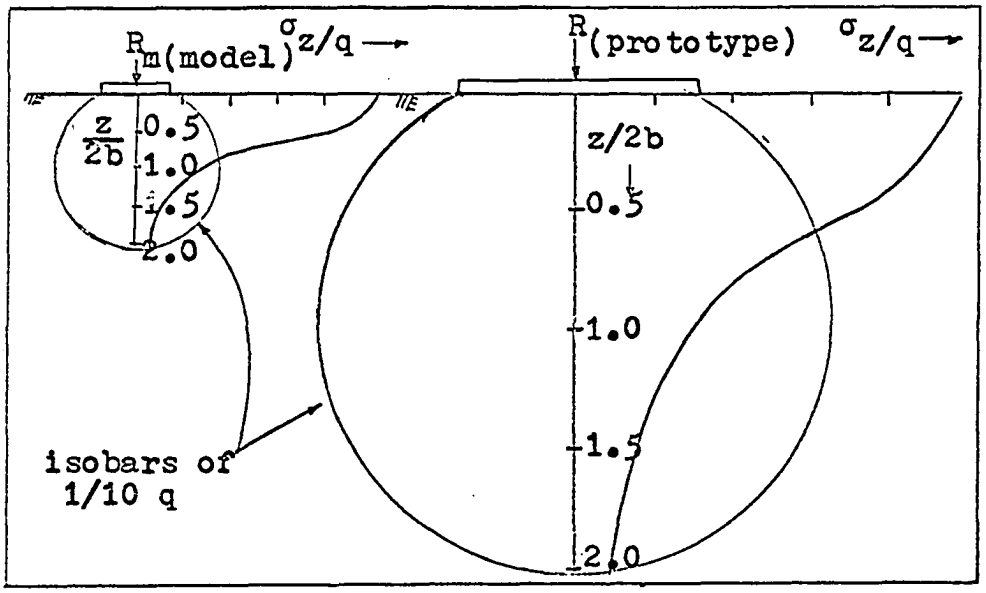

Figure 2a. Stress distribution in soil, model and prototype systems

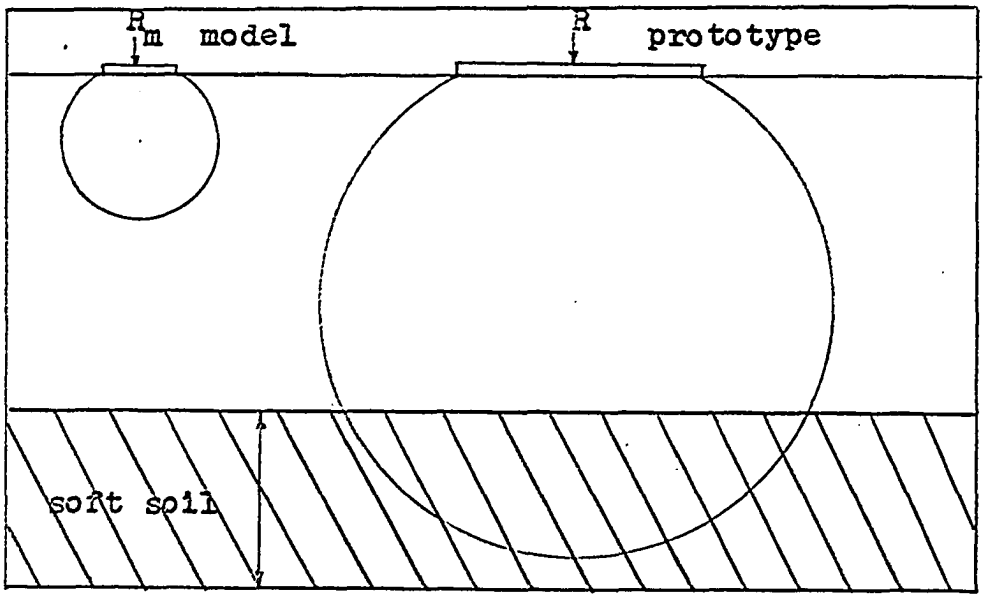

Figure 2b. Influence of buried soft soil on model load testing

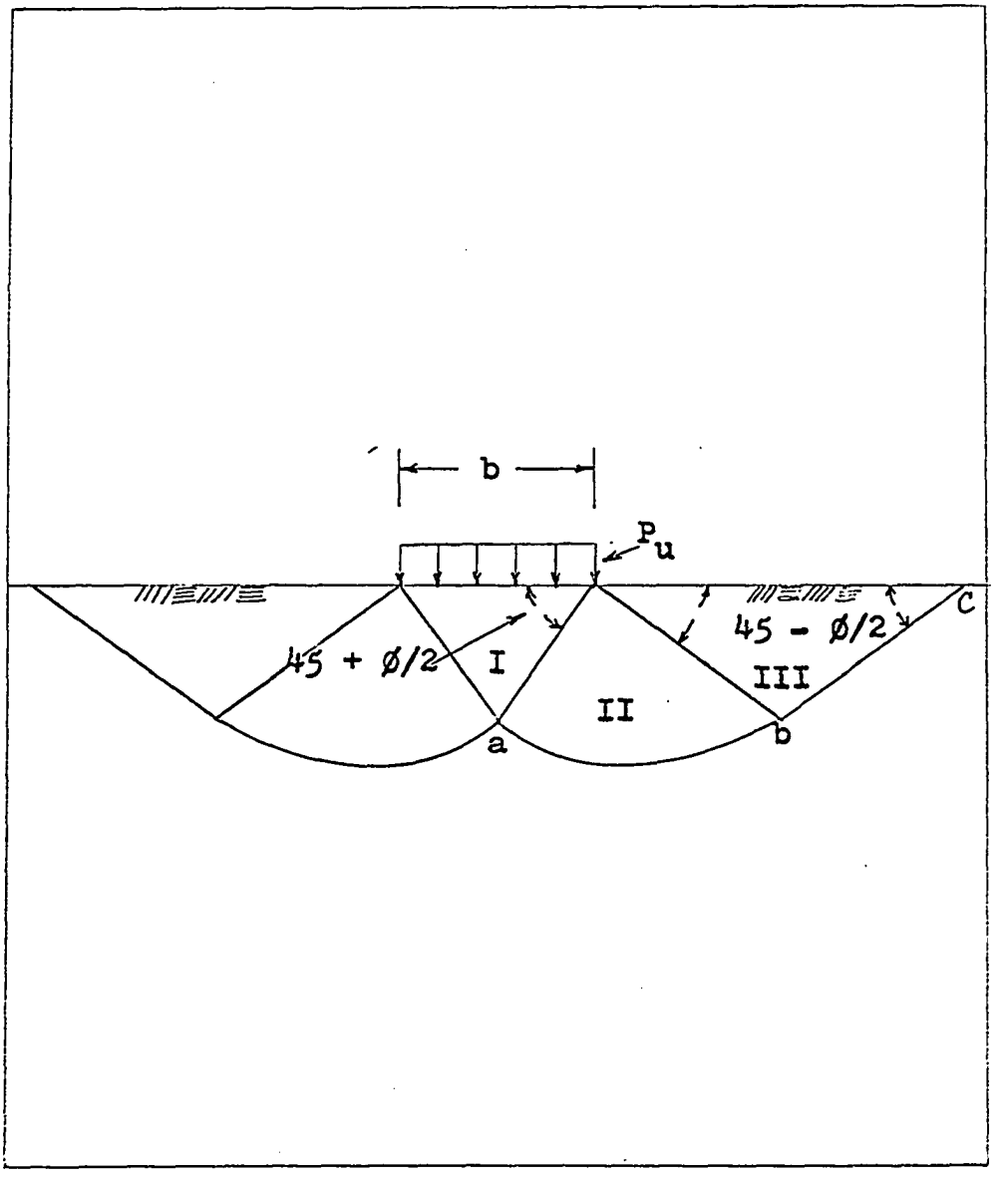

Figure 3. Prandtl's plastic equilibrium theory

equal. Therefore $y'''/y'''_m = t/t_m$. By definition $t = A'/r\, e^{\pi \tan \phi}$, where A' is the area previously specified and shown in Figure 3. r is the length abc in the same figure. Thus $t/t_m = \frac{A'/A'_m}{\frac{r\, e^{\pi \tan \phi}}{r_m e^{\pi \tan \phi_m}}}$ which is equal to $\frac{A'\, r_m}{A'_m\, r}$. From geometric similarity this is equivalent to n^2/n, or n. Thus $y''' = n y'''_m$.

Each of these three examples represents what can be considered a separate mechanism of settlement; immediate or elastic settlement, y', consolidation settlement, y", and shear rupture settlement, y'''. It is conceivable that all these mechanisms could occur simultaneously or that they could occur separately or not at all under different loading conditions and in different soils. If the model soil system and the prototype soil system are similar, then for each of these three examples, y should equal n times y_m.

Since $y' = n\, y'_m$

$y'' = n\, y''_m$

and $y''' = n\, y'''_m$, and since $y = y' + y'' + y'''$, $y = n y'_m + n y''_m + n y'''_m$, or $y = n y_m$. If the model and prototype systems are truly similar, as assumed in this analysis, then $y = y_m\, b/b_m$, or $y/b = y_m/b_m$. Therefore for different sized foundations on a homogeneous soil mass, a plot of $\frac{\text{settlement}}{\text{foundation width}}$ versus load intensity should converge. In practice this trend has been detected (11, 22), however, only some curves in certain soils and with a particular range of foundation sizes converge. The others do not converge.

In this section it has been shown that if one assumes the prototype and model soil-foundation systems to be similar, then by employing commonly used soil engineering equations describing the 3 common mechanism of settlement, elastic compression, consolidation, and shear, settlement in the prototype system should be equal to n times the settlement in the model. The fact that observations have shown that this is usually not achieved indicates that true similarity does not exist in the model and prototype systems. If the model and prototype systems could be made similar, or more similar (by reducing the amount of distortion), it would appear that settlement in the prototype system, y, would more closely approximate n times settlement in the model system, y_m. If a close approximation could be achieved with model foundation systems, reliable settlement predictions for prototype foundations may be possible.

C. Removal of Distortion in Settlement Problem

Since it has been shown that all design conditions may be satisfied and a true model system can be constructed if g_m can be made equal to n times g, the problem now is to determine a practical method of increasing the gravitational acceleration in the model system.

Gravity is defined as "The apparent force per unit mass with which the earth attracts bodies near its surface, as measured by the acceleration of a body in free fall relative

to the surface of the earth. This apparent force acting on a body of mass m at a point where the acceleration of gravity is g, is m·g, and is called the weight of the body." (19). Thus gravitational force is commonly called weight, and is equal to the mass of a body times gravitational acceleration, g. Weight = mass times g or g = weight/mass. g is known to vary slightly with elevation and position of the earth's surface, but it is close to 32.2 feet per second squared.

An artificial acceleration could be introduced within the model footing system to increase g beyond its normal 32.2 feet/sec^2. This approach has been taken to remove distortion in a similitude problem dealing with concrete arches by the use of centrifuges (10). The use of a centrifuge for the particular problem of settlement prediction in the field location appears impossible, or at best, impractical.

A second possible way to increase g would be to increase the gravitational force or weight (W) acting on a body. This could conceivably be done by a magnetic force application, although once again this appears impractical. A more practical manner of increasing the gravitational force appears to be in the application of an external force over an area, which could be applied by air or other fluid pressure. As far as has been determined this approach has never been attempted in a soil system problem. The method of increasing the gravitational force, W, acting on a mass, M, to increase g_m will be examined in detail.

A free body diagram of an element of homogeneous soil is shown in Figure 4. The gravitational force W_1, is the force required to cause this body to accelerate at 32.2 feet/ sec^2. If an additional body force, W_2, were applied to the free body diagram, as shown in Figure 2, g_m would now be $\frac{W_1 + W_2}{M}$. M has not changed, therefore g_m has increased from its original magnitude by the amount W_2/M. Thus if one can introduce a body force, W_2, into a soil mass, M, the effective gravitational acceleration, g_m of the model soil system can be increased.

For practical reasons, the additional body force, W_2, will be approximated by a surface force. If a large area of a soil mass is subjected to a surface force, and only a small volume of the mass is investigated, the surface force may closely approximate a body force. For example, consider the case of a rigid plate resting on a level soil surface as shown in Figure 5. A force W_2 is applied to the plate. The pressure distribution of the soil is known to depend on both the plate characteristics and the soil characteristics (53), as well as the magnitude of the load. To simplify the problem, the plate is assumed circular and perfectly rigid, while the soil is assumed to be a perfectly elastic material.

The force, W_2, divided by the plate area A, will be called the load pressure, P_2. If a volume of soil beneath the center of the plate with the dimensions as shown in Figure 5, is examined, the minimum vertical stress within this volume

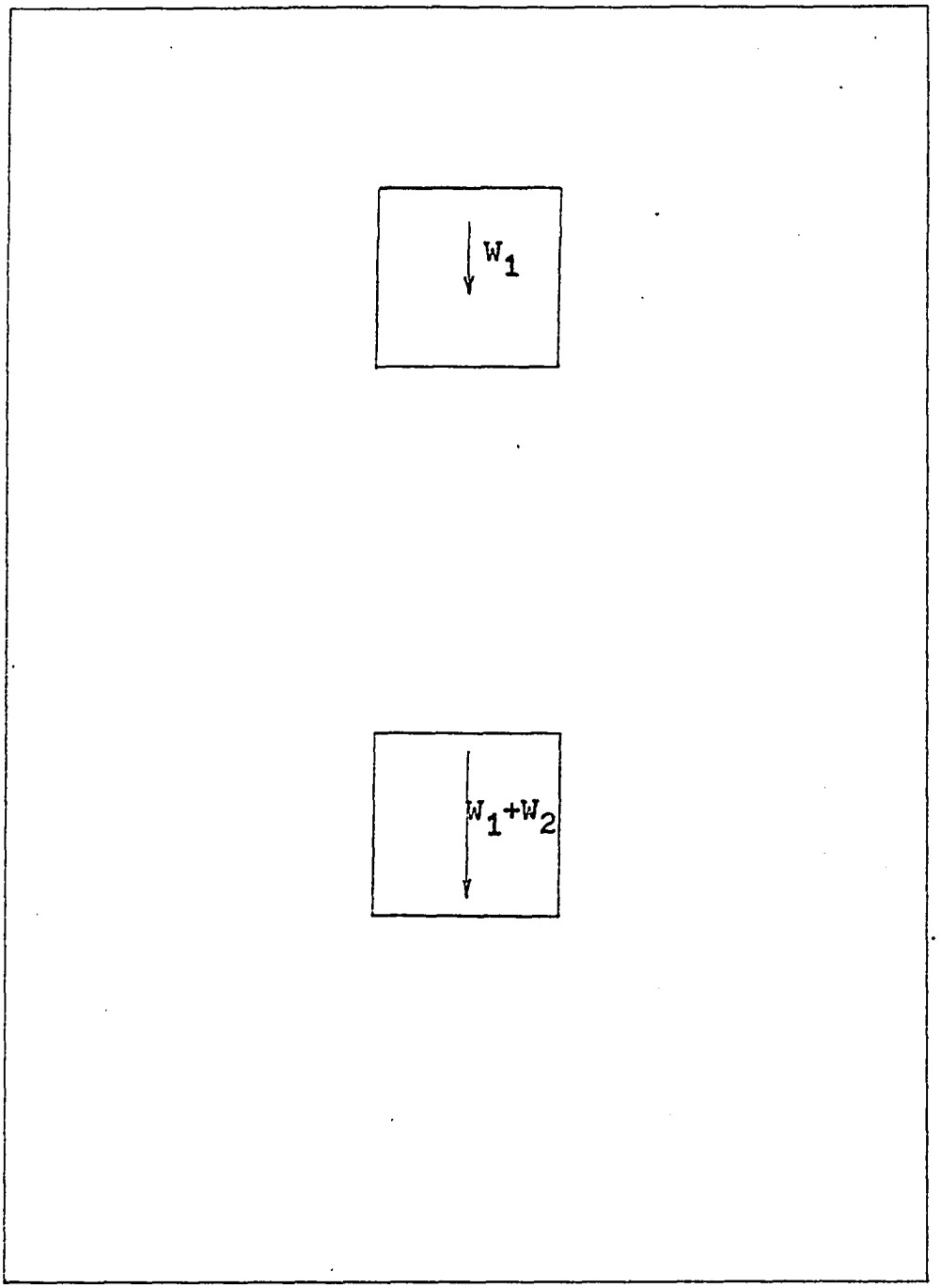

Figure 4. Free body diagrams of elements of homogeneous soil

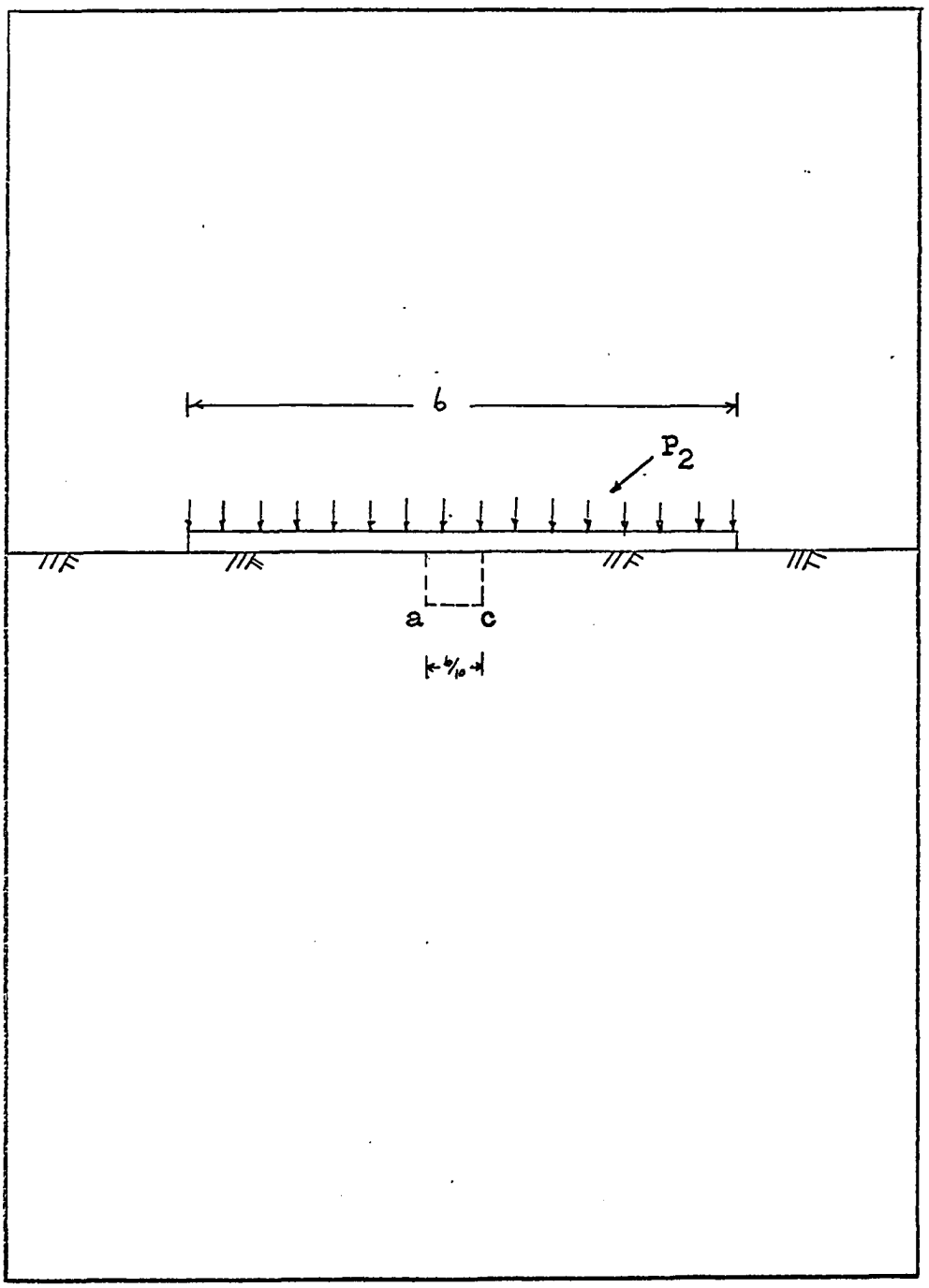

Figure 5. Surface pressure applied by rigid circular plate on ground surface

will occur at extreme points such as a and c. The vertical stress, σ_z, at a and c will be 0.97 times P_2 (60). All other elements in the mass of this small soil volume will be subjected to a vertical stress between 0.97 and 1.00 times P_2. Thus the vertical force per elemental area within this small volume will be quite uniform, and will be very close to P_2. The horizontal stress, σ_t within this volume will vary from 0.90 to 1.00 times P_2, while the shear stress Trz will vary from 0.00 to 0.01 times P_2. (60). Thus vertical stresses and horizontal stresses will be close to P_2, while shear stresses will be very close to zero.

The body forces in a soil mass due to gravitational acceleration will now be examined. The earth is represented as a perfect sphere. The solution to the problem of determining stresses induced in a sphere with internal and external pressure employing elastic theory has been solved (58). As shown in Figure 6, a is the radius of a cavity at the center of the sphere, b is the radius of the sphere, p_i is the internal pressure in the center cavity, p_o is the external pressure on the sphere surface. Since gravity is defined as the apparent force per unit mass with which the earth attracts bodies near its surface, this apparent force applied over an area can be considered an apparent pressure. This apparent pressure is represented in this analysis by p_o.

If σ_r is the radial normal stress within the sphere, and σ_t is the tangential stress, with T_{rt} being the shear

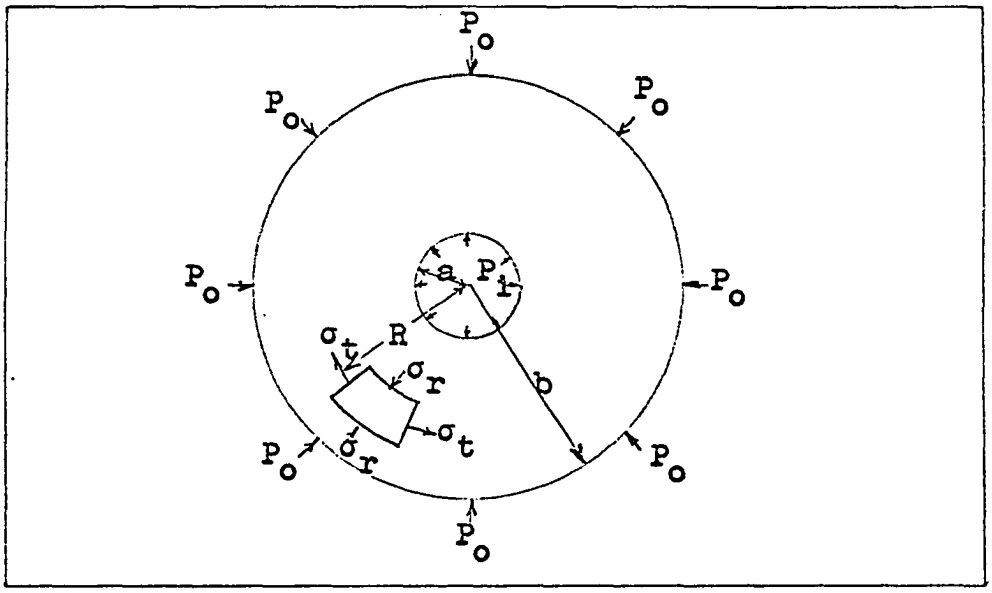

Figure 6. Sphere with external and internal pressure

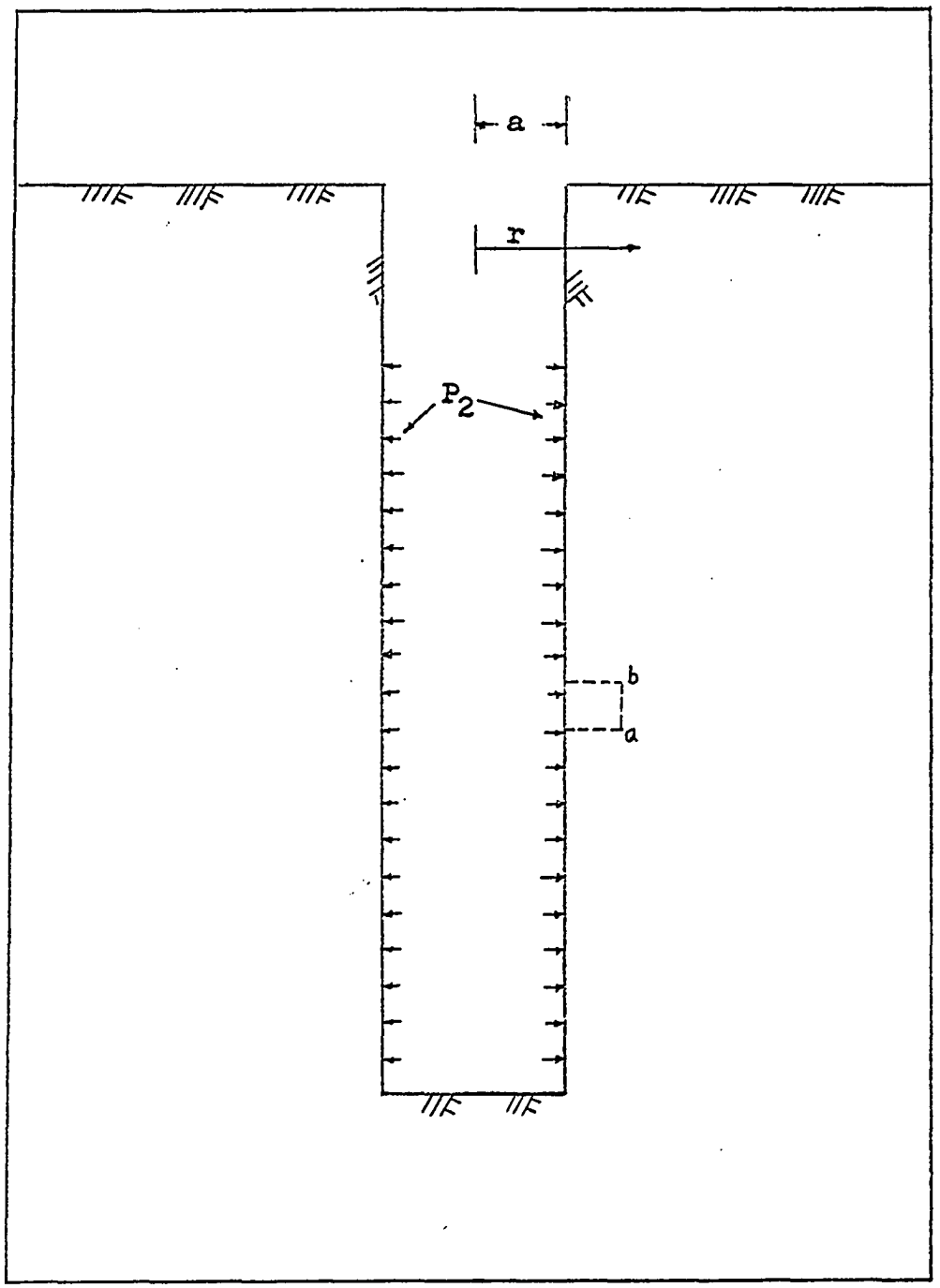

Figure 7. Surface pressure applied radially within a cylindrical hole

stress, then the following equations express the magnitudes of the stresses:

$$\sigma_r = \frac{p_o b^3(R^3 - a^3)}{R^3(a^3 - b^3)} + \frac{p_1 a^3(b^3 - R^3)}{R^3(a^3 - b^3)}$$

$$\sigma_t = \frac{p_o b^3(2R^3 - a^3)}{2R^3(a^3 - b^3)} - \frac{p_1 a^3(2R^3 + b^3)}{2R^3(a^3 - b^3)}$$

$$T_{rt} = 0$$

Another example of a situation in which a surface force may be applied to approximate a body force within a soil mass is the case of an cylindrical hole in an infinitely large soil mass. A force W_2 may be applied over an area of the hole as a pressure exerted radially on the sides of the hole as shown in Figure 7. This situation has the theoretical advantage that the system has a high degree of symmetry and elastic and plastic theories may be used in analyzing it. In addition, it has a practical advantage, since cylindrical holes, commonly called bore holes or drill holes, are required in the conduct of subsurface foundation site investigations.

Results of an elastic analysis, assuming the soil to be a perfectly elastic material, are: (58)

Radial stress, σ_r, = $-P_2\ a^2/r^2$, where a is the radius of the hole and r is the radial distance to any point within the soil mass. Tangential stress, σ_t, is = $P_2\ a^2/r^2$, or is equal to the radial stress, although opposite in sign. It is pointed out that both the radial stress and the tangential stress

are independent of material properties of the elastic soil. The vertical stress, σ_z, = $P_2(\frac{a^2}{b^2 - a^2})(\frac{3K - 2G}{3KG})$. G is the modulus of rigidity while K is the bulk modulus. Thus the vertical stress is not independent of material properties; however it is independent of r. For this problem, b = infinity, therefore the vertical stress is zero.

As in the previous case, a small volume of soil located within a large loaded area will be investigated. A volume of soil 1 1/2 inches by 2 inches by 2.25 inches as shown in Figure 7, will be examined. The hole radius is assumed to be 3.25 inches, and the length of hole which is subjected to the radial pressure P_2 is assumed to be infinite. The stress will be least at the extreme points such as a and b, as in the previous case studied. For these points, r = 5.25. Letting a = 3.25 and r = 5.25, and substituting into the equation for radial and tangential stresses, one finds that the radial and tangential stresses are equal to 0.382 P_2. The radial and horizontal stresses within the volume therefore are between 1.00 P_2 and 0.382 P_2. The average value for the radial and tangential stresses within this volume will be $1/5.25\text{-}3.25 \int_{3.25}^{5.25} P_2 \frac{a^2}{r^2}\, dr$, which equals 0.614 P_2. The bigger the hole, the closer these stresses will approach P_2. Table 1 shows a comparison of stress values for the sphere, the surface load, and the cylindrical load.

It is pointed out that soil is not a perfectly elastic material, and that stress dissipation in soils is generally

Table 1. Stress relationships, assuming elastic soil

Stress	Sphere	Surface load	Cylindrical load
σ_r	p_o	.985 p_o	.614 p_o
σ_t	p_o	.95 p_o	.614 p_o
T_{rt}	0	0	0

far less than computed by the elastic theory. Thus with a real soil, the average stresses within the volumes investigated will be considerably closer to P_2. It appears reasonable that a surface pressure might be applied radially within a cylindrical hole to approximate a body force within a small volume of soil, and that a pressure could be applied to the ground surface to approximate a body force within a small soil volume. This surface pressure which may be applied to approximate a gravitational body force within a small soil volume will be called "simulated gravitational pressure" (sgp).

The next problem is how to calculate the amount of "gravitational pressure" which is required to approximate an artificial gravitational force. Let $F_1 = Mg$, where F_1 is the normal gravitational force or weight of a body at the surface of the earth. F_1 can also be considered a force which is "equivalent" to 1 g. Let $F_2 = M\,ng$, where n is the linear scale factor. Since M and g are constant, $F_2 = n\,F_1$. Thus F_2 is equivalent to n g's. Thus the force required to corre-

spond to 10 g's is 10 times normal gravitational force, which is commonly called weight.

Assume a soil has a unit weight of 100 lb/ft^3. This is also $100/1728 = 0.0579$ lb/in^3. This force could be applied to one side of the one inch cube as a pressure of 0.0579 lb/in^2. which would simulate the gravitational or weight force of the top one inch layer of the assumed soil. The gravitational force of the top 2 inches of this soil could similarly be simulated by a pressure of 2 times 0.0579, or 0.1158 psi. Thus it is seen that the pressure required to simulate gravitational force in a soil mass varies with the depth of the soil to be affected as well as the unit weight of this soil.

Two approaches for determining the proper amount of sgp required to simulate the gravitational force of the soil mass are first, to assume a constant influence depth of soil for different sized model foundations, or second, to assume an influence depth of soil which is a function of the dimensions of the model footing. With the second approach if model 1 had linear dimensions 1.5 times larger than model 2, then the depth of the soil to be simulated with model 1 would be greater than that of model 2, probably 1.5 times as great.

Terzaghi (57) and subsequent investigators have observed that the zone below a footing within which at least 80% of the stresses occur extends to a depth of approximately 1.5 times the breadth of the loaded area. This approximation is of course a simplification, and the actual depth of the zone

which contains 80% of the induced stresses will be affected to some extent by the soil type and conditions such as moisture content.

The following conclusions are drawn from this discussion:

1) Since the required sgp varies with the depth of soil assumed to influence the settlement phenomenon, a depth of soil within which the weight force is to be simulated must be determined.

2) This depth of soil may be a constant depth for different sized models, or it may be a function of the size of the model plates.

3) The actual depth of influence of the sgp may depend on soil characteristics as well as model size.

4) Due to the depth-dependent relationship of the applied "gravitational pressure" and the weight force being simulated, and also due to the fact that surface stresses will dissipate in depth, a distortion must be assumed to be introduced with the application of any simulated gravitational pressure (sgp), whether this pressure is applied to simulate a constant depth, or one which is a function of model breadth.

The sgp applied in this study will be calculated to simulate the weight force of the soil at a constant depth of one inch for all models. The model dimensions will be 3 inches by 4 inches and smaller. The distortion induced by this method of sgp application will be evaluated in analyzing the results of the experiments performed.

Example sgp calculation: The assumed soil has a unit weight of 100 lb/ft^3. As previously shown, this is also 0.0579 lb/in^3. Thus the weight of the top 1 inch of this soil will be 0.0579 lb/in^2. This force may be approximated by a pressure of 0.0579 psi. If the model were 1/10th the size of the prototype, and n were 10, then the model soil should have a gravitational force of 10 g's. The weight force already existing in the soil, F_1, is 0.0579 lb. F_2, the weight force of the model soil must be 10 times 0.0579, or 0.579 lb. Furthermore, F_2will be the vector sum of F_1 and F_a, where F_a is the applied external force. When F_1 and F_a are acting in the same direction, which will occur when F_a is applied in the vertical downward direction, then $F_2 = F_1 + F_a$, or $F_a = F_2 - F_1$. When F_a is applied perpendicular to F_1, which will occur when the applied force is in the horizontal direction, then $F_2 = F_1 + F_a$. For example, if n = 10, F_2 will be 10 g and F_1 = 1 g. If F_a is applied in the vertical downward direction, F_a = 10 g - 1 g or 9 g. On the other hand if F_a is applied in the horizontal direction, F_2 = 10 g, = 1 g $+ F_a$, or 9.97 g. Furthermore, F_2 will act at an angle whose tangent if 0.10, or 5.7 degrees from the horizontal as shown in Figure 8.

It is seen that when F_a is applied horizontally, and n is increased, F_a will approach F_2 as a limit, and the direction of F_2 will approach the horizontal direction. It is again pointed out that the applied surface pressure will dis-

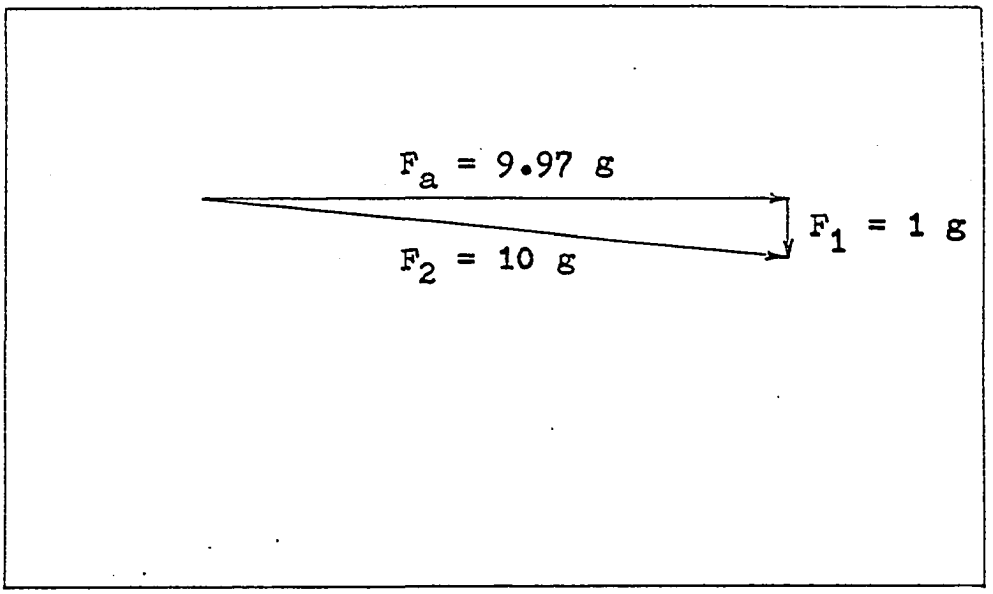

Figure 8. Vector forces

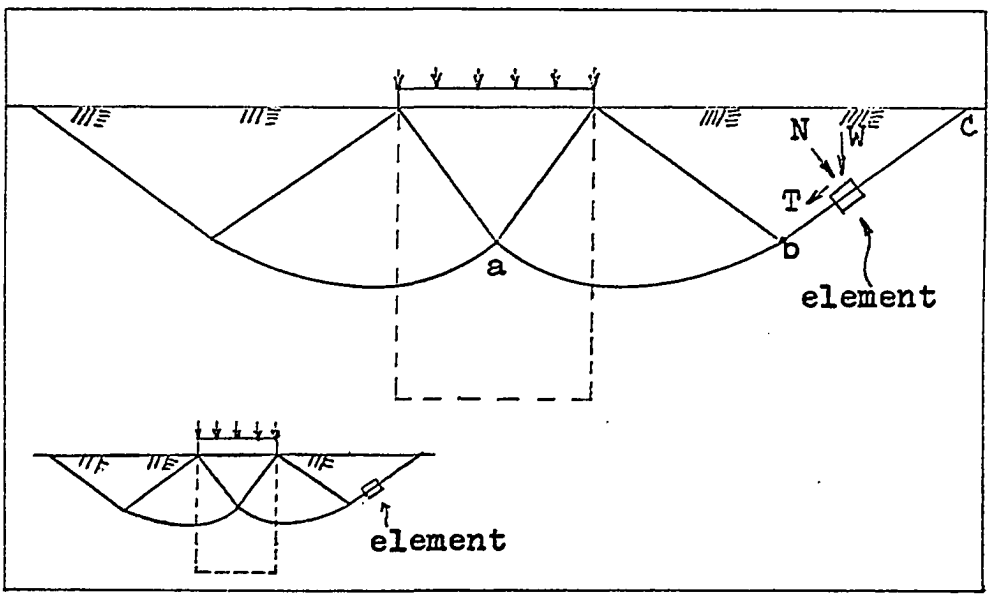

Figure 9. Element location for shear resistance force analysis

sipate in depth, although as long as the volume of soil being investigated is small in relation to the area over which pressure is being applied, the stress dissipation will be minimized.

D. Effect of Applied "Simulated Gravitational Pressure" on the Settlement Phenomenon

1. Introduction

According to the results of the previous similitude analysis, the distortion involved in the model-prototype soil-foundation systems can be eliminated by increasing the effective unit weight of the model soil by a factor of n times its original unit weight, where n is the linear scale ratio, prototype to model foundation. An application of a surface force applied over an area large with respect to the model foundation has been shown to approximate the body forces which would exist if the model soil actually weighed n times its normal weight. The following investigation will examine the effect of "sgp" in terms of classical theory.

The complexity of the phenomena associated with settlement is well recognized by those familiar with the field of soil mechanics. Three basic phenomena are widely acknowledged as occurring during settlement: primary compression, lateral flow, and secondary compression. Primary compression is divided into two parts, immediate or elastic compression, and primary consolidation. Lateral flow is generally considered

a plastic and irreversible process which involves no volume change. Both of these phenomena, primary compression and lateral flow, have been frequently observed and studied in laboratory and field situations. The third phenomenon, secondary compression, is often called viscous creep. Although it is known to occur in many soils, little is known or agreed upon concerning the causes or extent of this phenomenon.

Three force systems act during the settlement process. The three resisting forces which oppose settlement can be classified as the shear resistance force, the compressive resistance force, and the viscous resistance force. Ratios of these resistance forces with the applied force are dimensionless; in fact two had previously been chosen as pi terms, R/b^2C, the applied force to cohesive shear resistance pi term and RK/b^2, the applied force to compressive resistance pi term. Rt/b^3n, the applied force to viscous resistance force is the third force ratio in the settlement phenomena.

In fluid flow problems, when more than one force ratio pi term is involved, complete similarity is possible only for full-scale models, which is usually highly impractical; therefore incomplete similarity results (39). A parallel may be drawn between the settlement problem and fluid flow problems. Since both involve more than one force ratio, and complete similarity is impossible in the fluid flow problem, it appears reasonable that the same situation would exist in the soil problem. This parallel further strengthens the conclusion

that an inconsistency exists in the satisfaction of the design conditions, for this is an indication of incomplete similarity.

2. Shear strength

According to the Coulomb theory, the soil shear strength may be expressed by the two parameters, C and ϕ, which are considered inherent characteristics of the soil. It is recognized that this theory is a simplification of the actual shear phenomenon; however it usually is a good approximation, and has been widely used in the solution of many soil mechanics problems. C, the cohesive shear strength, may be defined as the shear resistance of a soil when no normal pressure is applied to the failure surface. By this definition, C will not change with an increase in normal stress. ϕ, the angle of internal friction, will not change with an increase in normal stress, since ϕ is assumed to remain constant by the Coulomb theory. However, it is known that ϕ will often increase with an increase in the density of a soil, particularly if the density of a loose sand is increased. Normal stress application can cause an increased density, which in turn could cause an increase in ϕ, however the assumption is made that ϕ will not change with an increase in applied normal stresses.

3. The Prandtl Punch theory

Prandtl employed the theory of plastic equilibrium in studying the penetration of hard metal punches into softer homogeneous materials. The theory developed by Prandtl has been applied to the problem of a hard body, such as a loaded plate, penetrating softer soil. Results of laboratory and field observations have verified the approximate validity of Prandtl's theory for this problem, although Terzaghi, Taylor and others have modified several of Prandtl's assumptions, and have arrived at different analytical expressions to describe the failure phenomenon. Prandtl's theory results in an assumed shape of rupture surface which depends on ϕ and the breadth of the foundation. The assumed rupture surface consists of arcs of a logarithmic spiral, and straight lines tangent to these arcs, and shown in Figure 9. This rupture surface has been found to correspond fairly well with the manner of failure observed in experiments for granular soils and stiff clays. It may be applicable to frictional and cohesive soils (C-ϕ soils), purely cohesive soils ($\phi = 0$), and purely frictional soils ($C = 0$). Limitations of this theory to the problem of settlement analysis include:

1) Elastic deformations are ignored. Since in most materials such as metals, elastic deformations are small in comparison with plastic deformations, the elastic part of the body was treated by Prandtl as a rigid body. Since soils are more compressible than metals, this assumption introduces

more error into soil systems, and limits the use of this theory in settlement or deformation analysis.

2) Prandtl's solution is not made for settlement, but for bearing capacity. Thus it is concerned mostly with determining allowable loads to prevent rupture or shear failure, and not with amounts of settlement. Although these two limitations should be kept in mind, the geometric shape of the various zones assumed to develop beneath the loaded surface by the Prandtl theory, and the processes which take place in the soil during loading are valuable tools in analyzing the settlement problem. In addition, shear strains developed prior to complete rupture result in some settlement.

The shear force ratio pi term, R/b^2C will be slightly modified for the purpose of analysis. C will be replaced by S, the shear strength, where $S = C + N \tan \phi$. Thus the modified pi term will be R/b^2S. A loading condition, that R/b^2 be equal in the model and prototype has already been established, therefore for this pi term to be equal in model and prototype system, S in the model must be equal to S in the prototype. Since $S = C + N \tan \phi$, and C and ϕ have been assumed to be equal for model and prototype, N, the normal stress on the failure surface in the prototype system, must equal N_m, the normal stress in the model system in order that the design condition established by this pi term may be satisfied. Figure 9 depicts the Prandtl theory, where the large system represents the prototype and the small system represents

the model. Superimposed on these figures in dotted lines is a simplified pressure distribution bulb which outlines the approximate location of isopressure lines representing 10% intensity of pressure. It is seen that the greater portion of the rupture surface abc, is unaffected by pressures in excess of 10% of the load pressure. If a free body diagram of the model and prototype is drawn from the area outside the pressure bulb influence, as shown in Figure 10, the only soil forces involved will be the weight force, the shear resistance force, and the actuating force. The actuating force will then be opposed by these two forces. The weight force may be resolved into two components, one normal to the rupture surface, the other parallel to it. The resistance to shear failure in the prototype system, in terms of force, is $CLd + NLd \tan \phi + TLd$, where L is the length of the element, d is the width or depth of the element into the plane of the paper, and T is the tangential component of the weight force.

The shear resistance force in the model system is $C_m L_m d_m + N_m L_m d_m \tan \phi_m + T_m L_m d_m$. Substituting $C = C_m$, $\phi = \phi_m$ and $n = L/L_m$ into the model equation results in : $CLd/n^2 + N_m Ld/n^2 \tan \phi + T_m Ld/n^2$ = model shear resistance force.

The ratio of the actuating forces, prototype to model are: $Rm/b_m^2 = R/b^2$ therefore, $R/R_m = n^2$ eq. 2. The ratio of applied forces to resisting shear forces are: Prototype: $R/CLd + N \tan \phi + TLd$; model: $R_m/\frac{CLd}{n^2} + N_m \tan \phi + T_m \frac{Cd}{n^2}$.

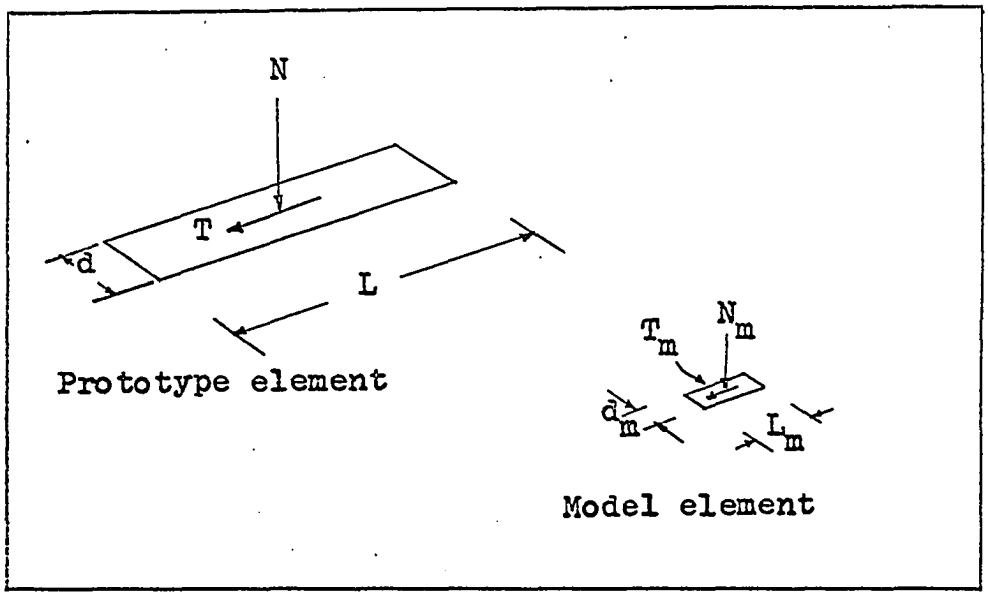

Figure 10. Elements on rupture surface

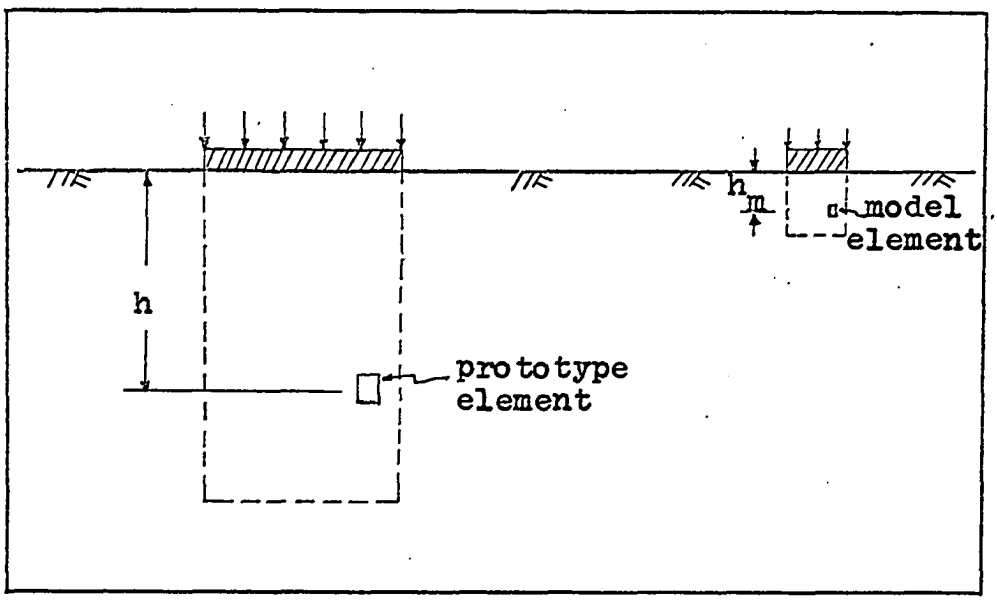

Figure 11. Elements for compressive resistance force analysis

Substituting eq. 2 into the model equation results in: $R/CLd + N_m \frac{\tan \phi}{n^2} + T_m/n^2$. These two force ratio equations can be made equal for the model and prototype only if N_m/n^2 and T_m/n^2 in the model are equal to N and T respectively. However, $W/W_m = N/N_m = T/T_m$ = volume in prototype times unit weight in prototype divided by volume in model times unit weight in model. Since n is the linear scale factor, the volume ratios, prototype to model, will be n^3, and $N/N_m = n^3 \gamma/\gamma_m$ eq. 3. Since we also know that N_m/n^2 must equal N, or $N_m = n^2N$, there now exist two equations involving N and N_m. Substituting N for N_m in eq. 3, yields $N/n^2N = n^3 \gamma/\gamma_m$, or $\gamma_m = n\gamma$. Therefore the unit weight in the model must be n times the unit weight in the prototype for the shear resistance design condition to be satisfied.

The next step is to determine the relationship between the applied force and the compression resistance forces as expressed in the pi term RK/b^2. Figure 11 depicts a simplified diagram of the compressed soil mass. Results of experiments have verified that the depth of influence, H, of the compressive stresses is about 1.5 times the breadth of the loaded area (57).

The vertical stress on the top of an element within the stressed zone has been shown by many investigators, including Bousinesq and Westergaard (53) to be proportional to R/H^2, or directly proportional to the applied force and inversely proportional to the depth squared. Therefore $\frac{\sigma_z}{\sigma_{zm}} = \frac{R/H^2}{R_m/H_m^2}$ eq.4.

Since $R/R_m = n^2$ (loading restriction), and $H/H_m = n$, $\frac{\sigma_z}{\sigma_{zm}} = \frac{R/H^2}{\frac{R}{n^2}\frac{n^2}{H^2}} = 1$. Thus $\sigma_z = \sigma_{zm}$.

The passive resistance stress developed on the sides of the elements are proportional to γHK_p from Rankine's earth pressure theory (53). The ratio of these lateral stresses for prototype to model are: $\gamma HK_p/\gamma_m H_m K_{pm}$. But K_p, the passive pressure coefficient is equal to $\frac{1 + \sin \phi}{1 - \sin \phi}$, and since $\phi_m = \phi$, $K_{pm} = K_p$ (K_p, the passive pressure coefficient should not be confused with K, the compressibility coefficient). Therefore the ratio of lateral compressive stresses, or passive resistance stresses on the sides of the elements as shown in Figure 12, is $\gamma HK_p/\gamma_m H_m K_{pm}$ or $n\ \gamma/\gamma_m$.

The applied force on the prototype element is $\sigma_z\ dxdz$; that on the model element is $\sigma_z\ dx_m dz_m$, or $\sigma_z \frac{dxdz}{n^2}$. The compressive resistance force on the side of the prototype element is $\gamma HK_p dxdy$; that on the model element is $\gamma_m H_m K_{pm} dx_m dy_m$, or $\gamma_m \frac{H}{n} K_p \frac{dxdy}{n^2}$. The ratio of the applied force to the compressive resistance force in the prototype element is $\frac{\sigma_z dxdz}{\gamma HK_p dxdy}$, and in the model element is $\frac{\sigma_z \frac{dxdz}{n^2}}{\gamma_m \frac{H}{n} K_p \frac{dxdy}{n^2}}$. Setting these two force ratios equal results in $\frac{\sigma_z dxdz}{\gamma HK_p dxdy} = \frac{\sigma_z \frac{dxdz}{n^2}}{\gamma_m \frac{H}{n} K_p \frac{dxdy}{n^2}}$ or $\frac{1}{\gamma} = \frac{n}{\gamma_m}$.

Thus γ must $= n\gamma_m$.

It has been demonstrated that an additional weight force

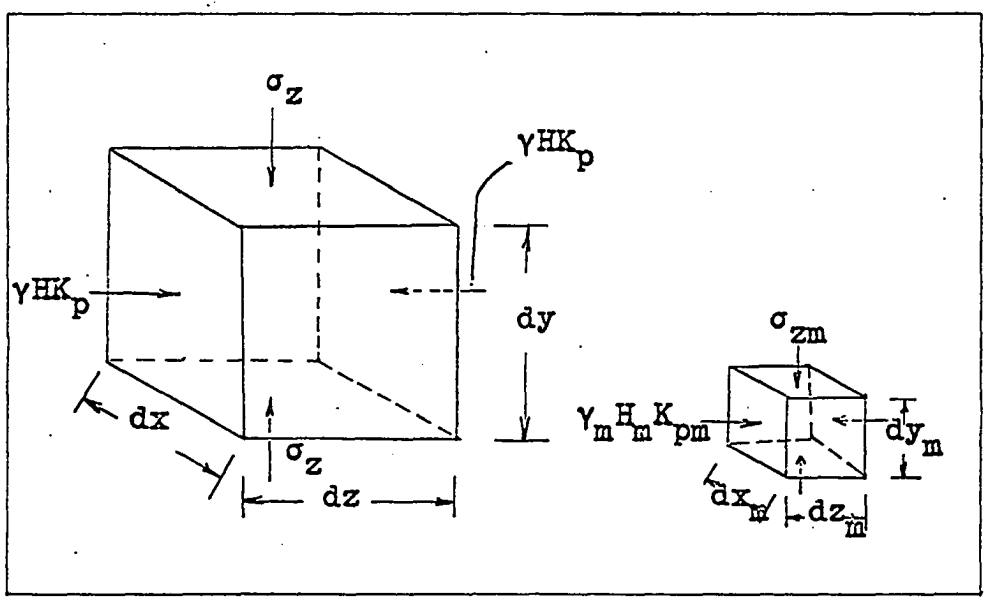

Figure 12. Elements in compressed soil mass

per volume, $n\gamma$, is introduced into the model system will result in the 2 force ratio pi terms, R/b^2S and RK/b^2 in the prototype system being equal to their respective pi terms in the model system. This analysis goes one step further than merely assuming that $S = S_m$ (or that $C = C_m$ and $\phi = \phi_m$) and $K = K_m$.

In the viscous resistance force ratio, with R/b^2 ratios equal, it is seen that t_m/n_m must equal t/n. However, due to practical conditions of the test, the duration of loading in the model system must be much less than in the prototype system. Although the duration of loading may have an effect on the viscosity, it appears evident that the great difference in loading times will prevent this design condition from ever being completely satisfied. This fact may induce some distortion into the problem.

E. Design and Operation of Model Settlement Apparatus

A basic requirement of the Model Settlement Apparatus was that it would be inserted in a drill hole and test the soil at the sides of the hole. This requirement was imposed for practical reasons, since the device should be capable of testing soils at various depths. Testing at the sides of a hole allows for the hole to be drilled to completion prior to the beginning of testing within the hole.

A second general characteristic of the Model Settlement Apparatus was that it use a pair of model foundations mounted in order to act diametrically in opposite directions on the

sides of the hole. This would enable the soil itself to act as a reaction to the penetration force, rather than necessitate a dead load or other type of reaction. The direction of penetration of the model foundation plates would therefore be in a plane perpendicular to the longitudinal axis of the drill hole. The amount of settlement, or penetration of the plates within the soil would have to be measured.

A third characteristic of the Model Settlement Apparatus was that a method of "gravitational pressure" application must be incorporated, separate from the load application on the model foundation plates.

Finally, two sets of different sized model foundation plates would be placed within the apparatus, since this would allow for experimental verification of the similitude theory, and enable the measurement of the magnitude of distortion remaining in the model system for different soils to be made.

As a direct result of these four general characteristics, model #1 shown in Figure 13 and Figure 14 was constructed. Based on the results of testing with this apparatus, a second and improved model shown in Figure 15 and Figure 16 was designed and constructed.

As shown in the photographs, the apparatus is cylindrical in shape, with a rubber membrane fastened to the two end discs, much as in a laboratory triaxial test apparatus. In fact, the rubber membranes used were standard 0.025 inch thick triaxial rubber membranes. The two sets of foundation

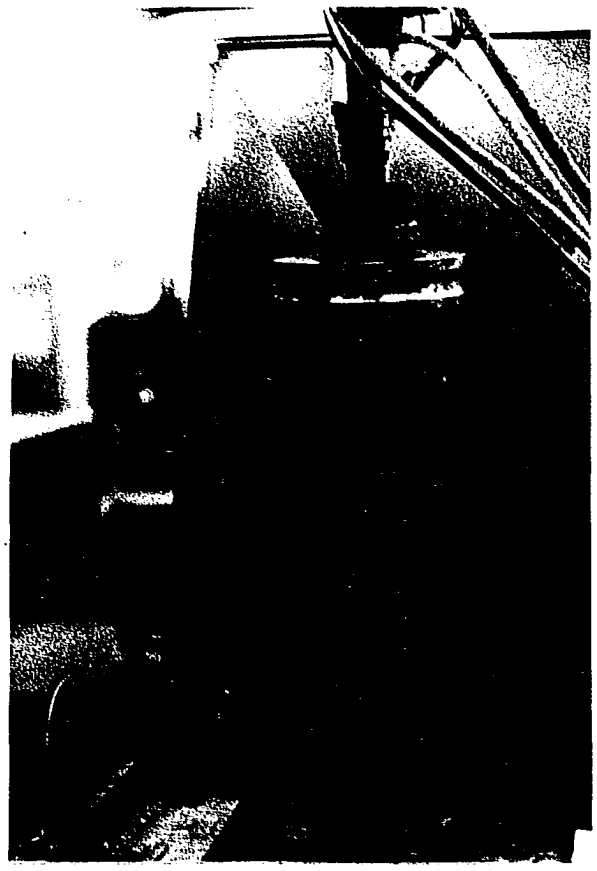

Figure 13. Model #1 without membrane

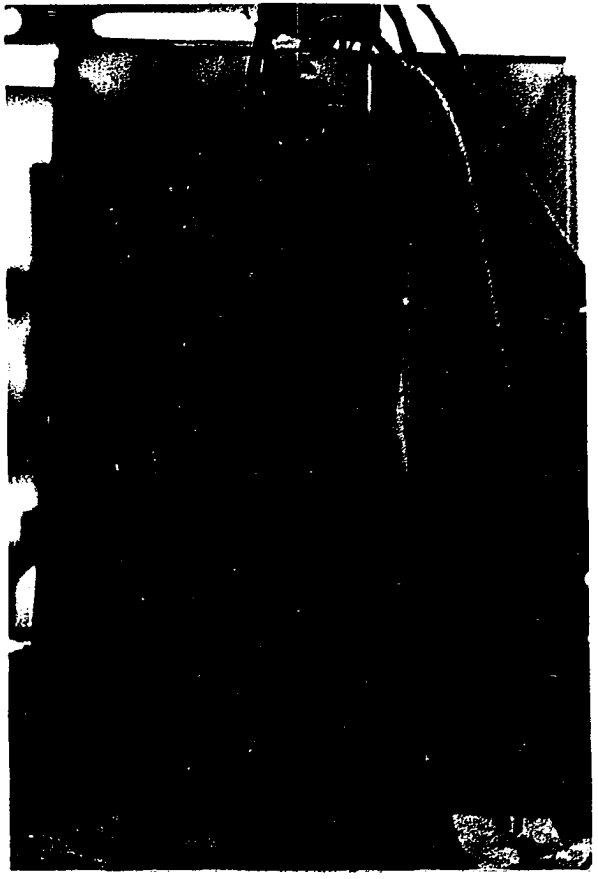

Figure 14. Model #1 with membrane

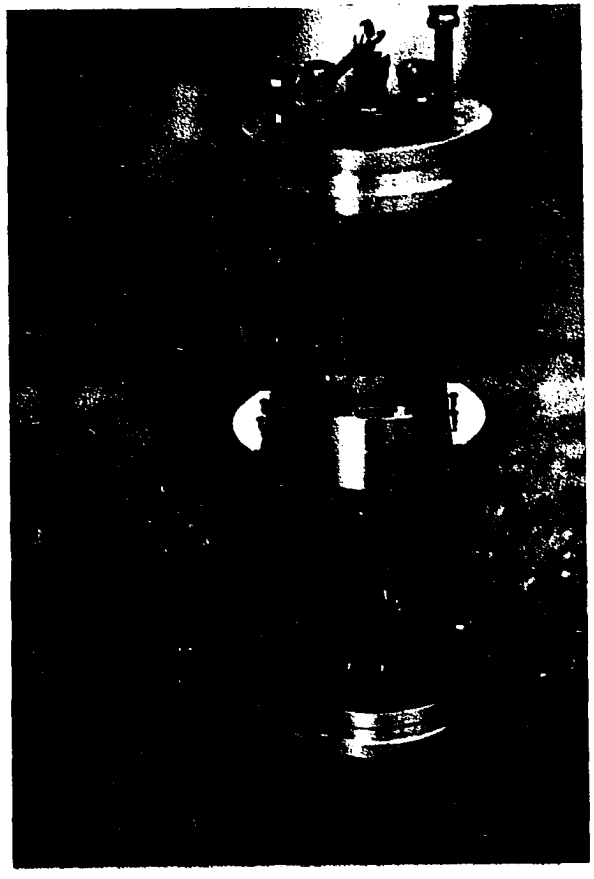

Figure 15. Model #2 without membrane

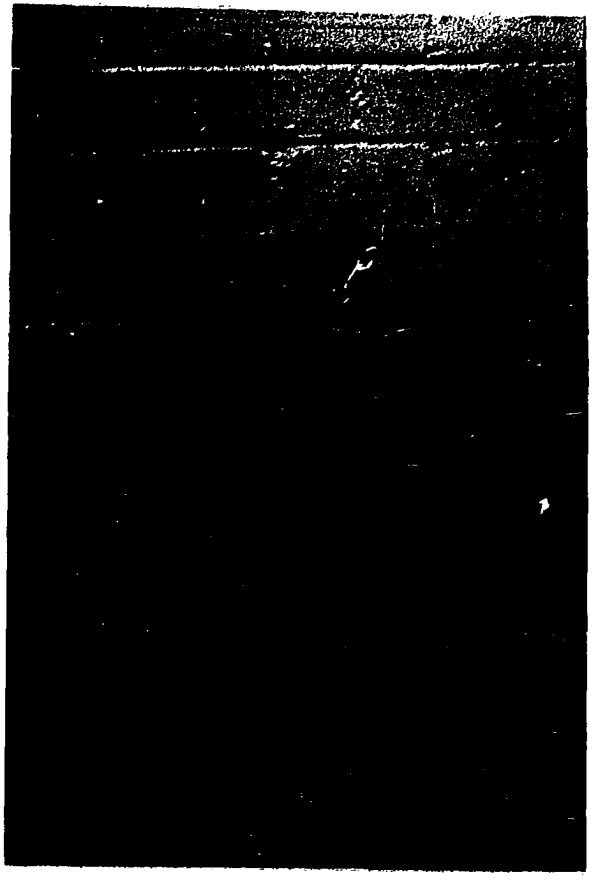

Figure 16. Model #2 with membrane

plates are mounted so that their directions of settlement are perpendicular to each other. The foundation plates are curved with the same curvature as that planned for the drill hole, 3.25 inch radius. The large plates measure 3 inches in width by 4 inches in length measured along the curved surface. The small plates measure 2 inches in width by 2.67 inches in length, again measured along the curved surface. If the smaller plates are considered as the models, and the larger plates are the prototypes, the linear scale ratio n is 1.5. The two sets of plates are not completely geometrically similar, since each set has the same radius of curvature. In the analysis of test results and interpretations we will assume geometric similarity, and any distortion which may be induced will contribute to the over-all distortions present in the system.

Each plate in a set is fastened to a piston which moves within a common hydraulic cylinder. The plates are loaded by means of hydraulic pressure applied by an hydraulic pump located at the ground surface. The magnitude of load is calculated from the hydraulic fluid pressure read on a standard bourdon tube pressure gage.

The amount of relative movement of the plates is measured by means of SR-4 strain gages mounted on opposite sides of a stainless steel cantilever beam (actually a 6" flexible steel ruler) located at one end of the set of plates as shown in Figure 17. A woven brass wire connects the free end of the

Figure 17. Model #2, showing cantilevered ruler with strain gages

Figure 18. Accessory equipment

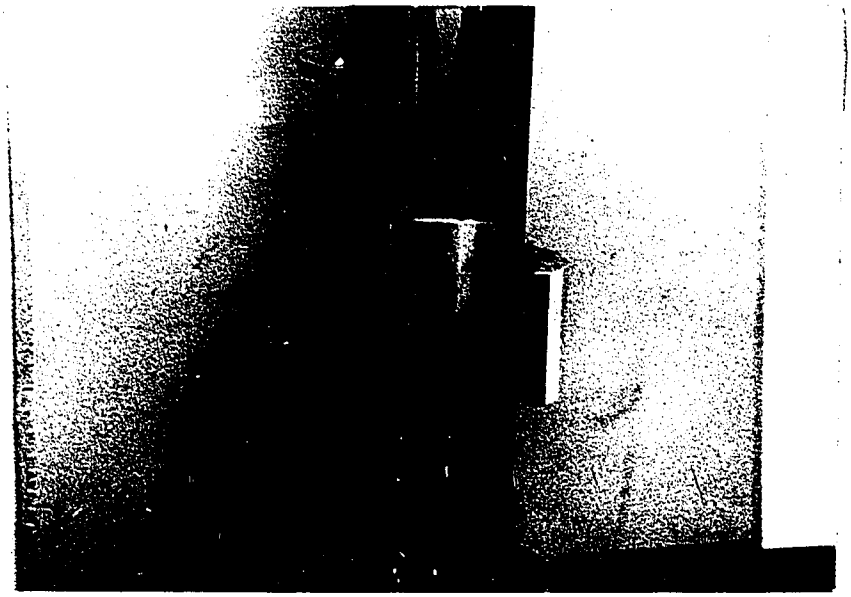

cantilever with a bar on the opposite end of the set of plates. As the plates expand, the bar and cantilever separate, bending the cantilever so that with proper calibration the strain gages measure the amount of total movement of both plates. Each set of plates is allowed to "float" within the apparatus so that equal loads and settlements can be expected of each plate. The second model is better equipped to float due to suspension of the plate sets by 8 springs. Only one piston exists within each plate set, so that a true action-reaction situation is created. Upon load application, the piston moves outwardly and the plate fastened to that piston moves to engage the soil. Once the soil is engaged, the opposite plate is moved by the movement of the cylinder assembly itself. This will continue until both plates engage the soil, and an equal load is transmitted to both plates. Since the strain gage arrangement measures penetration of both plates into the soil, the measured values are divided by 2.

The gravitational pressure is applied by air pressure within the rubber membrane. This air pressure is provided by a compressed air tank located at the ground surface. Figure 18 shows the accessory equipment mounted on a portable carrier. The hydraulic pump for application of model foundation load is shown at A; the air compressor for application of "gravitational pressure" is located at B. The SR-4 strain gage indicator, model A-7 is shown at C.

The mechanics of operation of the apparatus can be il-

lustrated in 3 basic steps (Figure 19).

The first step is the lowering of the apparatus into the bored hole to the desired depth for test.

The second step is the application of air pressure in the rubber membrane. This causes the rubber membrane to expand and engage the soil, exerting a radial pressure on the sides of the hole.

The third step is the application of a predetermined hydraulic pressure to force the plates into the soil. The amount of movement of the plates is read on the strain indicator after the first load application. When the rate of movement slows down to less than 0.002 inches per minute, the next load application is applied to the plates. This repeated load application is continued for as many loads as desired.

The complete test sequence involving steps one through three is first performed with the large plate set. After the test has been completed, the large plates are retracted and the air pressure in the membrane is increased in accordance with the sgp theory, and the small plate set is tested, employing steps two and three. Thus the two plate sets test the soil in the hole at two depths that differ by only about 2 inches.

When the small plate set test is complete, the small plates are retracted and the air pressure in the rubber membrane is released. The apparatus is then ready to test at

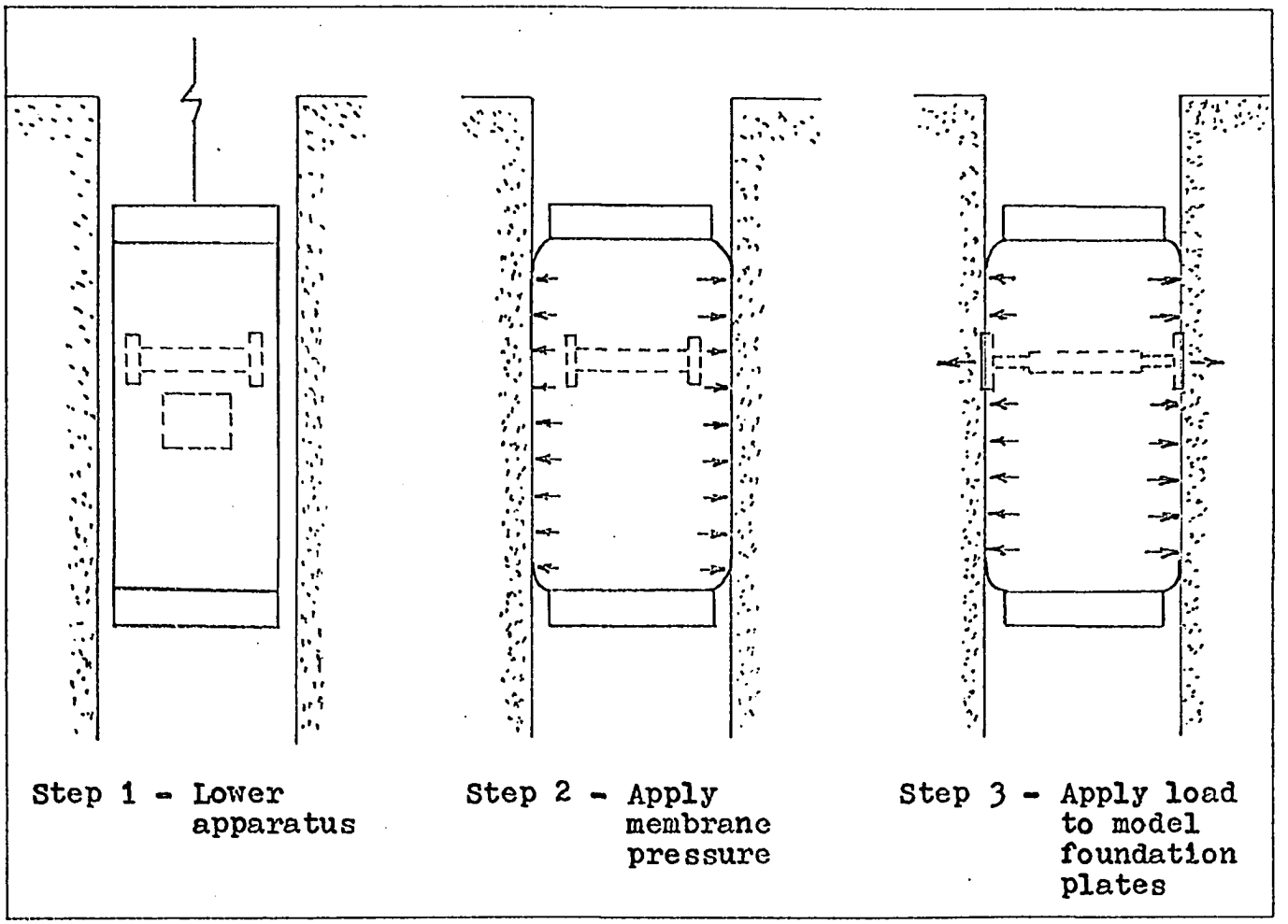

Figure 19. Settlement apparatus operation

another depth within the hole, or in another hole. The device does not have to be removed between tests for cleaning or other purposes.

The apparatus was calibrated in the laboratory prior to use in the field. The penetration force was determined by placing the apparatus so that one plate rested on a fixed base, and the opposite plate engaged the bottom of a calibrated proving ring. The force measured by the proving ring was divided by the area of one plate to obtain the load pressure.

The strain gages were calibrated by means of Ames dials reading to 1/10,000 of an inch. Each dial was mounted to read the sum of the movements of opposite plates, similar to the operation of the strain gages.

A circular ring with an inside diameter of 6.5 inches was placed over the rubber membrane for calibration. The air pressure was slowly increased within the membrane until the amount of pressure that caused the membrane to touch the ring was determined. This pressure was then considered the opening pressure, which added to the calculated pressure gives the gage pressure.

F. Differences Between Model and Prototype Systems

1. Different directions of applied settlement load

Model settlement loads with the Model Settlement Apparatus are perpendicular to the longitudinal axis of the bore

hole, which will normally be in a vertical orientation. Thus the settlement load is applied in the horizontal direction, whereas in the prototype foundation the settlement load is vertical. The question arises as to what effect this difference may have.

Two areas for examination of this difference are anisotropicity of the soil physical properties, such as shear strength, compressibility and permeability, and anisotropicity of stress distributions within the soil.

It is reasonable to assume that soil physical properties may vary for different orientations of applied load. Jakobson (28) found however, in a study of a non-homogeneous varved, post-glacial clay, that the clay was virtually isotropic in regard to compressibility and shear strength. He tested samples in the laboratory which had been obtained from vertical holes, horizontal holes, and holes oriented at an angle of 45 degrees.

Schmertmann (47) reports that field tests with the vane shear test in soft, normally consolidated clays resulted in an average shear strength difference amounting to a ratio of 1.8 for the shear strength of a horizontal test (shear stress was applied circumferentially about a horizontal axis) divided by the shear strength of a vertical test (shear stress was applied circumferentially about a vertical axis).

Field tests conducted with the Bore Hole Direct Shear Device (18) indicate an anisotropic shear strength in loess,

wherein the ø obtained from a horizontal test was greater than the ø obtained from a vertical test.

The anisotropicity of some soils with respect to permeability is well known by those familiar with earth dam construction. This difference probably influences the time required for consolidation under the applied settlement load.

It is recognized that the amount of anisotropicity of soil with respect to the soil properties of shear strength, compressibility, and permeability vary with the soil being investigated. Since anisotropicity will result in a distortion in the model system, the amount of distortion should vary with the soil. The amount would be discernable if a Model Settlement Apparatus test were performed in a horizontal hole with the model plates directed upward and downward. The practicality and necessity for such tests should be further investigated.

2. Effect of curvature of model foundation plates

It has been pointed out that the 2 "model plates and the 3" model plates each have a 3.25 inch radius of curvature, in order to fully engage the surface of the hole. Furthermore, the prototype loading plate, and prototype foundations have flat bottom surfaces (an infinite radius of curvature). Thus the model foundations are not truly similar to the prototype foundations, nor are they truly similar to each other, since for true similarity, the radius of curvature in the 2"

plate should be 2/3 that of the 3" plate.

Figure 20 shows qualitative stress distributions beneath a rigid flat loaded surface on 3 general soil types under different loading intensities (57). Cylindrical depressions on the surface of an infinite elastic solid will cause an elliptical distribution of stresses (16). The stress distribution beneath a cylindrical surface will result in a different stress distribution than that shown in Figure 20, therefore the curvature of the surface can be expected to effect the stress distribution within the soil. The extent of this effect can be examined from experimental results with model and prototype tests. Since the radius of curvature of the 2" plate is larger than that of the 3" plate with respect to the plate dimensions, the 2" plate is more similar to the flat prototype plate with an infinite radius. If test results show a consistently closer relationship in predicting settlement of the prototype plate than does the 3" plate, it would appear that the stress distribution difference caused by the curved surfaces would be of considerable importance.

3. Time effects

According to the similitude analysis, duration of load application for the model should be 1/n times that of the prototype. This is a desirable relationship, since model load durations from practical necessity are short compared with prototype load durations (which last for the lifetime of the

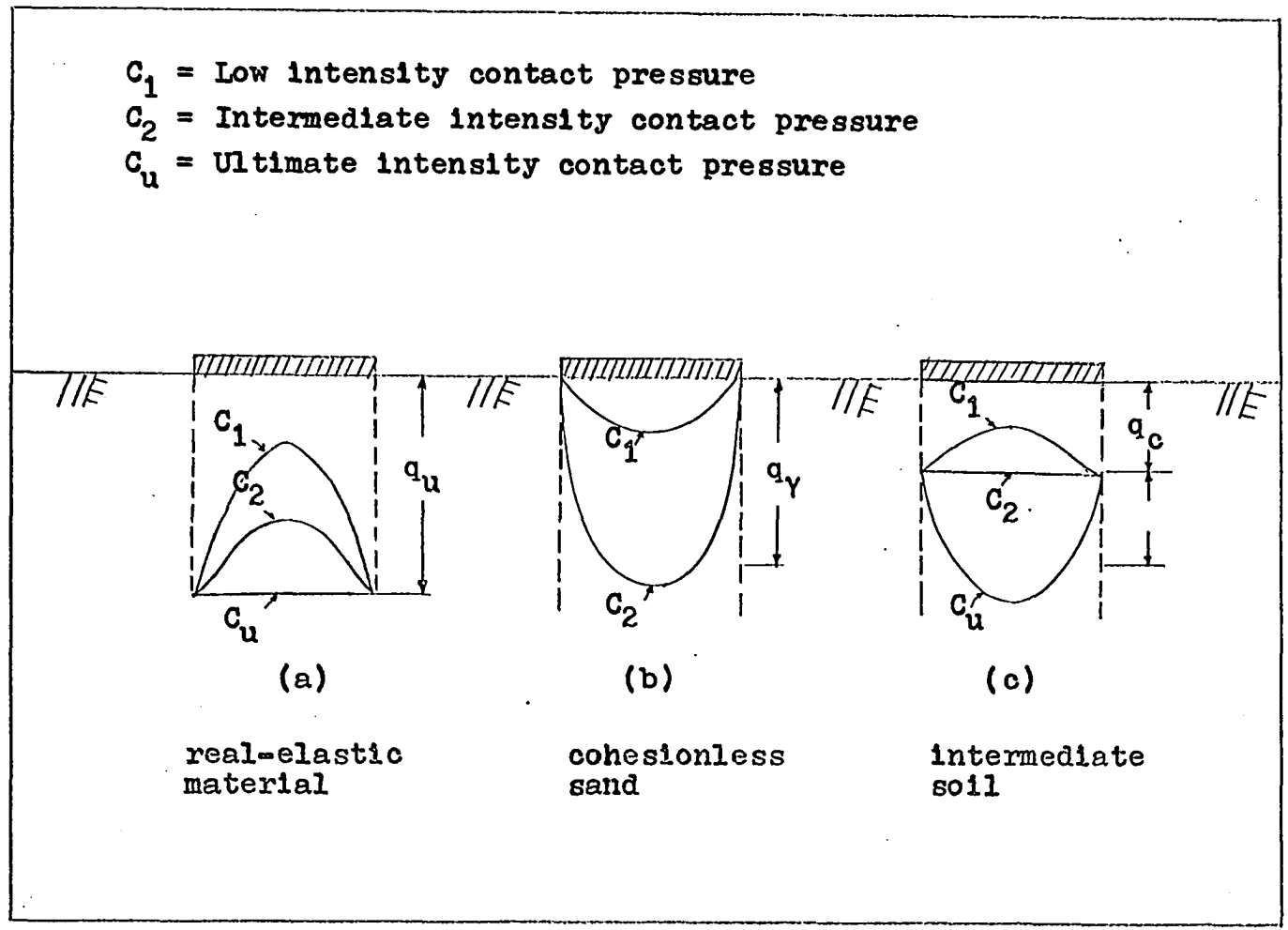

Figure 20. Contact pressure on the base of rigid, flat foundations

structure). However, model load durations will probably be less than the 1/n ratio, and this shortening of load duration may introduce some distortion.

With sufficient membrane pressure, and plate load intensities of sufficiently low intensity that shear rupture is prevented, consolidation should occur; however, full consolidation in fine-grained soil may take years to accomplish, and a model test duration of 1/n years would be impractical. However, a method of load testing similar to that outlined in ASTM, in which 90% consolidation is reached, may be practical.

One problem in this area is that the permeability of the soil may be different for the different orientations of the model and prototype load applications. The 1/n ratio for duration of loading is therefore not suggested as a prescribed loading time. Rather than specifying a particular duration of load increment application, it was decided that settlement should reach some set minimum rate prior to the next load increment application.

4. Base roughness

Little mention has been made on the effect of roughness of the base of the foundation on the settlement. As previously mentioned, roughness of the base often affects the amount of settlement of a foundation.

Lee (34) has shown that roughness has little effect on the normal stress distribution along the contact face of a

footing resting on an elastic medium. Meyerhof (37) has reported that most prototype foundations have a perfectly rough base, that is, the full shearing strength of the soil directly beneath the foundation is mobilized.

In the model system, the model foundation plates contact the rubber membrane; therefore the actual interface between soil and foundation is a soil-rubber interface. Furthermore, the rubber is stretched. From field observations it appears that the stretched rubber interface forms a rough surface with the soil, and the assumption that this interface is perfectly rough is reasonable. Under this assumption, the base roughness will be the same in the model and prototype systems, and no distortion should result due to roughness of the bases.

5. Soil stresses in the vicinity of the bore hole

Terzaghi has shown that the distribution of stresses on horizontal sections in the soil surrounding a cylindrical hole are similar to those shown in Figures 21a and 21b. If the soil is in a state of elastic equilibrium, the stress distribution will be similar to that shown in Figure 21a. If the soil is in a state of plastic equilibrium, the stress distribution will be similar to that shown in Figure 21b. Since the shearing stresses on the cylindrical surface are equal to zero, Terzaghi proposed that one could replace the soil which had been located within the hole by a liquid with a unit weight of $K_o\gamma$ without changing the state of stress in the

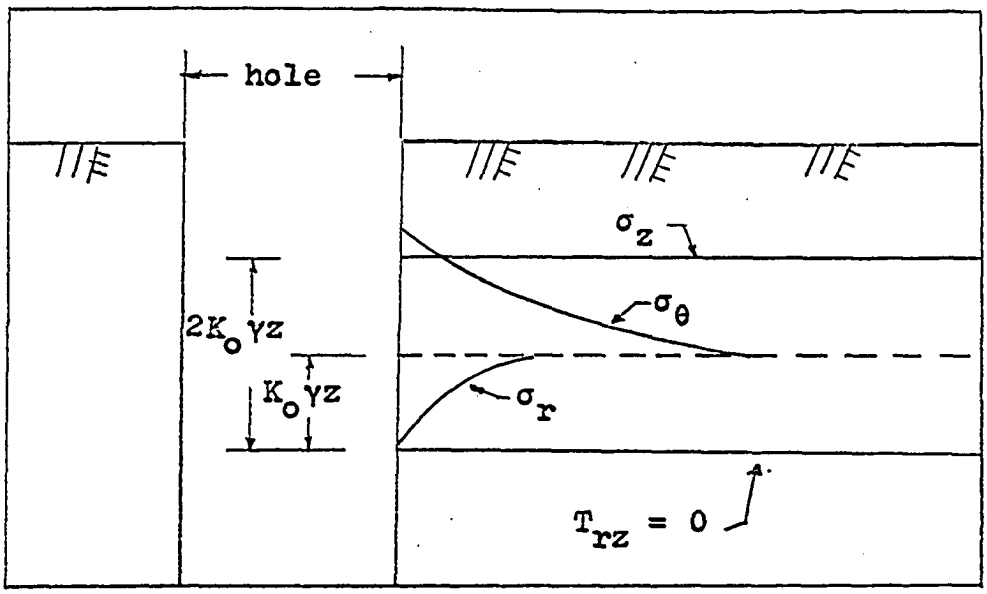

Figure 21a. Stress distribution in the vicinity of a cylindrical hole in perfectly elastic material

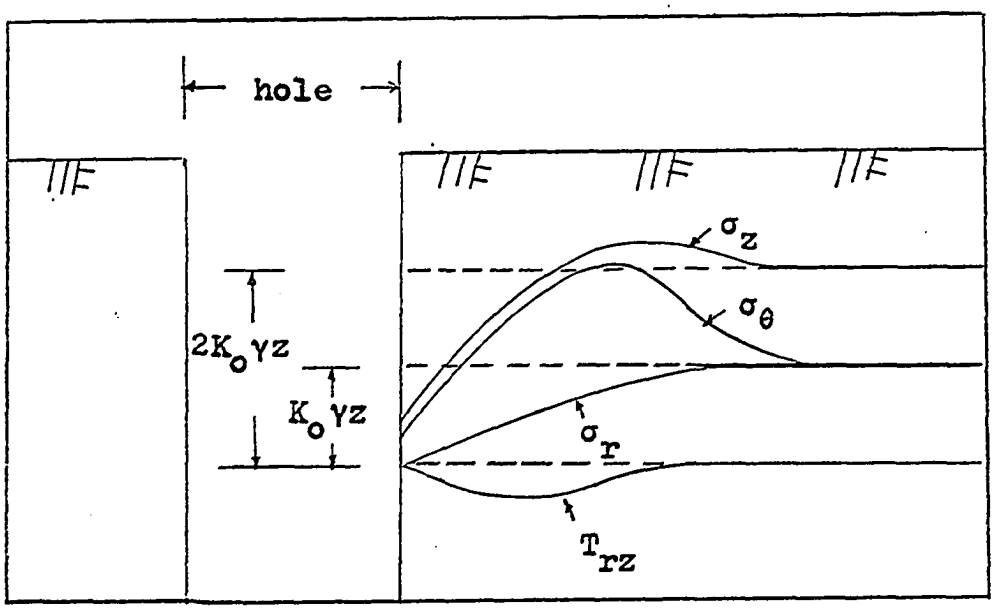

Figure 21b. Stress distribution in the vicinity of a cylindrical hole in plastic material

surrounding soil. σ_z represents the vertical stress, σ_r represents the radial stress, σ_θ represents the tangential stress and T_{rz} represents the shear stress. K_o is the coefficient of earth pressure at rest, z is the depth to the plane being investigated.

There are no universally accepted methods of determining K_o, although the formula $K_o = 1 - \sin \phi$ is commonly used. The stresses acting in the soil surrounding the hole can be resolved into two parts, one due to the weight of the over-lying soil, the other due to the pressure exerted by the liquid. The sum of these stress components will equal the stresses in the soil prior to the hole being bored, as represented in the following equations:

$$\sigma_z = \gamma z$$

$$\sigma_r = K_o \gamma z$$

$$\sigma_\theta = K_o \gamma z$$

$$T_{rz} = 0$$

Thus it appears possible that the stress distribution in the soil surrounding the hole may be restored to its approximate original state by the application of a pressure $= K_o \gamma z$. This could be applied by means of the rubber membrane in the Model Settlement Apparatus. For example, if a soil had a unit weight of 100 pcf and a K_o of 0.75, then at a depth of 20 feet the "stress restoring" pressure would be (.75)(100)(20) = 1500 psf or 10.4 psi.

If this procedure were used, the normal stresses on a soil element would be similar to those shown in Figure 22a.

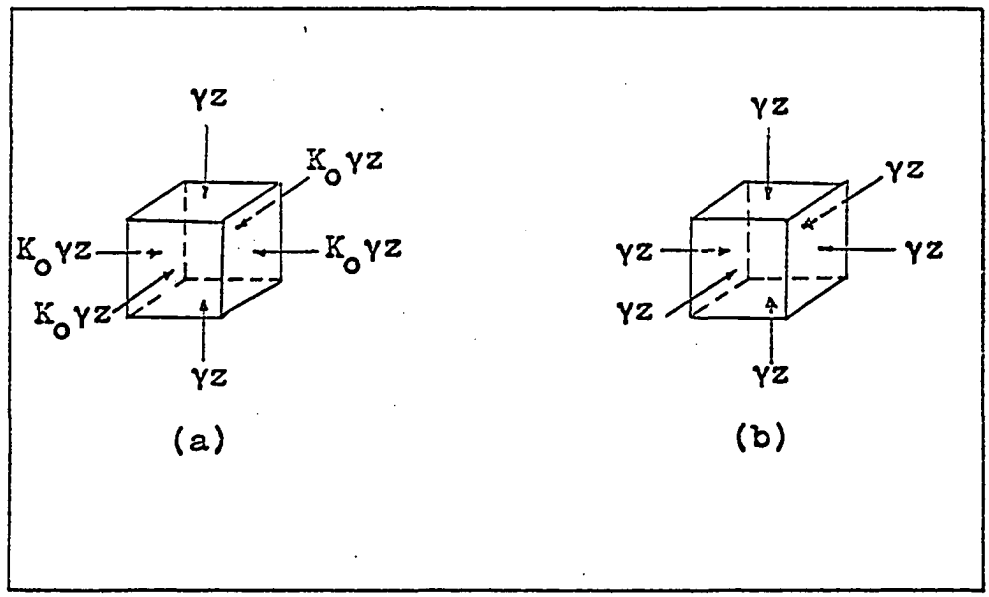

Figure 22. Elements of soil in the vicinity of cylindrical hole, with applied radial pressures of $K_o\gamma z$ and γz

If a surcharge pressure = γz were applied, the normal stresses would be similar to those shown in Figure 22b. The model plate will be directed horizontally, so the question still exists, which procedure will result in a more similar test?

Aboshi (1) reports that when the direction of major principle stress is changed with respect to the plane of deposition, the coefficient of compressibility in a sedimentary soil becomes a little smaller. This implies that for that soil, an effect, although it is a small effect, on compressibility results due to a change in stress orientation. Although it might appear that the situation in Figure 22a is better, since the stresses on the element are the same, and only the direction of load application is different, determination or close approximation of K_o may be difficult. Also if the surcharge pressure method is employed, γz is always greater than $K_o \gamma z$, so the effect of the soil being removed from the hole will be more than compensated by the application of surcharge pressure. Even though the use of the surcharge pressure method may introduce some distortion, the ease of determining γ, and the difficulty of approximating K_o may well result in the adviseability of the surcharge method.

IV. EXPERIMENTAL INVESTIGATION

A. Objectives

The objectives of the experimental investigation were:

1) To conduct a series of tests in 3 different general soil types; sand, clay, and silt (loess), employing the Model Settlement Apparatus.

2) To employ the gravitational pressure concept in testing and to analyze the results in light of the similitude analysis.

3) To conduct test series in which no gravitational pressure was applied and compare these results with those in which gravitational pressure had been applied.

4) To employ distorted model theory with the results of both the gravitational pressure tests and the tests with no gravitational pressure.

5) To test a prototype foundation by forcing a rectangular plate (with length and width dimensions of the same ratio as the model foundation plates) into the soil.

6) To employ the results of the similitude analysis to predict the amount of settlement of the prototype plate, and determine the amount of error in the prediction.

B. Procedures

Holes were drilled in the soil by means of hand augers. The holes were enlarged and smoothed by means of a hand-op-

erated reamer, or cutting tool. This reamer consisted of a cylindrical pipe with an outside diameter of 6.5 inches, and the lower edge sharpened.

The apparatus was then lowered into the hole to the desired test depth by means of a wire cable fastened to a wrist pin of the apparatus. The cable was then fastened to a quick-release clamp supported on a tripod. The apparatus was thereby allowed to hang suspended prior to the application of the air pressure in the membrane. Steps two and three of the test sequence were then performed. The air pressure was applied within the membrane, forcing the membrane against the sides of the bore hole, with a pressure equal to the sum of the desired surcharge pressure and the sgp. Hydraulic pressure was then applied to one set of model plates, forcing the plates against the rubber membrane. This plate load, transmitted through the membrane to the soil, caused the soil to compress. The plate load was maintained at a constant level until the rate of compression (settlement) was less than 0.002 inches per minute. Strain gage readings were then taken and recorded, and the next plate load increment was applied.

Care was taken to apply identical initial load pressures with the two plate sets. Additional load increments were also applied equally, so that the load restriction that R/b^2 be the same in the model and prototype was followed.

Soil density measurements were made in field locations so that the unit weight of the soil being tested was known.

This unit weight was necessary for calculation of the gravitational pressure, as previously discussed.

C. Description of Soils

The sand tests were conducted in a fine sand classified as Thurman loamy fine sand by the Story County Soil Survey Report (35). This sand was chosen because of its uniform nature, its very low cohesion, and the large amount of information that had previously been obtained from it. Soil identification tests performed on this soil were: moisture content, liquid limit, plastic limit, grain size analysis. Results of these tests are shown in Table 2. In addition to the identification tests, laboratory direct shear and triaxial shear tests and field bore hole direct shear tests were conducted in the soil (17). Density tests were also made. Results are shown in Table 3.

The loess soil tests were performed in a cut of Wisconsin age loess, a wind-deposited silt known for its ability to stand in steep faces. Soil identification tests performed on the loess are shown in Table 2. Field density measurements were taken. Field bore hole direct shear tests and laboratory triaxial and direct shear tests had previously been performed in the loess, and results of these tests are shown in Table 3 (18).

The clay soil tests were performed in alluvial clay located within the Missouri River floodplain. Field density

Table 2. Soil property data

Soil Type	Dune Sand[a]	Loess[b]	Clay[c]
Classification			
AASHO-ASTM	A-2-4 (0)	A-4 (8)	A-7-6 (20)
Unified	SM	ML	CH
Plasticity			
Liquid Limit, %	16.2	30	88.8
Plasticity Index	NP	5	58.7
Size Gradation, %			
Gravel (2mm)	0.0	0.0	0.0
Sand (2-.074mm)	87.9	1	0.6
Silt (.074-.002mm)	7.2	84	19.0
Clay (.002mm)	4.9	15	80.4
Dry Density, pcf	99.0	83.3	93.2
Moisture Content, %	4-8	17	33

[a]Field location - N.W. 1/4 Sec. 20, T83N, R23W, Story County, Iowa. Test depth from 12 inches to 30 inches.

[b]Field location - N.W. 1/4 Sec. 3, T77N, R44W, Harrison County, Iowa. Test depth from 14 inches to 20 inches.

[c]Field location - N.W. 1/4 Sec. 8, T78N, R44W, Harrison County, Iowa. Test depth from 14 inches to 20 inches.

measurements were made, laboratory unconfined compressive strength tests and direct shear tests were performed on remolded samples (molded to standard proctor density) obtained from the same area. Results of these and other laboratory tests are shown in Tables 2 and 3.

Table 3. Soil shear parameters

Soil	ø, °			C, psi		
	Bore Hole[a]	Direct shear[b]	Triaxial[c]	Bore Hole[a]	Direct shear[b]	Triaxial[c]
Sand	36.9 .5	36.5 .3	35.8	0.4 .3	0.3 .3	(0.3)[d]
Loess	24.0-29.5	24.1-24.7	28.9	0.7-4.3	0.2-1.8	2.4
Clay	-	4.5	-	-	15.0	15.5[e]

[a]Ref: Olson.

[b]Ref: Akiyama.

[c]Ref: Handy and Fox.

[d]Assumed value, only one test performed.

[e]From unconfined compressive strength tests.

V. PRESENTATION OF DATA

Load-settlement results of the model tests in sand are shown in Figures 23 through 33. L designates large plate tests, S refers to small plate tests. The prototype settlement test with a 15 inch by 20 inch plate is shown in Figure 34.

Results of the model settlement tests in loess are shown in Figures 35 through 43. L and S again refer to the large model plate set and the small model plate set respectively. The prototype settlement test is shown in Figure 44.

Results of the model settlement tests in clay are shown in Figures 45 through 49. The prototype test is shown in Figure 50.

The amount of settlement shown in the graphs was obtained by dividing the amount of settlement of both opposite plates by 2.

Time-settlement information from the sand and loess tests was not obtained. As previously explained, the time of duration of load application in these tests was determined by the rate of settlement and not by an arbitrary or predetermined duration. Time-settlement data were obtained from the clay tests. Settlements were recorded immediately following load application and at intervals following load application. The tests were not conducted to 90% consolidation due to equipment limitations, in which the air membrane pressure could not be

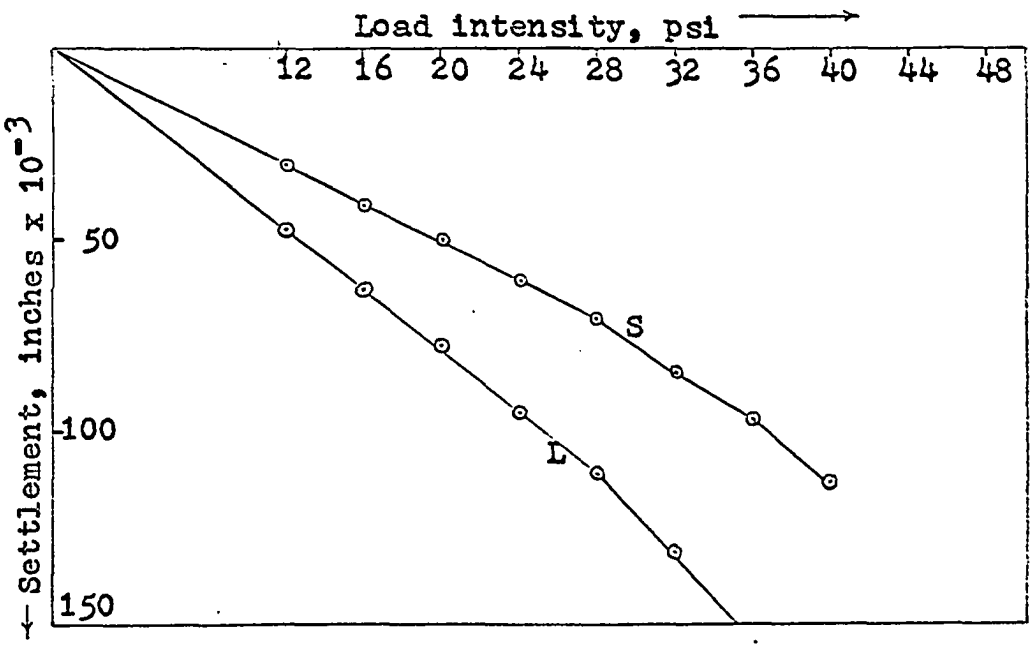

Figure 23. Field tests 1 and 2, sand

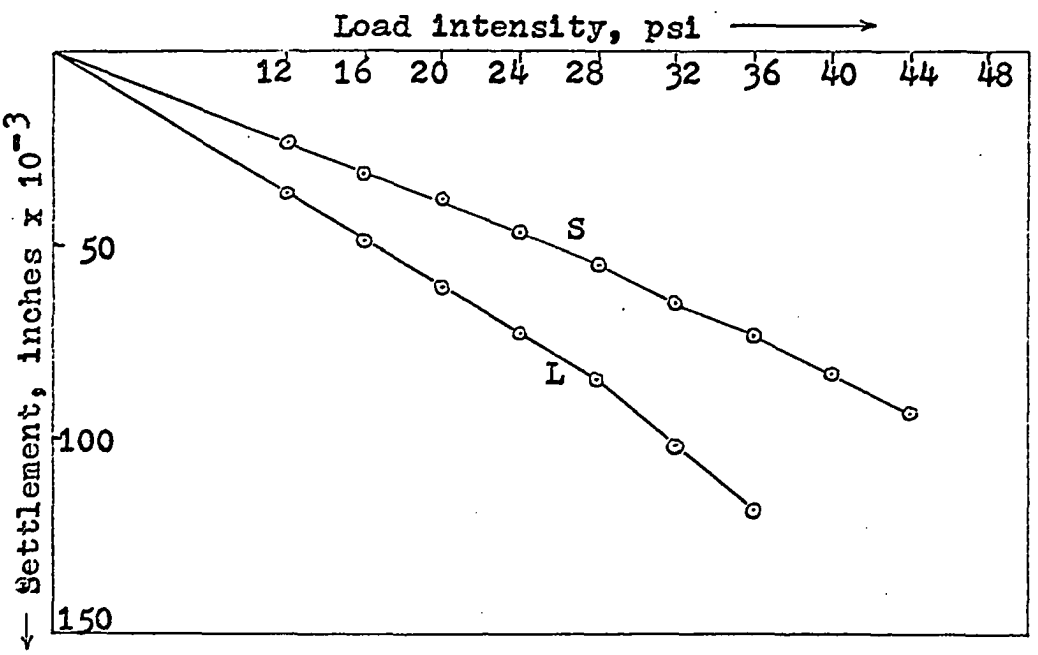

Figure 24. Field tests 3 and 4, sand

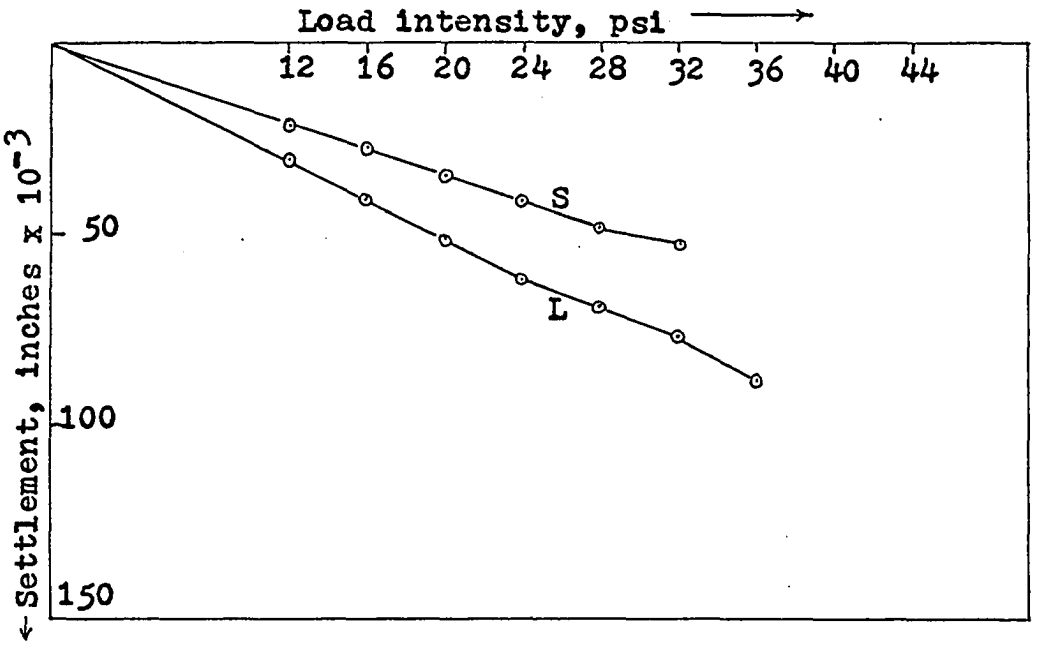

Figure 25. Field tests 5 and 6, sand

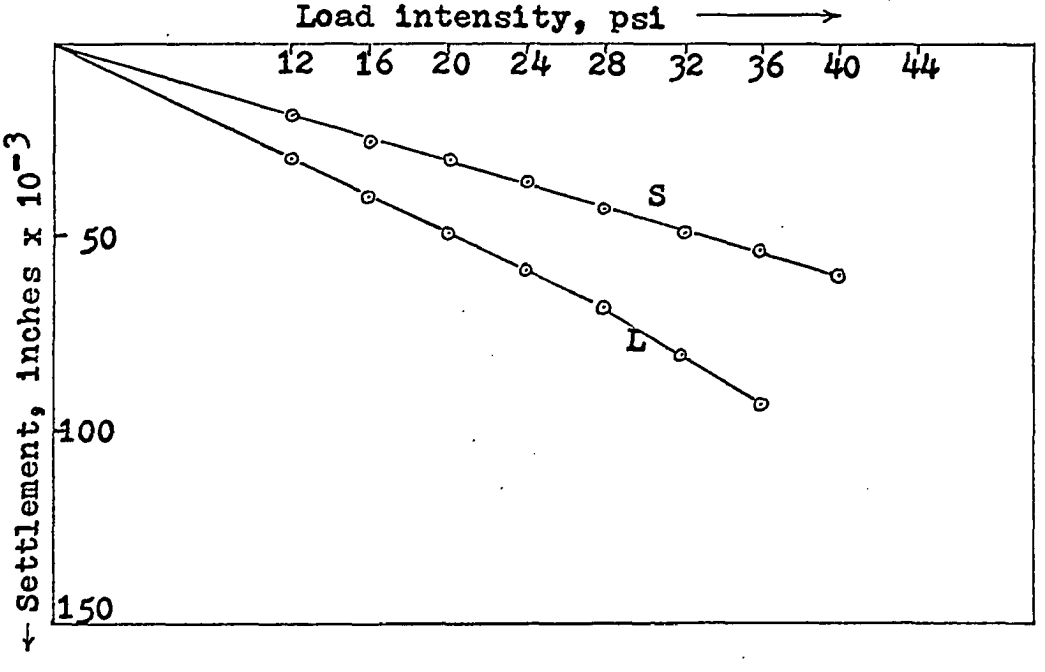

Figure 26. Field tests 7 and 8, sand

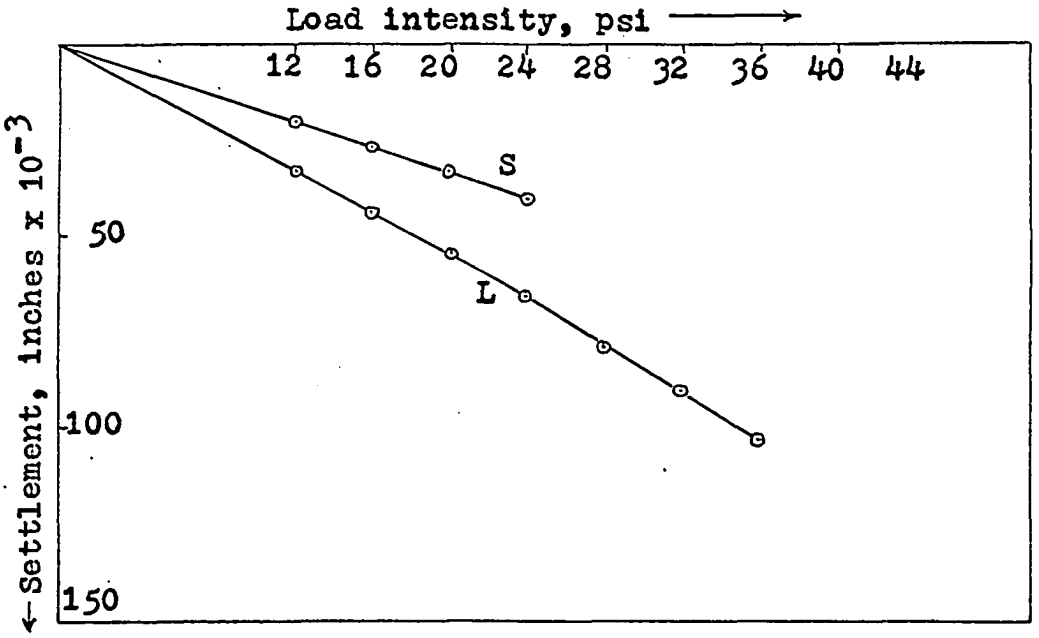

Figure 27. Field tests 9 and 10, sand

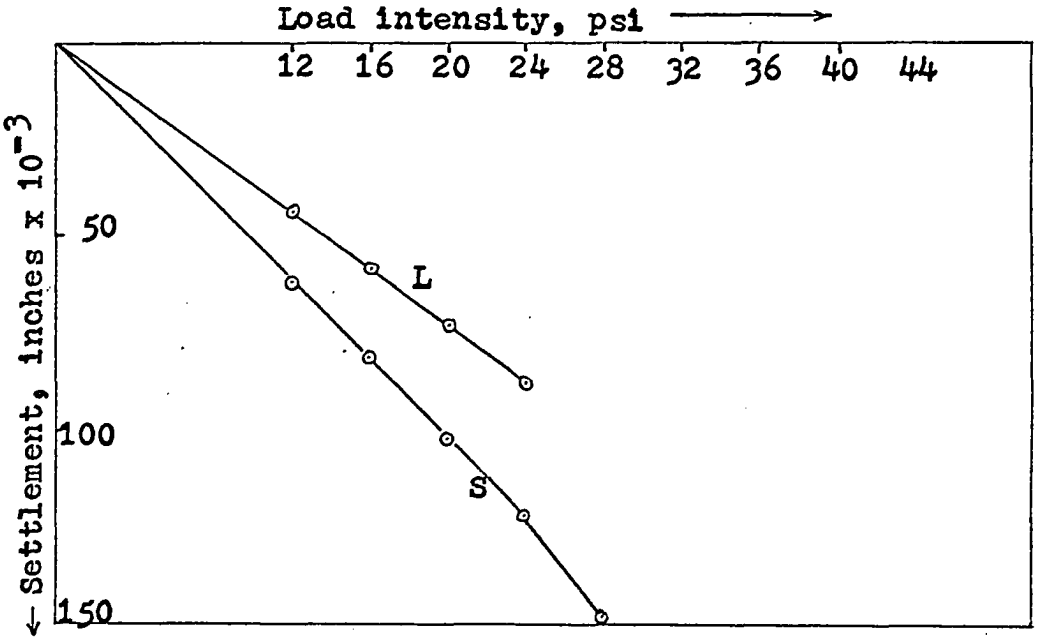

Figure 28. Field tests 11 and 12, sand

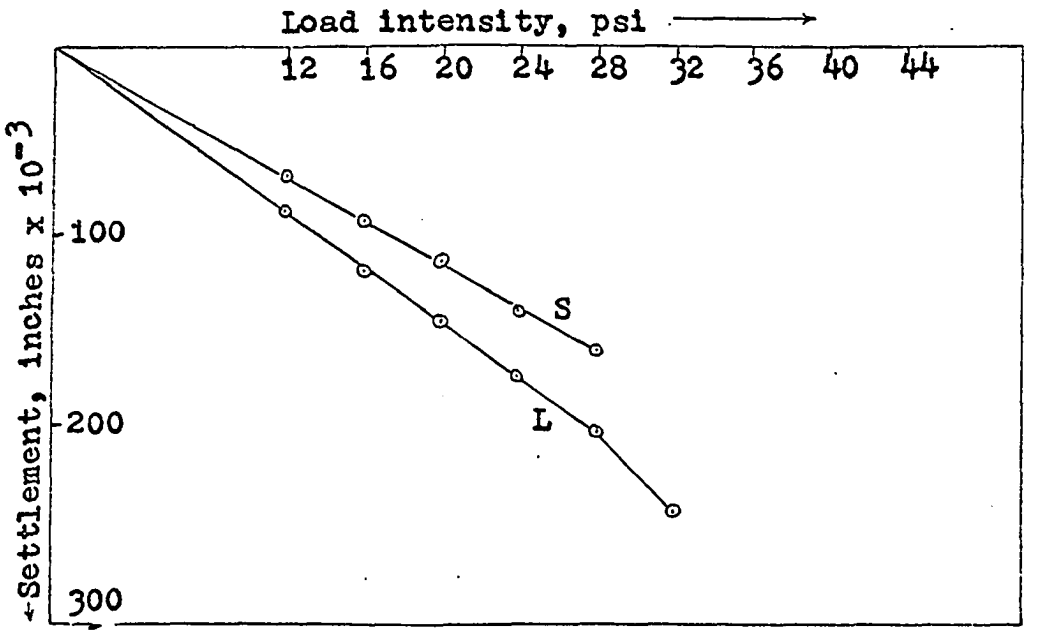

Figure 29. Field tests 13 and 14, sand

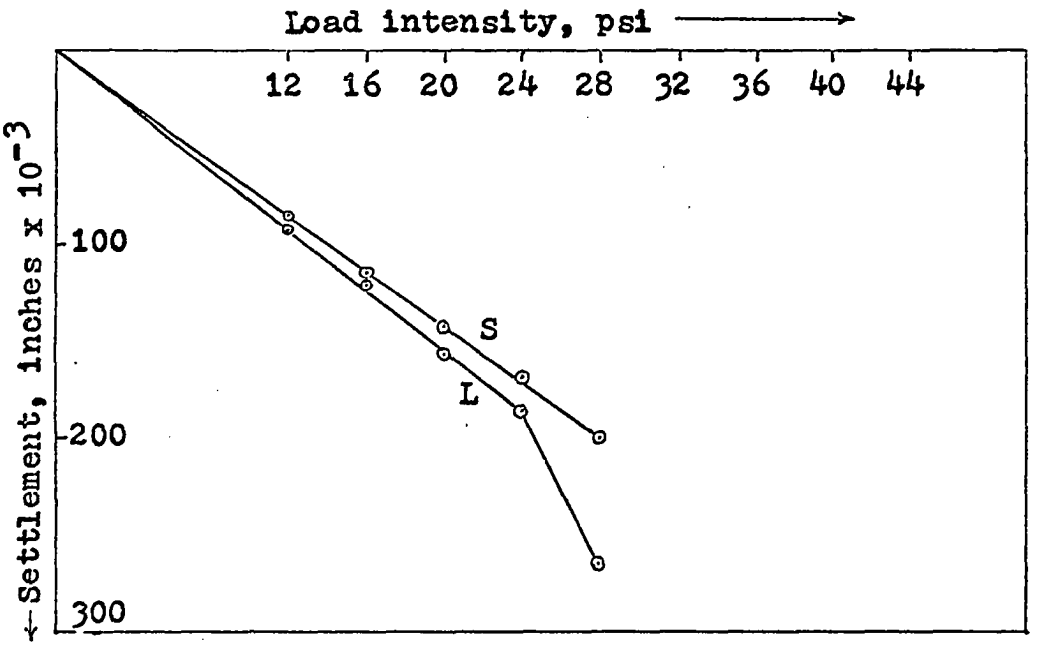

Figure 30. Field tests 15 and 16, sand

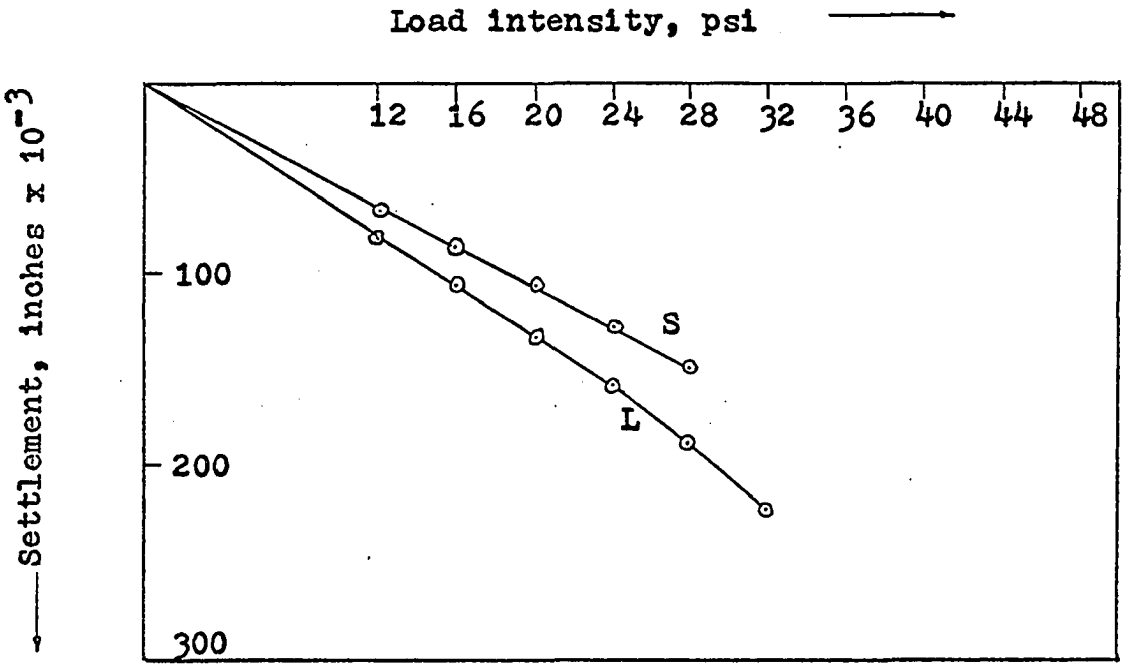

Figure 31. Field tests 17 and 18, sand

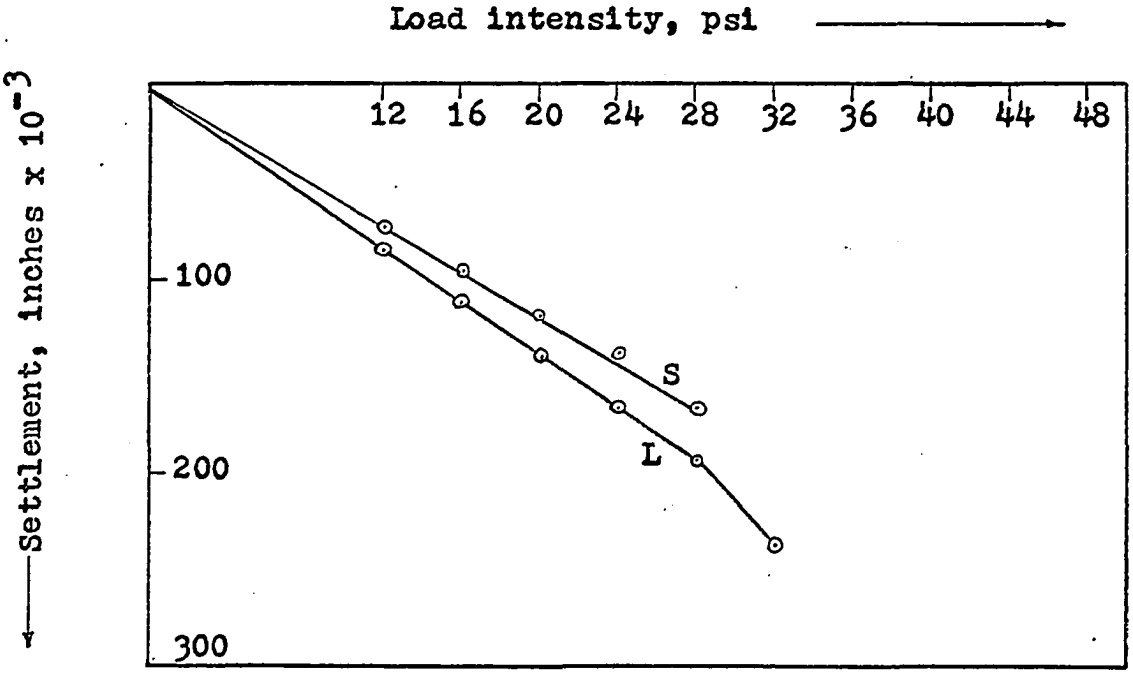

Figure 32. Field tests 19 and 20, sand

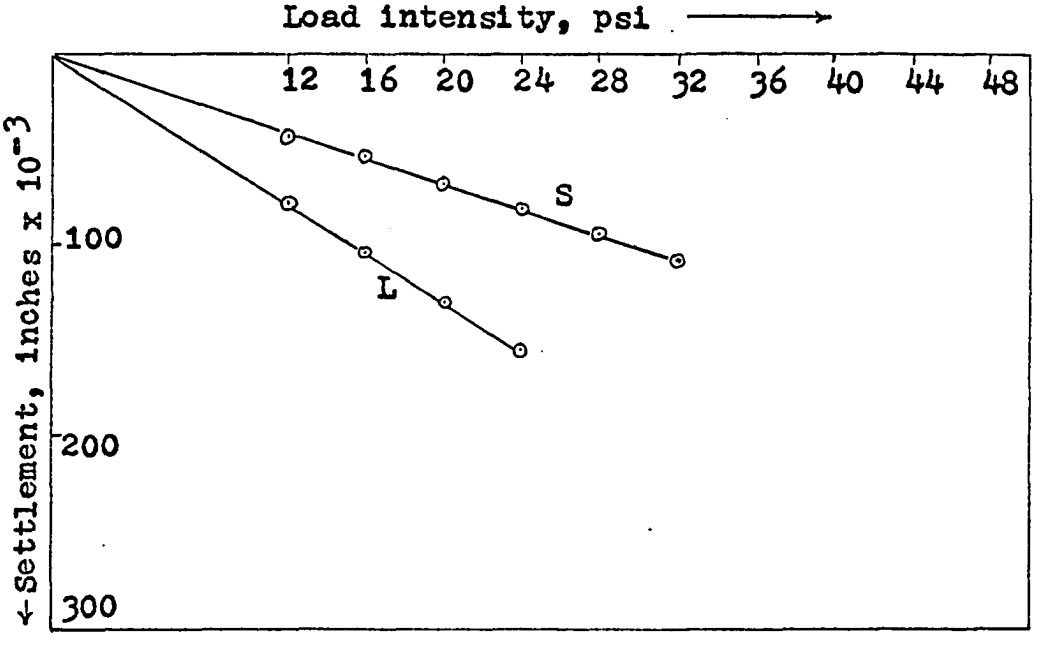

Figure 33. Field tests 21 and 22, sand

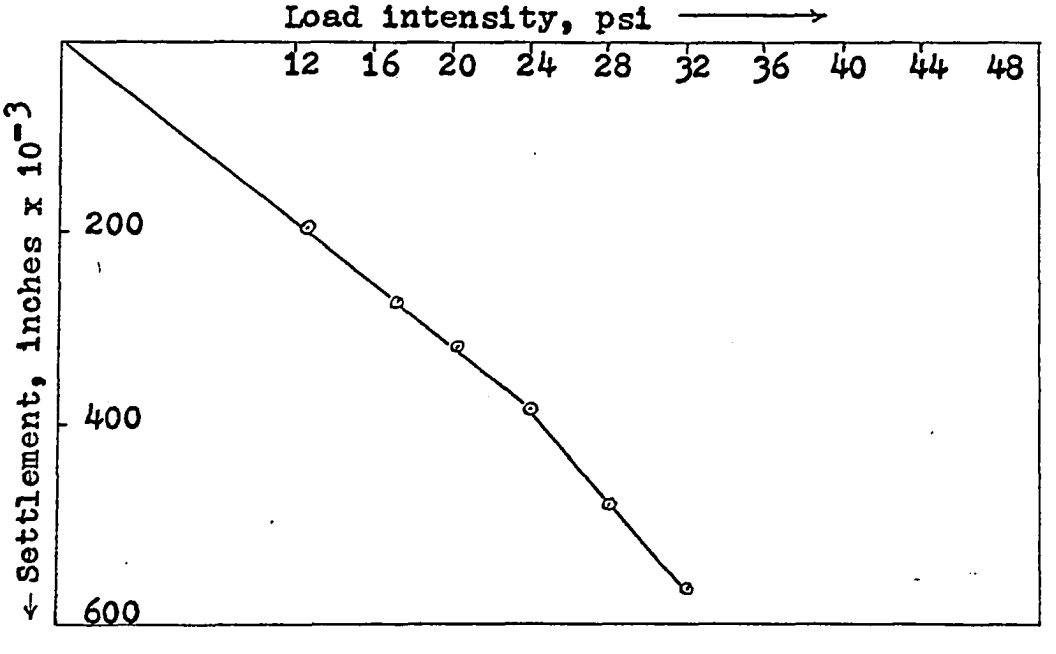

Figure 34. Prototype test, sand

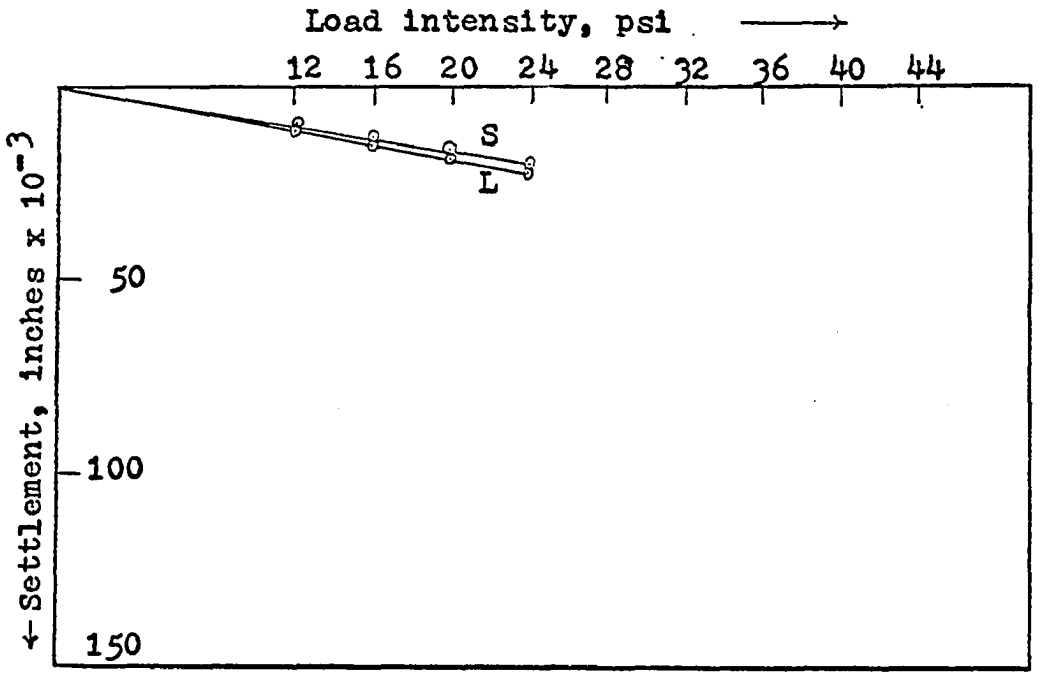

Figure 35. Field tests 23 and 24, loess

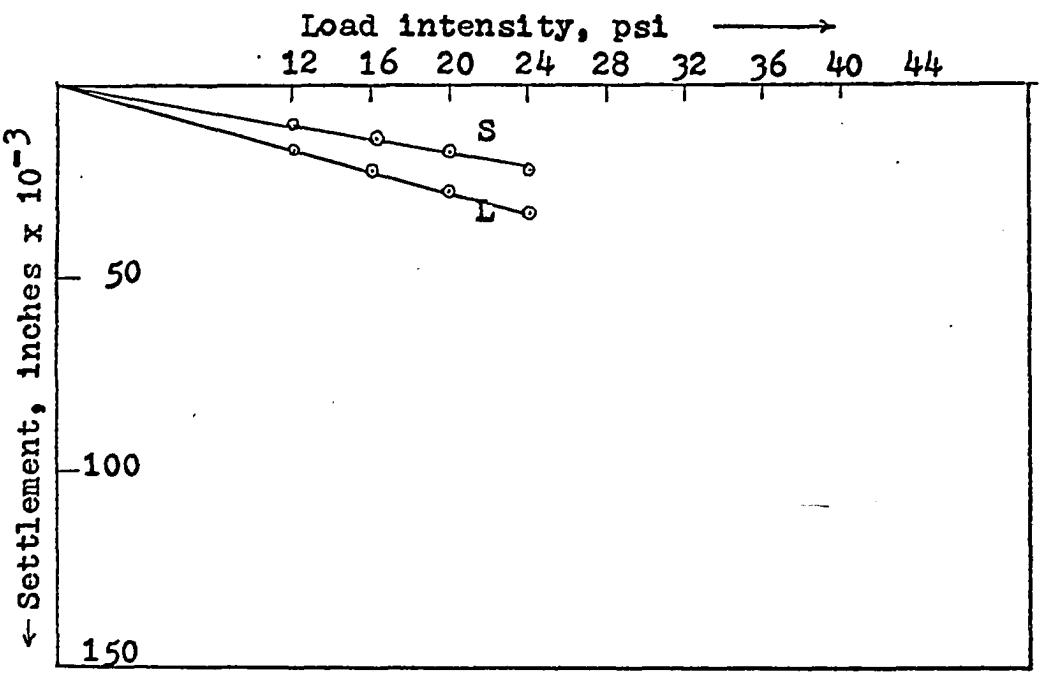

Figure 36. Field tests 25 and 26, loess

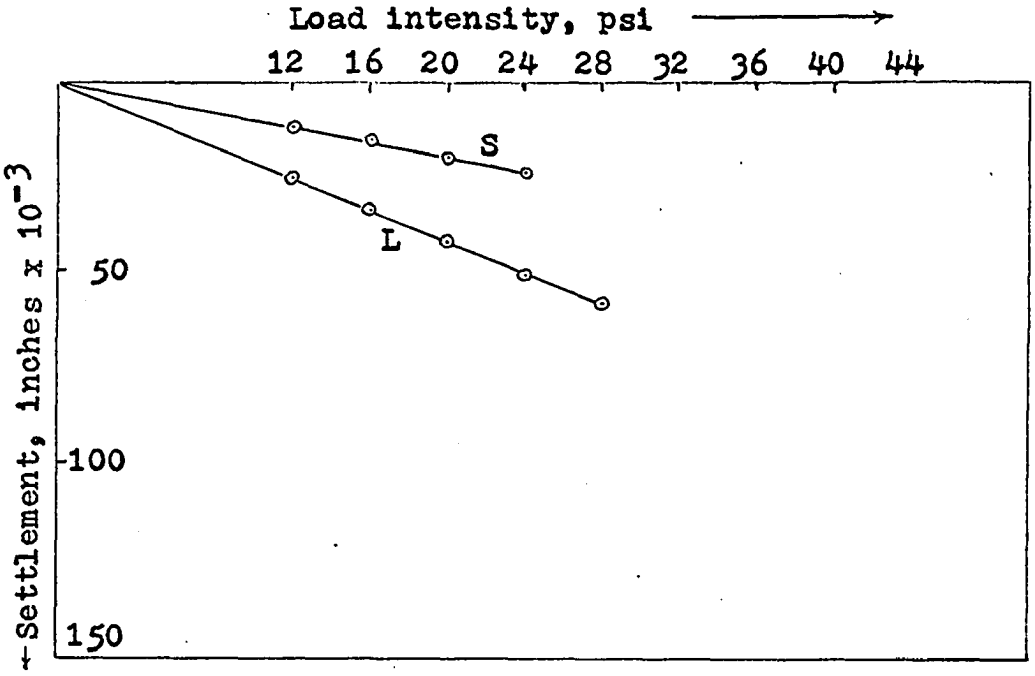

Figure 37. Field tests 27 and 28, loess

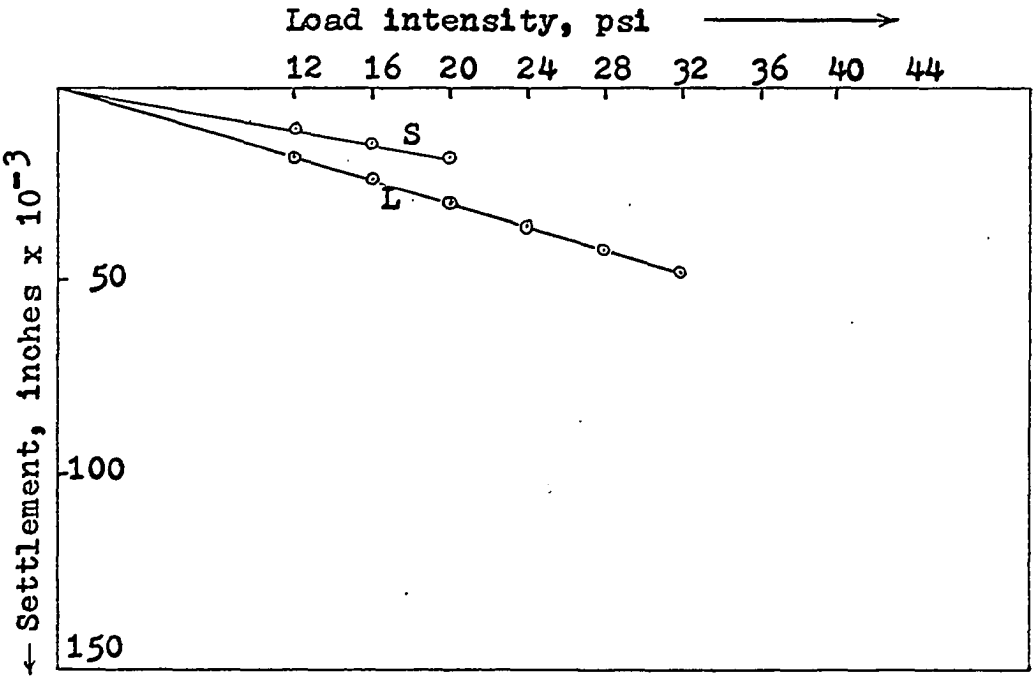

Figure 38. Field tests 29 and 30, loess

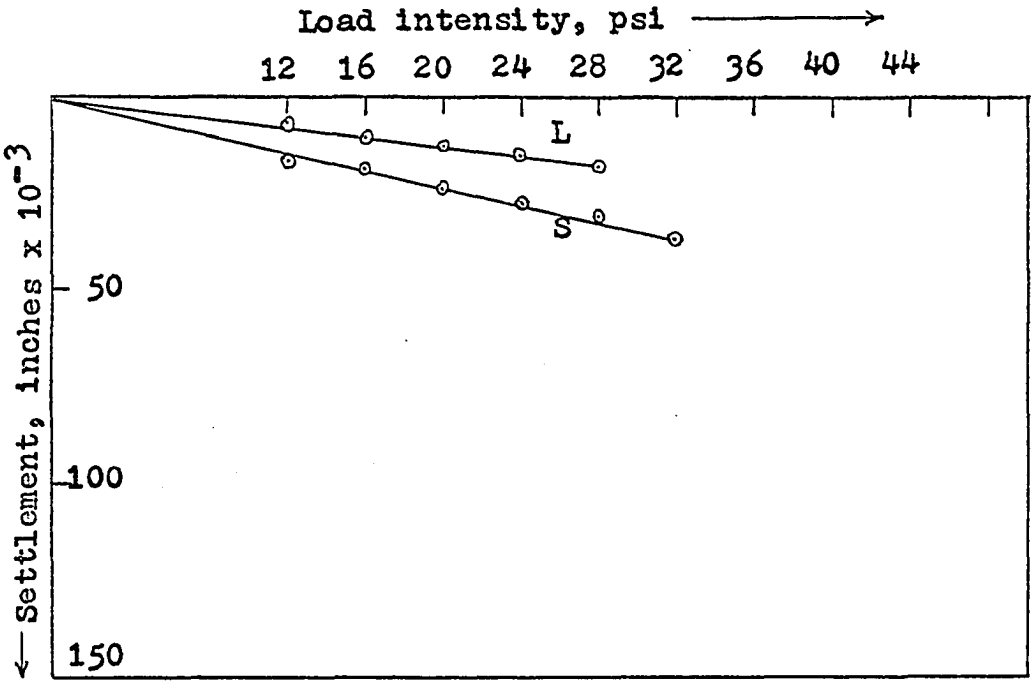

Figure 39. Field tests 31 and 32, loess

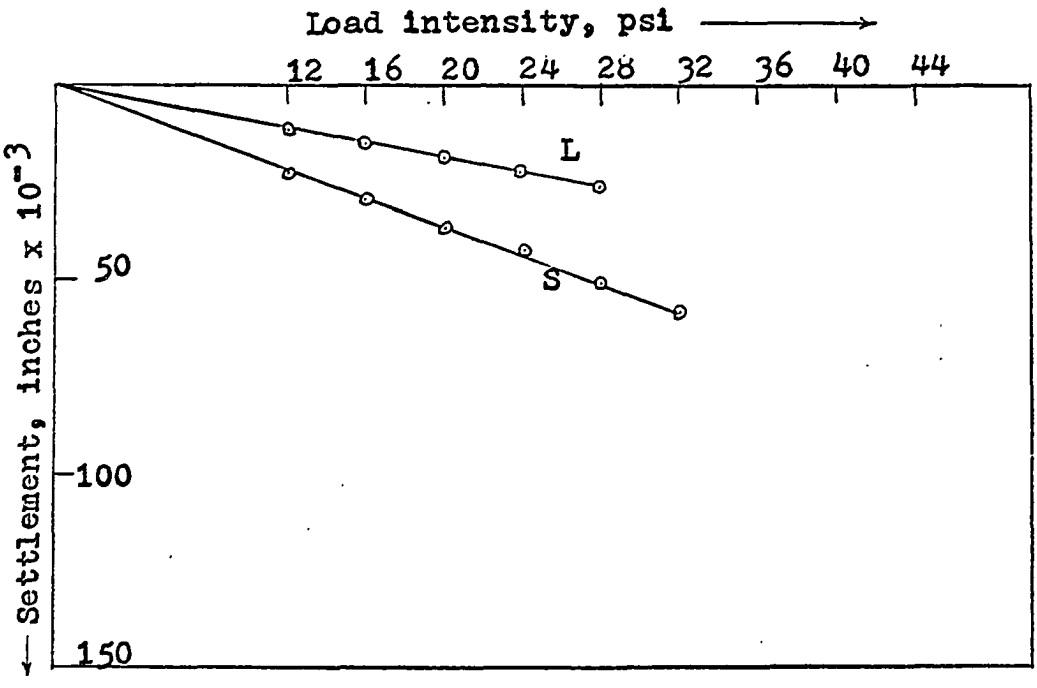

Figure 40. Field tests 33 and 34, loess

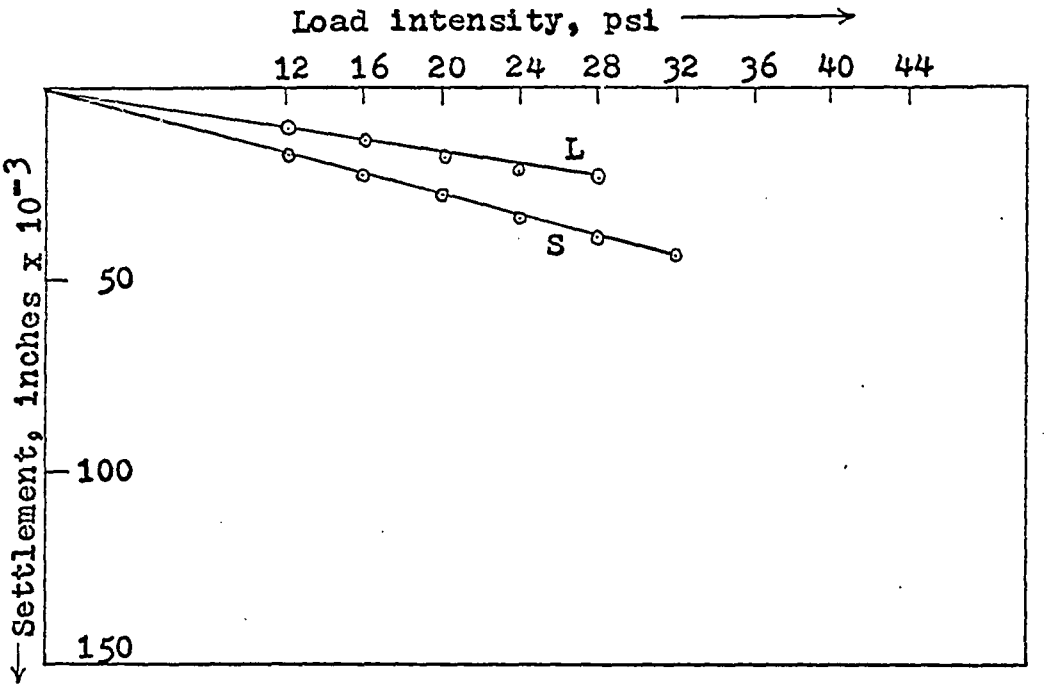

Figure 41. Field tests 35 and 36, loess

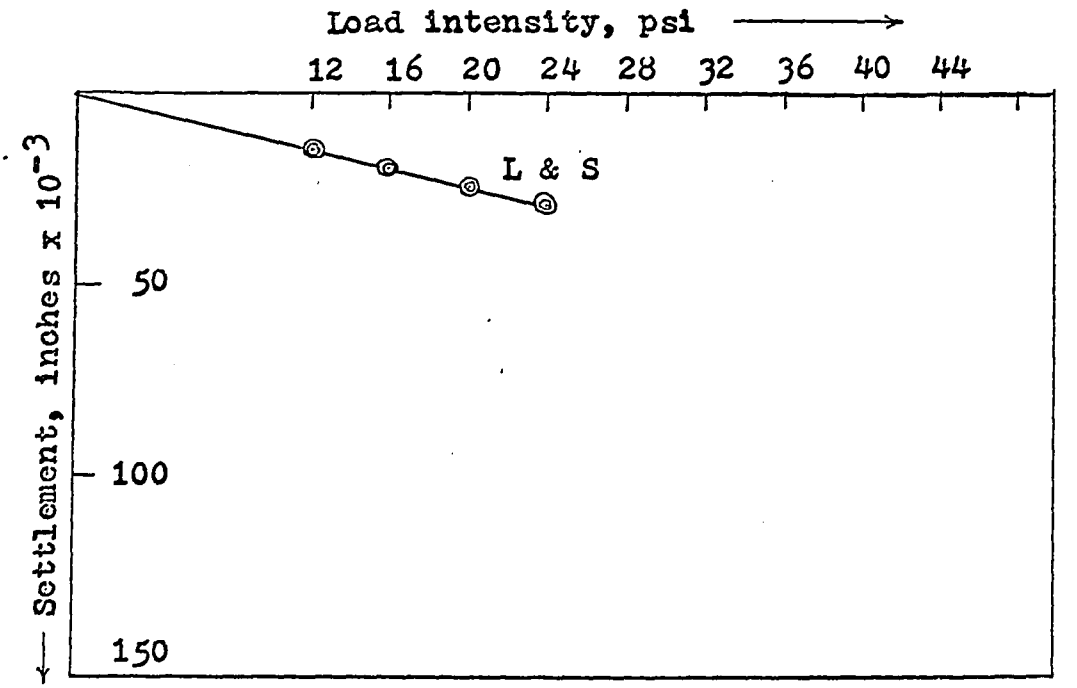

Figure 42. Field tests 37 and 38, loess

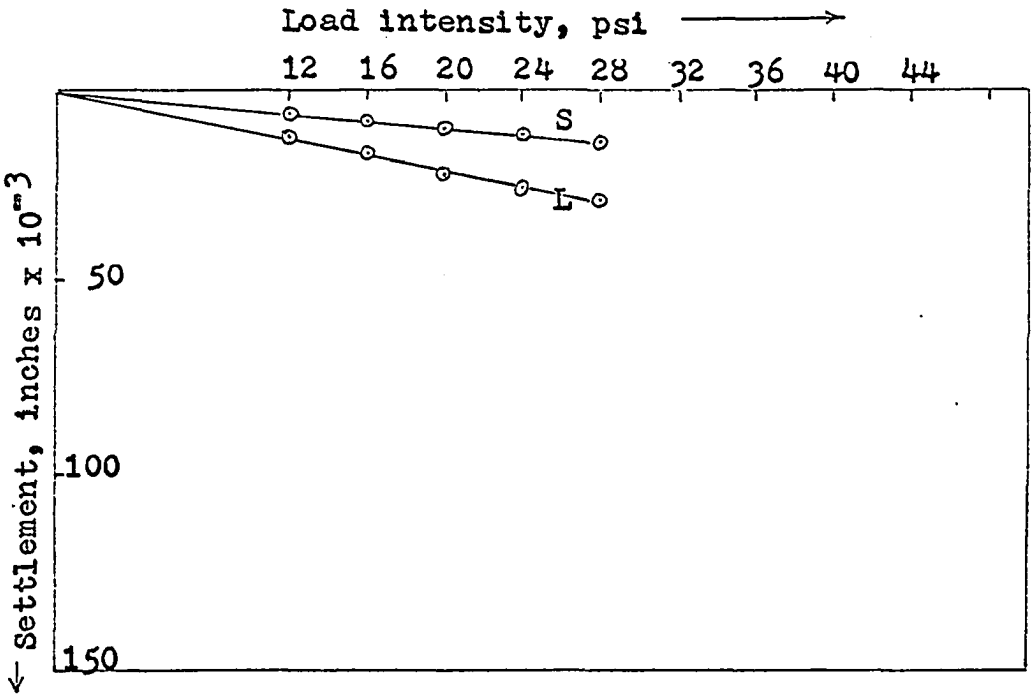

Figure 43. Field tests 39 and 40, loess

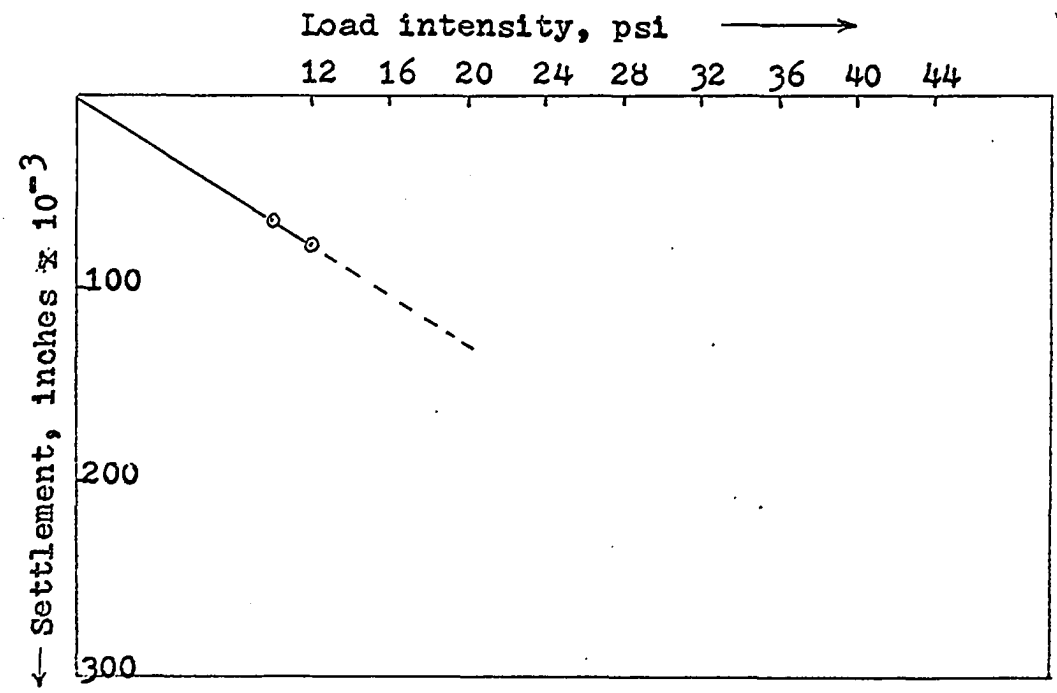

Figure 44. Prototype test, loess

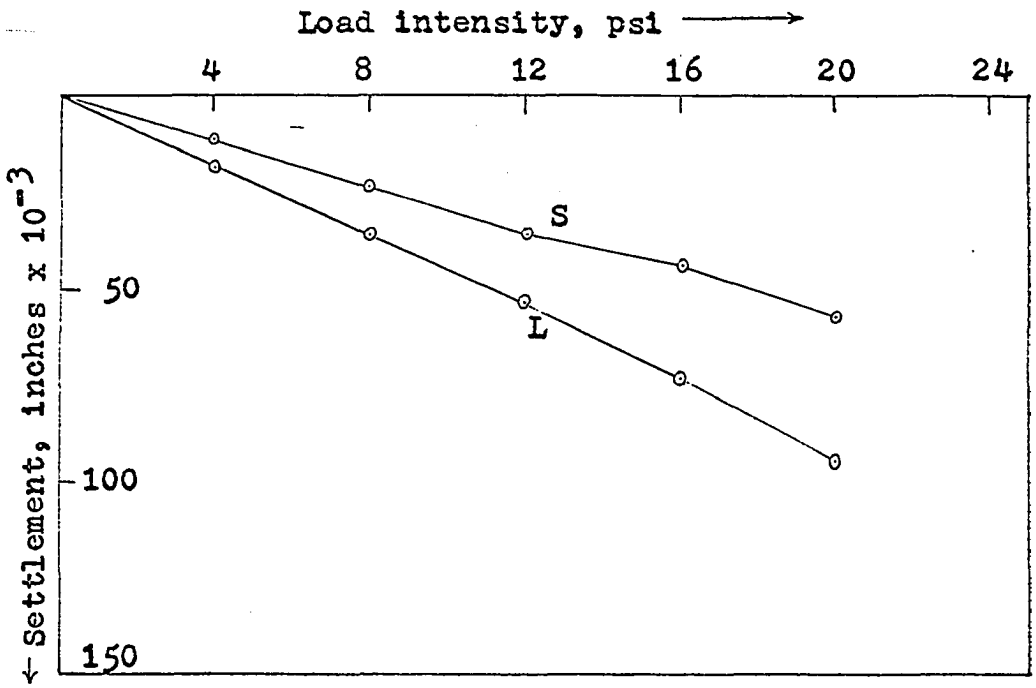

Figure 45. Field tests 41 and 42, clay

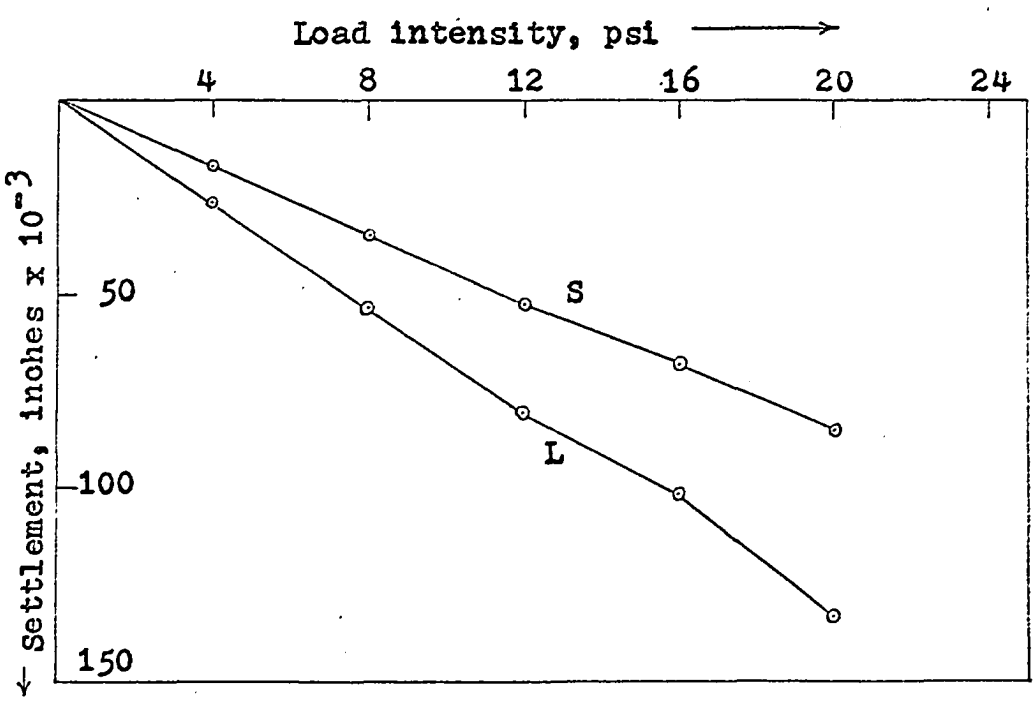

Figure 46. Field tests 43 and 44, clay

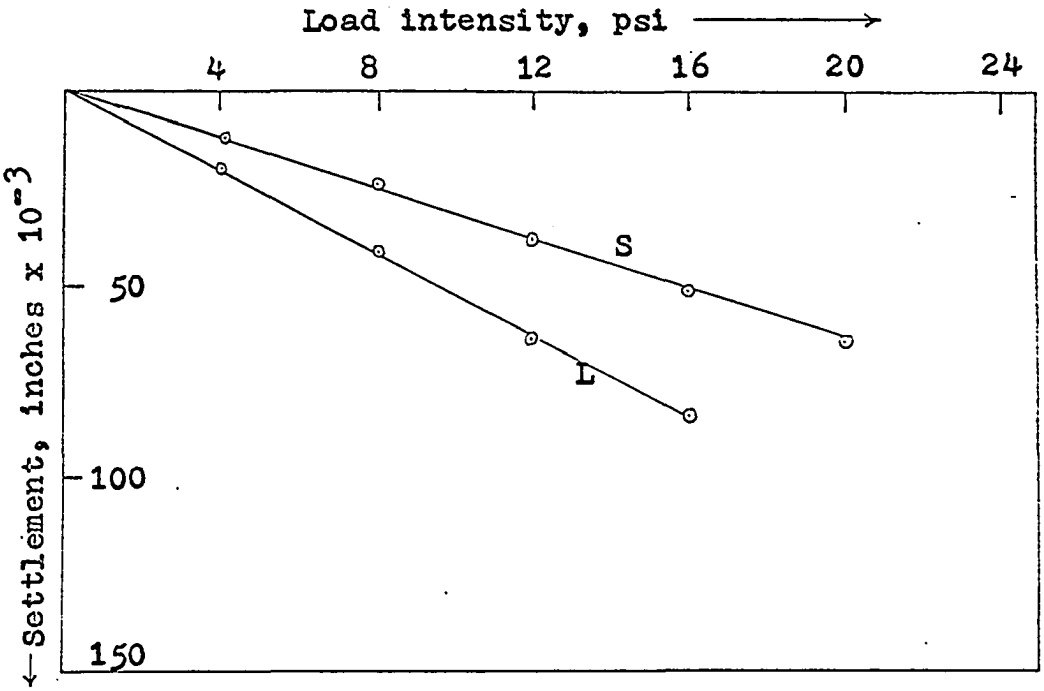

Figure 47. Field tests 45 and 46, clay

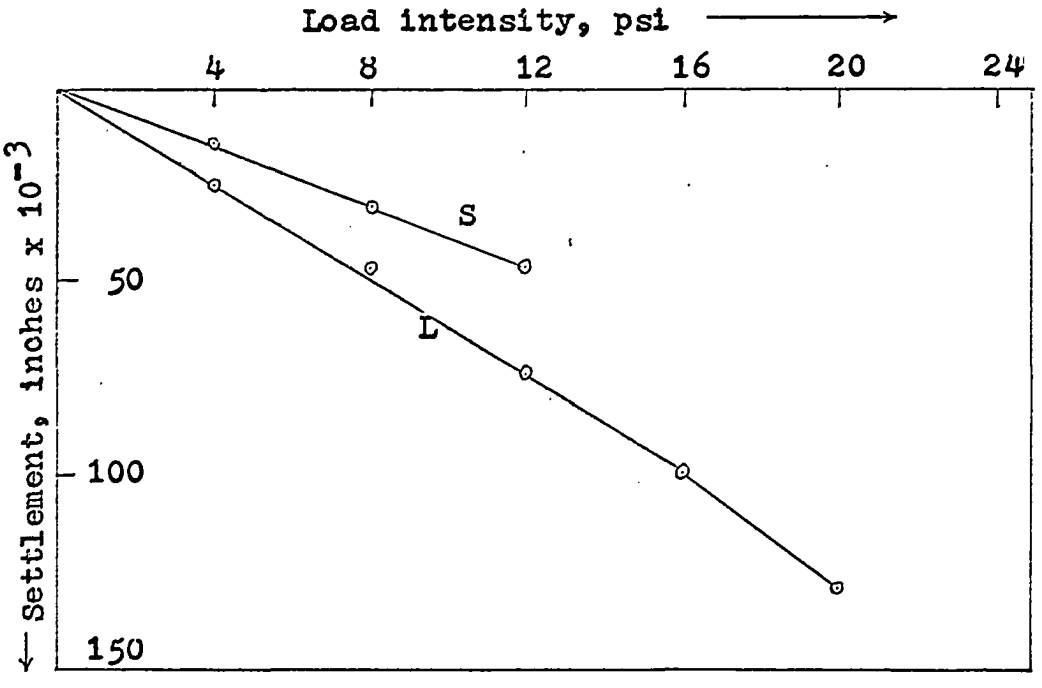

Figure 48. Field tests 47 and 48, clay

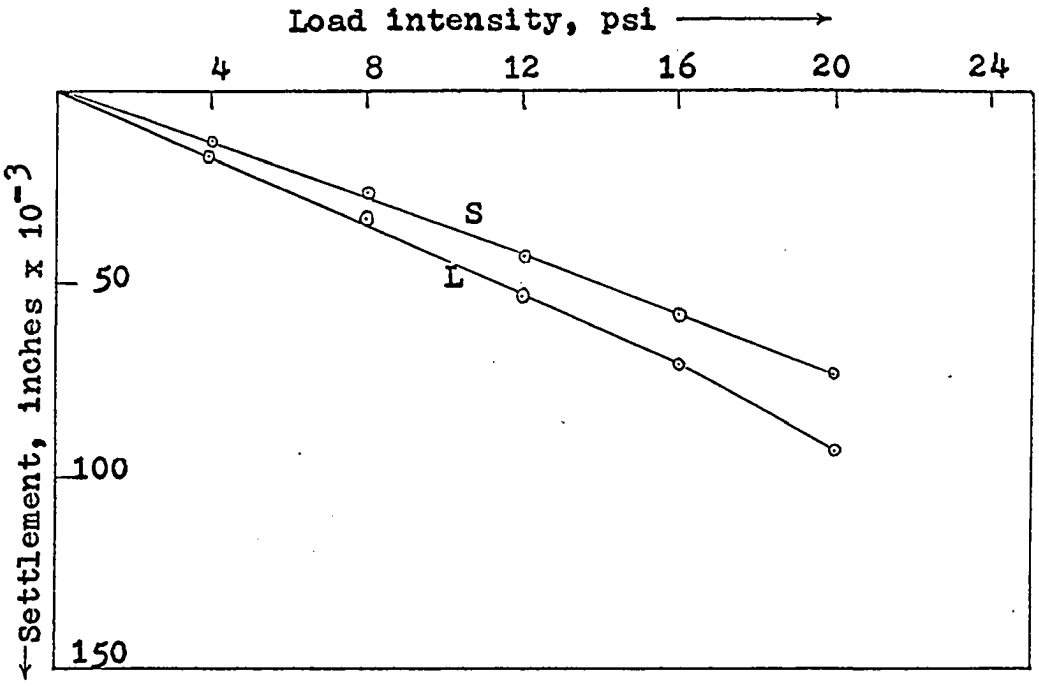

Figure 49. Field tests 49 and 50, clay

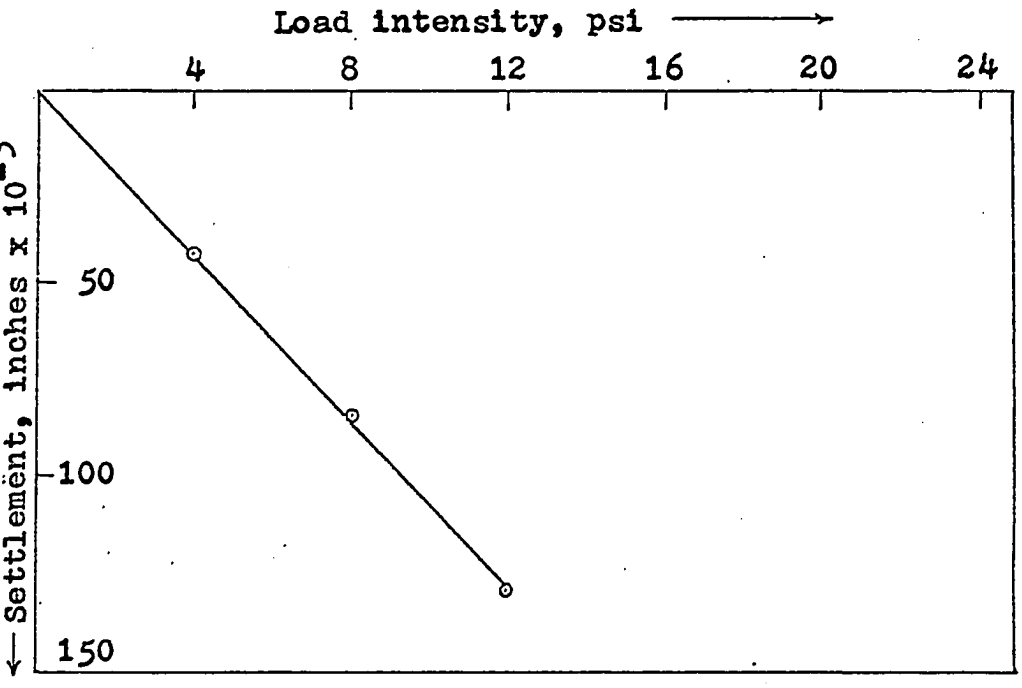

Figure 50. Prototype test, clay

maintained for the time duration required. Time-settlement data are shown in Table 7. This table shows only the absolute magnitude of settlements at two time intervals following the initial settlement reading. For example, a value of 4.4 corresponding to an interval of 0.71 minutes means that the model plate settled 4.4 thousands of an inch during that time. The amount of immediate settlement is not included in Table 7.

VI. DISCUSSION OF RESULTS AND PRACTICAL APPLICATIONS

A. Analysis of Experimental Results

1. Sand

The field tests in sand show a very fine straight line load-settlement curve until at least 28 psi for all tests, with and without gravitational air pressure. The curves generally began to show an decrease in slope between 28 and 32 psi. The absolute values of settlement corresponding to a load of 20 psi are shown for the various tests in Table 4. Also included in this table is a ratio of settlement of the larger (3 inch by 4 inch) model plate divided by the settlement of the smaller (2 inch by 2.67 inch) model plate, again at a load of 20 psi. Since in all tests the load-settlement will be the same for any corresponding points of equal load on the curves.

Tests 1 through 12 were conducted with membrane pressure. The membrane pressure employed was the sum of three component air pressures. The first component was the constant opening air pressure required to inflate the membrane against the sides of the hole. The second component was the surcharge pressure corresponding to γz, where z is the depth from the surface to the plane of the bottom of the prototype footing. This method of approximating surcharge pressure has often been used by Terzaghi (56), and has been used in model load testing by Burmister (11) and others. The surcharge pressure

Table 4. Sand model settlement data

Test	Settlement Ratio	3 Inch Plate Settlement	2 Inch Plate Settlement
1&2	1.56	.0759 inch*	.0507 inch*
3&4	1.55	.0600 inch	.0387 inch
5&6	1.47	.0512 inch	.0350 inch
7&8	1.41	.0495 inch	.0350 inch
9&10	1.62	.0550 inch	.0340 inch
11&12	0.71	.0730 inch*	.1020 inch*
Mean Value	1.53	.0539 inch	.0357 inch
Standard Deviation	0.083	.0047 inch	.0011 inch
13&14	1.28	.144 inch	.112 inch
15&16	1.10	.156 inch	.142 inch
17&18	1.21	.133 inch	.109 inch
19&20	1.17	.140 inch	.120 inch
21&22	1.89*	.130 inch	.069 inch*
Mean Value	1.19	.1406 inch	.1208 inch
Standard Deviation	0.076	.0102 inch	.0148 inch

*Rejected data.

will also be the same for both small and large model footings. The third component of air pressure is the simulated gravitational pressure. The amount of sgp varies with model plate size, and was determined by the equation $\gamma sgp = \frac{\gamma n}{1728}$, where sgp is in psi and γ is in pcf. The prototype was a 15 by 20 inch plate; therefore n was 7.5 for the small model plates and 5.0 for the larger plates.

The rejection criterion used was that any measurement was rejected when the magnitude of its deviation from the mean was such that the probability of the occurrence of all deviations that large or larger was less than 1/2m, where m is the number of measurements taken (39). Two probable causes for incorrect or non-representative readings were instrument error, such as is known to have occurred in several loess tests when the strain gage connector became loose, and soil irregularities, such as crotovinas (holes), stones, roots, and so forth.

As shown in Table 4, one large-to-small-plate settlement ratio out of the six sets of sand tests with membrane pressure was rejected, and the mean of the other five was 1.53. This is very close to the predicted ratio of 1.50, indicating that the test results agree closely with the similitude theory. The error is 2% with a sample standard deviation of only 0.083. The results of tests 1 and 2 which were rejected, had standard deviations of 0.00465 inches for the larger plates and 0.00105 for the smaller.

Tests 13 through 22 were conducted in the same sand area, but without an application of membrane pressure. One settlement ratio was rejected, as shown in Table 4, and the mean settlement ratio was 1.19, rather than the 1.50 which should have resulted if no distortion had existed in the system. The fact that the ratio was less than the 1.50 shows that size effects of the two model plates was less in this soil than

predicted. This fact agrees with the observations of many past model load tests in sand, that size effects are often small, and sometimes negligable (45). More important, it substantiates the similitude analysis conclusion that the soil-foundation system is a distorted system. If it were not, the ratio would have been 1.50.

The standard deviation for the settlement ratios in sand with no membrane pressure was very small, being 0.076. This was somewhat smaller than that of the sand tests with membrane pressure, although the difference may not be significant.

An examination of actual model settlements from tests 13 through 22 illustrate several important trends. First, the settlements without membrane pressure were almost three times those obtained with membrane pressure. This shows the tremendous effect of only several psi (2.83 to 3.35) applied to the soil surface, on the settlement of the plates.

The predictions of the settlement of the 15 by 20 inch prototype were obtained by multiplying the small model plate settlement measurements by 7.5, and the larger model plate settlement measurements by 5.0. Results of these multiplications are shown in Figure 51. The mean prediction for the eight model plate tests was 0.269 inches.

Performance of a plate load test gave a prototype settlement of 0.313 inches indicating the error in prediction was 14.1%. Many factors could have contributed to this error. Probably the two largest sources of error were non-similarity

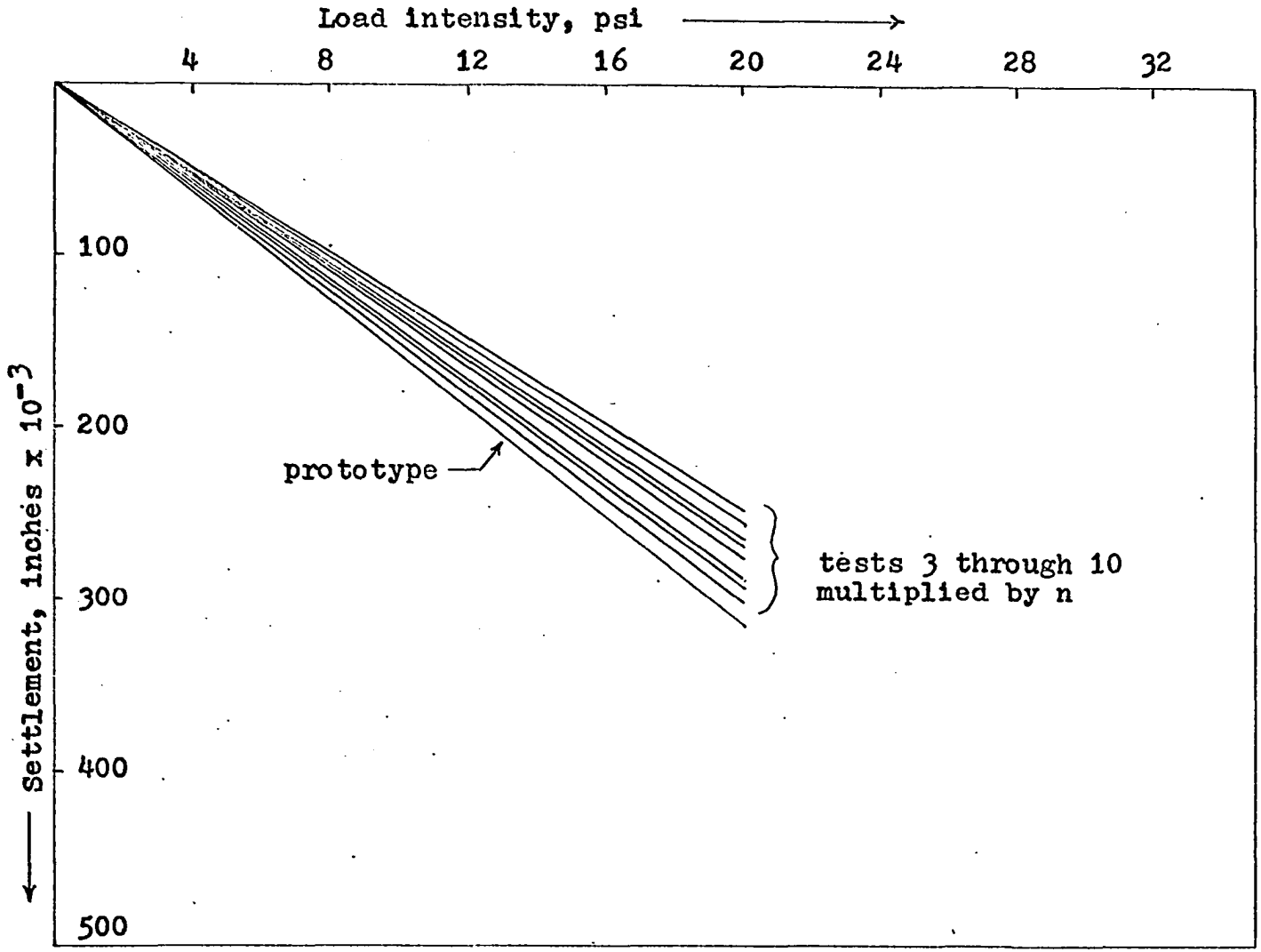

Figure 51. Sand settlement predictions

of model and prototype, and the horizontal direction of settlement in the model systems in contrast to a vertical settlement in the prototype system. The magnitude of error however, is not considered excessive for settlement prediction. More important, the error appears to be reproducable in this soil, so that corrections could be made for further settlement prediction which would result in a smaller error. The prediction factor, δ, which is equal to the prototype settlement divided by the model settlement (or mean model settlement) is 313/269 = 1.16. Corrected predictions could therefore be the calculated predictions multiplied by 1.16.

The data from the sand test series (tests 13-22) conducted with no membrane pressure, and therefore no gravitational pressure, present an opportunity to employ distorted model theory. From the distorted model analysis, $y = \delta n y_m$. Thus $\delta = y/ny_m$ Let the settlement from the small model plate be y_{m1}, and that from the larger model plate be y_{m2}. The settlement from the prototype will be y.

$\delta_1 = y/7.5\, y_{m1}$, or $0.313/(7.5)(.121) = 0.345$

$\delta_2 = y/(5)y_{m2}$, or $0.313/(5)(.141) = 0.444$

$\delta_3 = y_{m1}/(1.5)(.y_{m2})$, or $0.141/(1.5)(.121) = 0.777$

In the similitude analysis, design condition (h) was shown to be distorted. $R_m/\gamma_m b^3_m \neq R/\gamma b^3$. The inequality may be made an equality by the introduction of a distortion factor, α. Thus $R_m/\gamma_m b^3_m = \alpha R/\gamma b^3$ (design condition h'). γ_m is assumed to equal γ, and the loading restriction was that

$R_m/b^2_m = R/b^2$. Substituting these values into equation (h') results in $1/b_m = \alpha/b$, or $\alpha = b/b_m$. Therefore $\alpha = n$, the linear scale factor. A plot of the prediction factor, δ, versus the distortion factor, α, will show the effects of distortion on the prediction factor. Figure 52 shows a plot of δ versus log α. The three experimentally determined points fit closely to a straight line, therefore an equation may be written describing δ as a function of α. The following equation is derived from the δ versus log α curve: $\delta = -0.072 \log \alpha + 0.885$.

It is significant that δ appears to be a function of α. In multiple distortion situations, the prediction factor may also be a function of one or more pi terms in addition to the distortion factor (s) (39). Since the prediction factor for the sand tested is a function of the distortion factor, and the distortion factor is equal to n, prediction factors can be calculated from the linear scale ratios. It is pointed out that the range of scale ratios used in the experiment was from 1.5 to 7.5. Extrapolation of the linear relationship between δ and log α beyond these limits is not recommended.

Figure 53 shows settlement predictions for prototype settlement from the separate model tests performed with no membrane pressure, and the plate load (prototype) settlement. A large amount of error is seen to exist. Figure 54 shows settlement predictions from the same model tests, but corrected by injecting the prediction factors into the equations $y = \delta n y_m$. It is pointed out that these prediction curves were

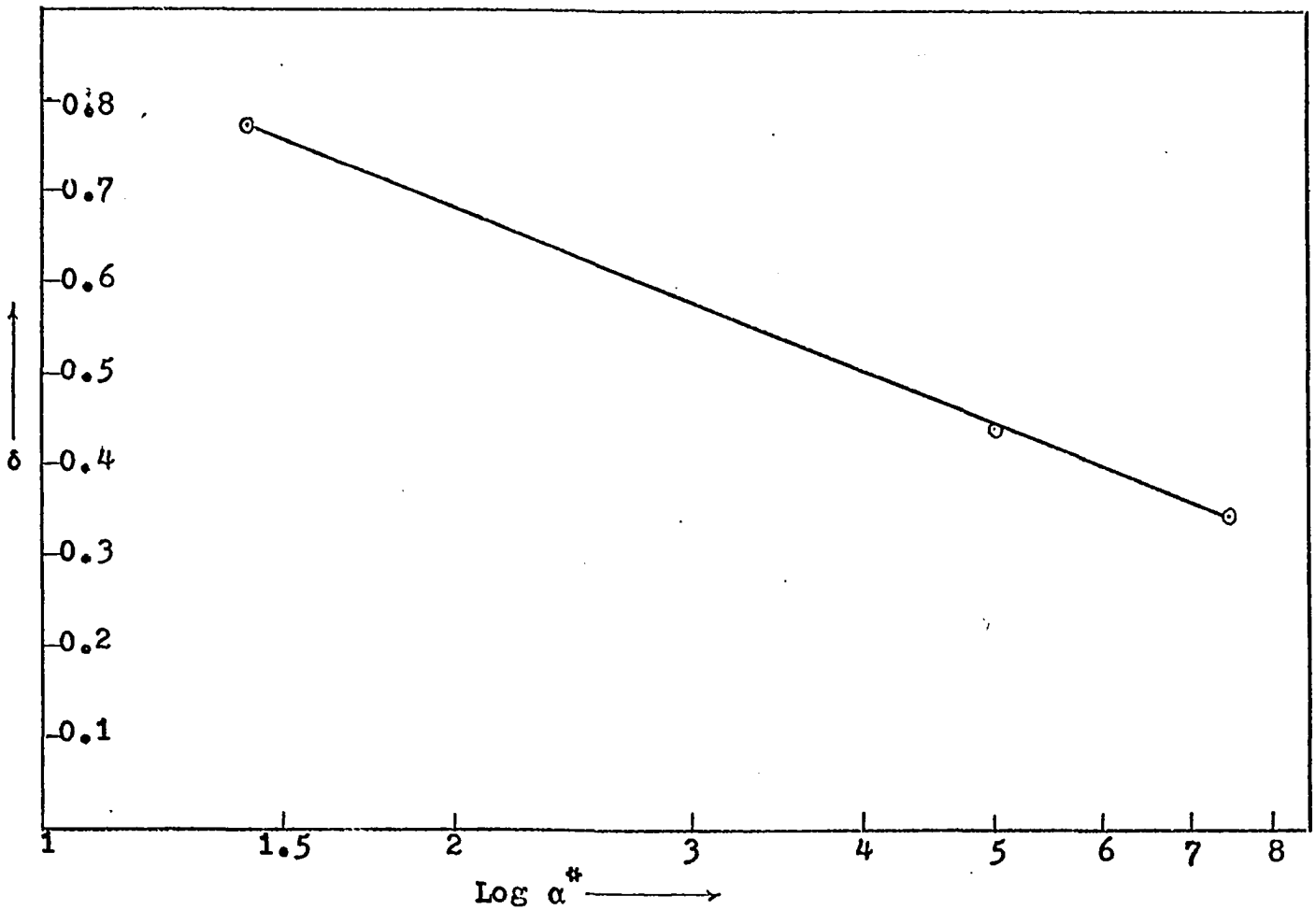

Figure 52. Effect of distortion on prediction factor - sand * α = n

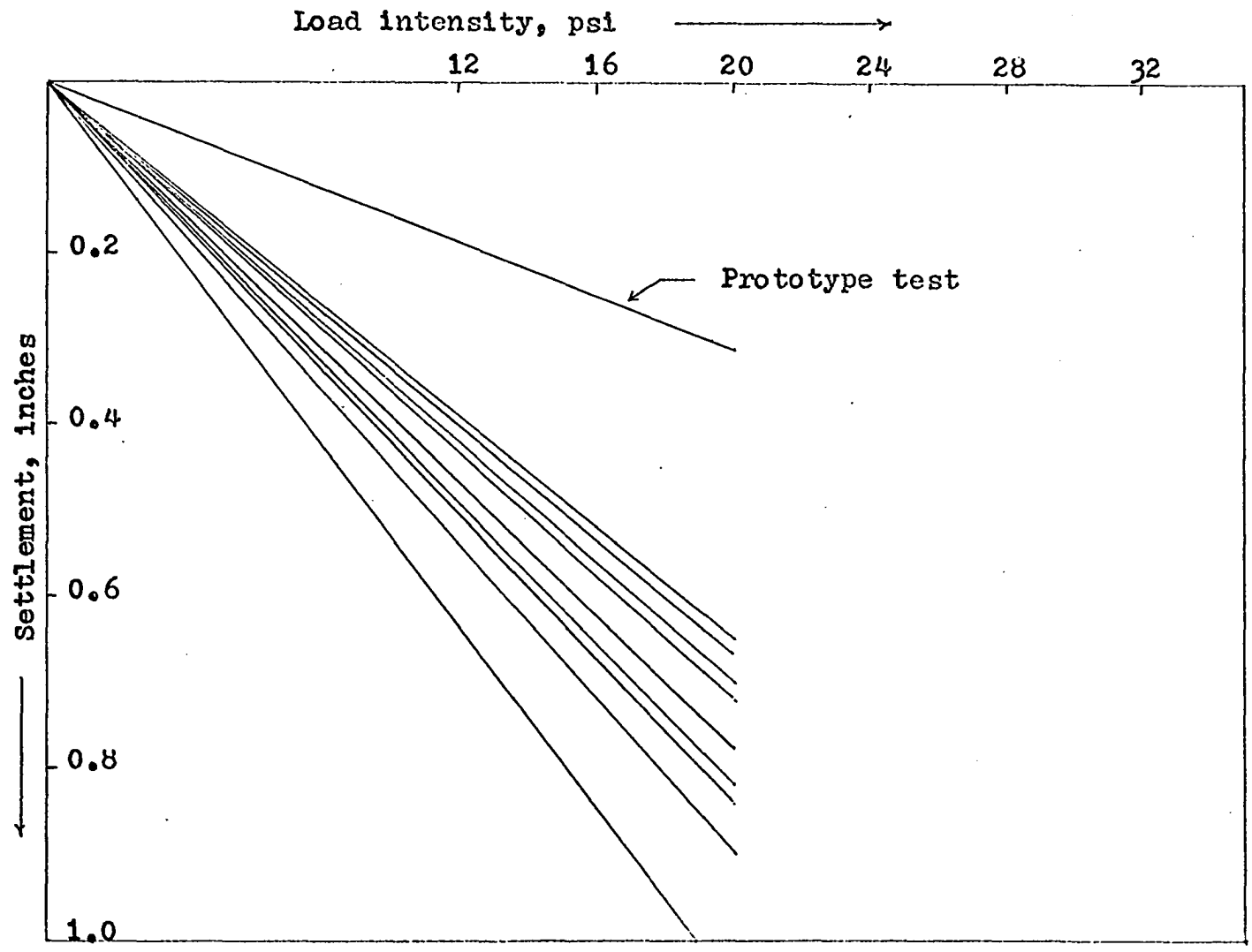

Figure 53. Sand settlement predictions with no membrane pressure

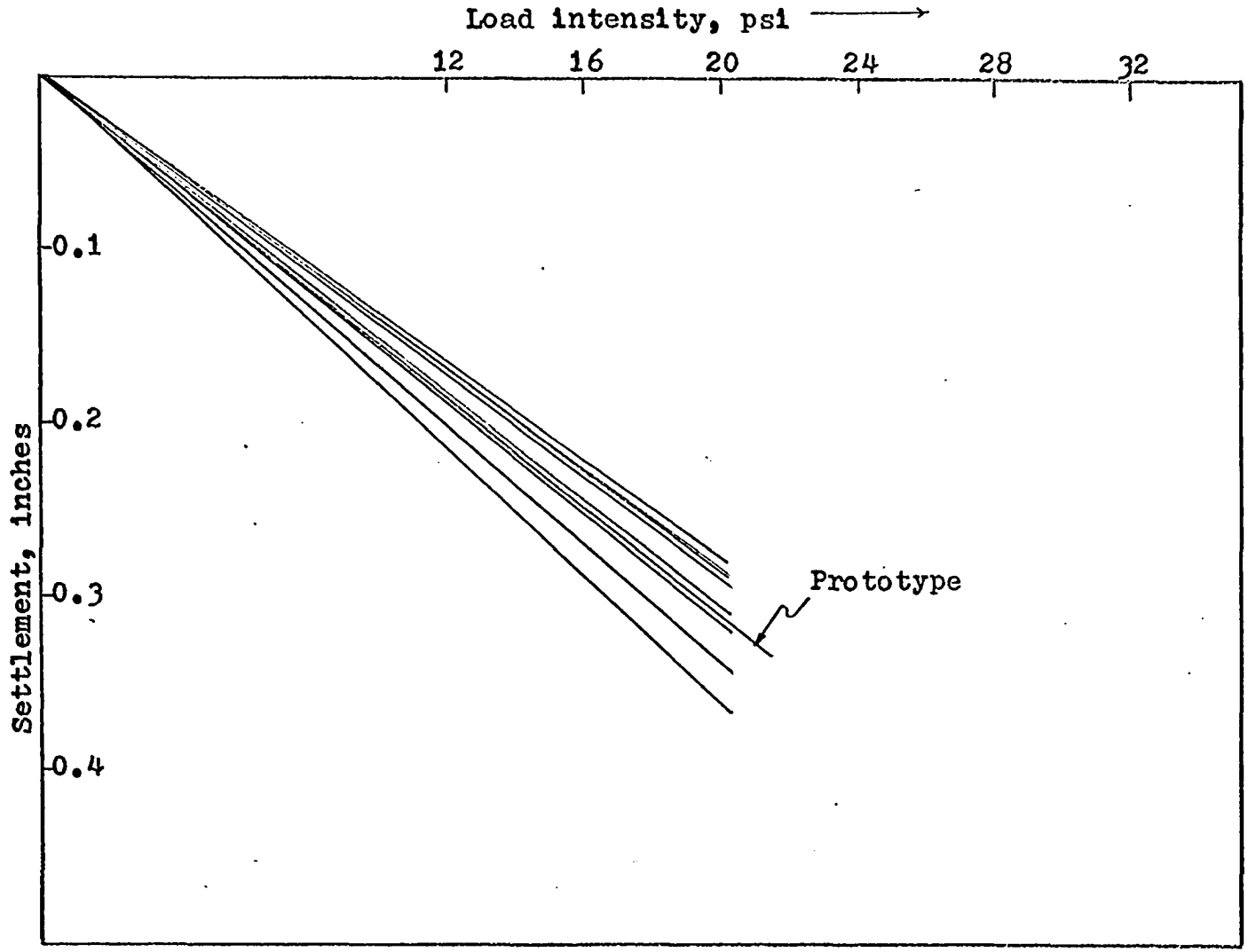

Figure 54. Sand settlement predictions, no membrane pressure, using prediction factors

determined from δ, which was obtained from three test values, small (2") model plate settlement, larger (3") model plate settlement and the plate load settlement. The prototype test was therefore used in adjusting the prediction curves for the prediction of the prototype test.

2. Loess

The field model tests in loess also gave a very good straignt line relationship. Tests 23 through 30 were conducted with membrane pressure calculated to account for the opening air pressure, plus one foot of surcharge pressure (since the prototype was to be placed at a depth of one foot) plus the gravitational pressures corresponding to n = 7.5 for the small plates and n = 5.0 for the larger model plates. Figures 35 through 43 show the results of these tests. Table 5 lists the settlement ratios for each set of tests performed in the same hole, the values of the settlements corresponding to the 20 psi load, the standard deviations and mean values. This table also lists the results of nine tests conducted with the model plates with no membrane pressure.

It is seen that for the 4 sets of tests with membrane pressure, only 2 result in settlement ratios in the vicinity of 1.5. However, an examination of the absolute settlements measured reveals that 2 large plate settlements should be rejected, whereas all 4 small model plate settlements are consistent. This information led to the discovery that the

Table 5. Loess model settlement data

Test	Settlement Ratio	3 Inch Plate Settlement	2 Inch Plate Settlement
23&24	1.06*	.0185 inch*	.0175 inch
25&26	1.52	.0285 inch	.0188 inch
27&28	2.10*	.0420 inch*	.0200 inch
29&30	1.60	.0298 inch	.0185 inch
Mean Value	1.56	.0291 inch	.01868 inch
Standard Deviation	.057	.0009 inch	.0010 inch
31&32	0.52	.0125 inch	.0240 inch
33&34	0.52	.0190 inch	.0370 inch
35&36	0.58	.0165 inch	.0285 inch
37&38	1.00	.0250 inch	.0250 inch
39&40	2.10*	.0210 inch	.0100 inch*
Mean Value	0.65	.0188 inch	.0286 inch
Standard Deviation	.232	.0047 inch	.0059 inch

*Rejected data.

larger model plate strain gage was not functioning properly. It also points out the advantage of having two sets of different sized model plates within the apparatus. Anomolous test results may be detected, and a rational criterion for rejection may be established. Therefore in computing standard deviations and mean values from these tests, the 2 erroneous large plate results have been ignored. The mean value of 1.56 for a settlement ratio is close to the theoretical value of 1.50. The standard deviations for both small and larger

model plate settlements is very small, being 0.00088 and 0.00103 inches respectively. Results of the nine tests performed with no membrane pressure gave a standard deviation of 5.90, considerably larger than those with membrane pressure. The same relationship had been observed with the sand test results.

Figure 55 shows the results of the prototype test and the predicted settlement from the 6 model tests with membrane pressure. The error from the mean prediction compared to the actual prototype settlement was 11.7%.

Figure 56 shows the results of the nine tests conducted without membrane pressure, and settlement predictions which would have been made if the distortion had been ignored. As with the results of the sand tests, it is seen that the settlement was greater for the tests with no membrane pressure, and that predictions ignoring the distortion involved with no membrane pressure are highly inaccurate.

Tests 35 through 38 were conducted with erroneously computed membrane pressures. Tests 35 and 36 represent one set from the same hole in which the unit weight of the loess was assumed to be 90 lb/ft^3. Tests 37 and 38 represent one set from the same hole in which the unit weight of the loess was assumed to be 128 lb/ft^3. Field density measurements determined the actual unit weight to be 97.5 lb/ft^3, and this latter value was used in computing the membrane pressure for tests 23 through 30. The results of these two erroneous test

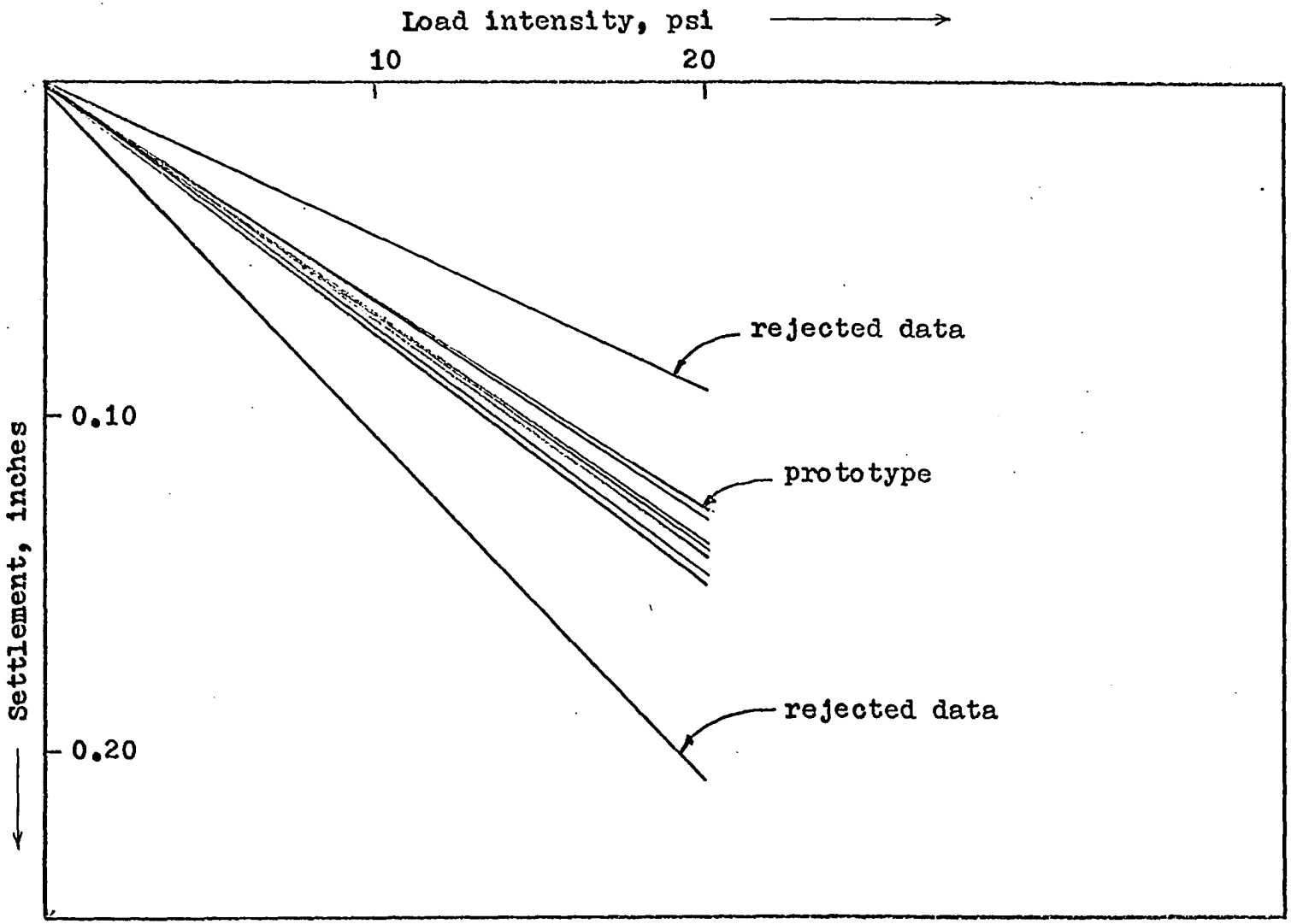

Figure 55. Loess settlement prediction

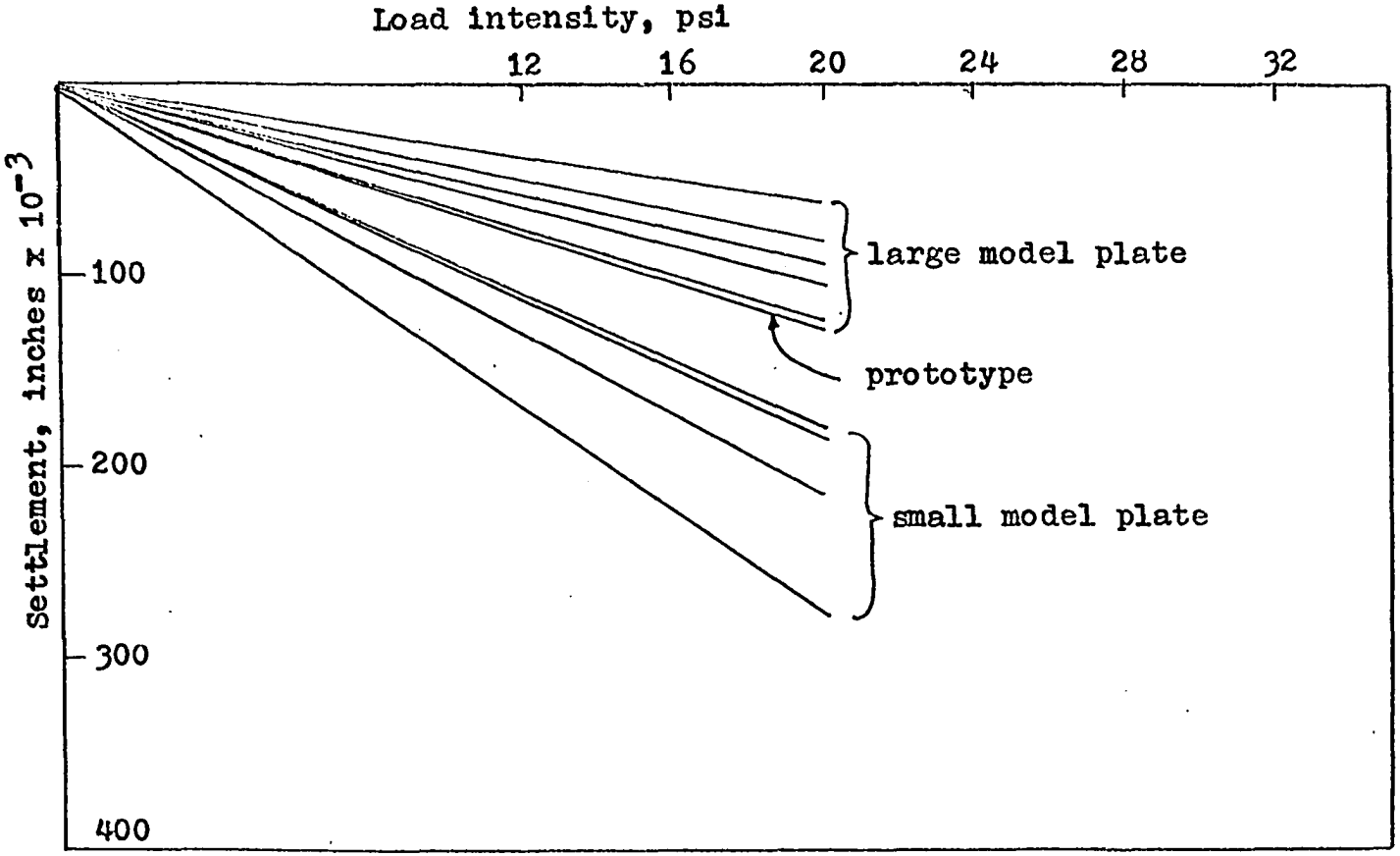

Figure 56. Loess settlement predictions with no membrane pressure

sets are shown in Figure 57 and Figure 58. Air pressures for the larger plate tests were the same in each set, 1.95 psi. Membrane pressures for the small plate tests were different, 2.08 psi for test 36 and 2.14 psi for test 38. This small difference in air pressure appears to have had a great effect in the settlement of the small plates, as shown in the figures. The settlement ratio for the first set (tests 35 and 36) is 1.35. That for the second set (tests 37 and 38) is 2.51. A plot of assumed density versus settlement ratio as shown in Figure 59 offers an interesting relationship. Since the theoretical settlement ratio is 1.50, a vertical line through 1.50 was drawn to intersect a straight line between the two ratio versus density points. The intersection of these two lines corresponds to a density of 95.0 lb/ft^3. Moreover, if the mean settlement ratio of 1.56 is used rather than the theoretical ratio of 1.50, the intersection is seen to correspond to a unit weight of 97 lb/ft^3, very close to the unit weight determined by field measurement.

This relationship between density and settlement ratio shows the apparent sensitivity of the model system to small differences in membrane pressure, and presents further evidence that the gravitational pressure concept for removing or greatly reducing the distortion involved in the settlement phenomenon is valid. It is emphasized that only one test set was performed at each of the erroneous densities, therefore the results are less substantial than would be the case

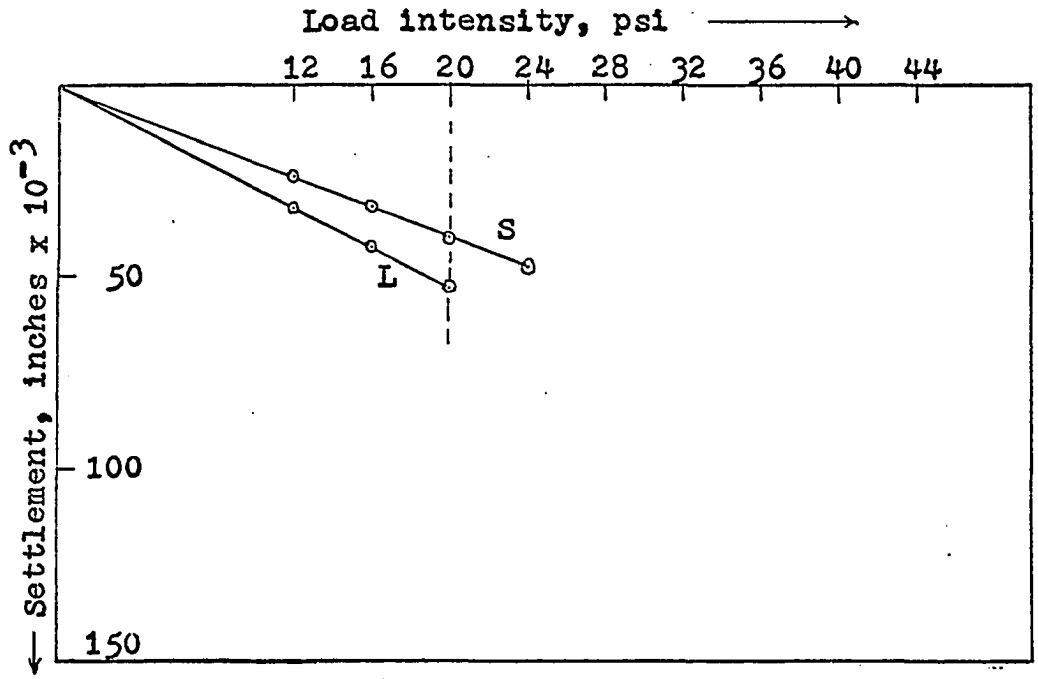

Figure 57. Field tests 41 and 42, in loess - assumed unit weight - 90 pcf

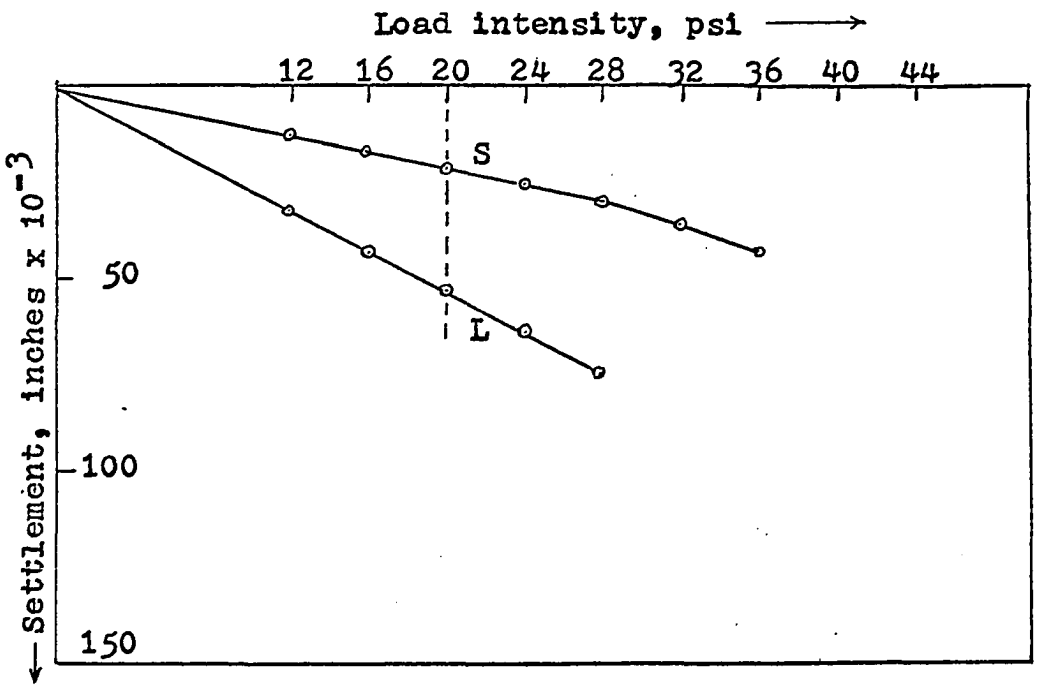

Figure 58. Field tests 43 and 44, in loess - assumed unit weight - 128 pcf

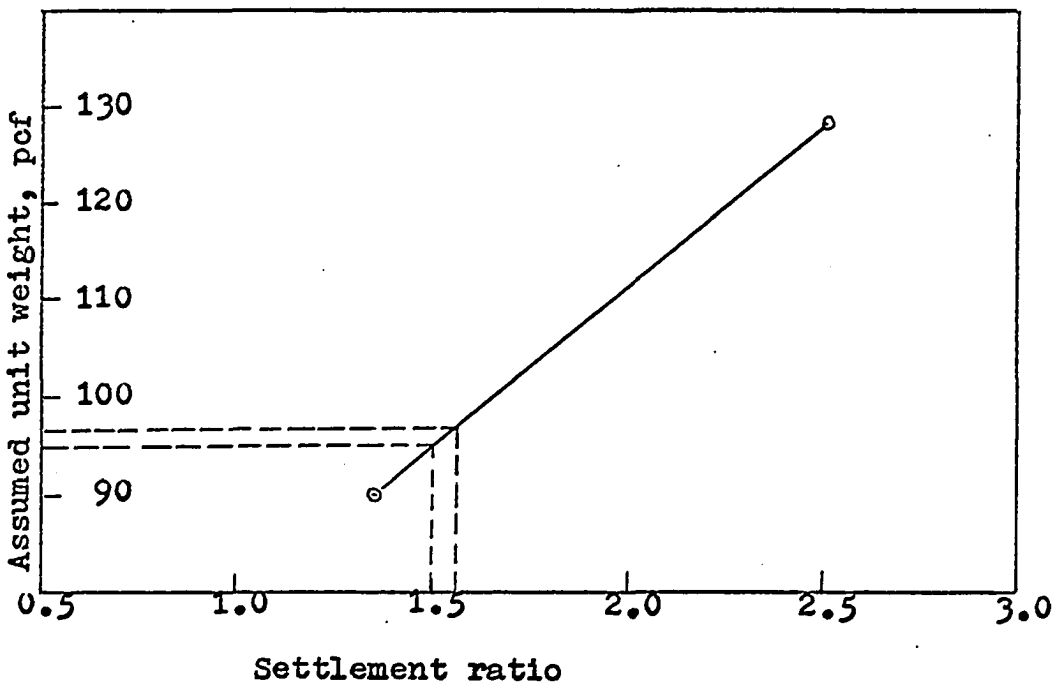

Figure 59. Unit weight prediction

if several test sets had been performed.

3. Clay

The field model tests in clay resulted in a straight line plot to at least 12 psi load intensity for all tests performed. The clay model tests were performed with the improved model settlement apparatus (model 2), whereas the other two soils had been tested with model 1. Membrane pressure for tests 41 through 48 included the sgp, the opening pressure, and one foot of surcharge pressure. Figures 45 through 48 show the results of these tests. Table 5 lists the settlement ratios for each set of tests performed in the same hole, the values of settlements corresponding to the 12 psi load intensity, the standard deviations and the mean values. This table also shows the results of two tests performed with no membrane pressure (tests 49 and 50).

All four sets of tests with membrane pressure resulted in settlement ratios in the vicinity of 1.50, with the value of 1.64 being the furthest from 1.50. Comparison of absolute settlements resulting from the same size model test (Table 6) show a scatter of up to 46.8%. This probably reflects a non-homogeniety in soil properties either in plan, in depth, or both. Each test set was performed in a different bore hole, the holes being six feet apart. The test depth varied up to a maximum of 6 inches.

The settlement ratios obtained from these four test sets

Table 6. Clay model settlement data

Test	Settlement Ratio	3 Inch Plate Settlement	2 Inch Plate Settlement
41&42	1.51	.0545 inch	.0360 inch
43&44	1.51	.0800 inch	.0530 inch
45&46	1.64	.0625 inch	.0380 inch
47&48	1.61	.0740 inch	.0460 inch
Mean Value	1.57	.0677 inch	.0432 inch
Standard Deviation	.068	.0114 inch	.0078 inch
49&50	1.22	.0540 inch	.0440 inch

varied only up to 8.6%. This fact, that absolute settlements varied up to 46.8% while settlement ratios only varied up to 8.6%, indicates the sensitivity of the model settlement apparatus and testing procedure. Each of the two sets within one set is conducted in essentially the same soil, therefore soil variability affects both 3 inch and 2 inch models equally, and does not greatly affect the settlement ratios from the two tests.

The two tests conducted with no membrane pressure resulted in a settlement ratio of 1.22. Less size effect apparently occurred with no membrane pressure as opposed to tests with membrane pressure. This appears reasonable since size effects for settlement of model footings in clay have generally been considered to be relatively unimportant (45). Therefore the ratio of settlements with no air pressure might be

expected to be closer to 1.0 than the ratio with air pressure.

The ratios of average velocities (velocities are in thousands of an inch per reading) for the 3 inch model divided by the 2 inch model for load intensities from 4 to 12 psi are: 4.55/3.70 = 1.23; 4.97/4.20 = 1.18; 5.30/3.45 = 1.53; 6.60/4.35 = 1.51; 4.55/4.45 = 1.02; 6.02/4.70 = 1.28.

The mean value of these ratios is 1.28 with a standard deviation of 0.198. Thus, if V = the velocity of penetration from the 3 inch model, and V_m = the velocity of penetration from the 2 inch model, then $V/V_m = 1.28$ from experimental results.

Design equation (j) from the similitude analysis was: $V^2_m/g_m d_m = V^2/gd$. If $g_m = ng$, and since $d/d_m = n$, $V_m = V$. If $g_m = g$ however, $V_m = V/\sqrt{n}$ or $V/V_m = \sqrt{n}$. For these tests $n = 1.5$, therefore $\sqrt{n} = 1.23$. Therefore, $V/V_m = 1.23$ theoretically, if $g_m = g$. The mean experimental result, that $V/V_m = 1.28$, is very close to the theoretical result, the difference being only $\frac{1.28 - 1.23 \times 100\%}{1.23} = 4.06\%$. It appears that the application of sgp does not affect the velocity of penetration if the Froude Number pi term V^2/gd is assumed to govern the velocity. The time-settlement data for the tests conducted with no membrane pressure, shown in Table 7, show too much scatter for a similar velocity ratio investigation.

Settlement predictions from model tests for the settlement of the prototype 15 inch by 20 inch flat plate were too high. The mean value of the 3 inch model plate tests corre-

Table 7. Time-settlement data from clay tests

Test	Load, psi	Settlement, 0.71 minutes after load application (inches x 10^{-3})	Settlement, 0.100 minutes after load application (inches x 10^{-3})
41 (3 inch plate)	4	4.4	5.25
	8	6.2	7.1
	12	4.4	5.25
42 (2 inch plate)	4	-	-
	8	2.2	3.2
	12	3.7	4.2
43 (3 inch plate)	4	4.7	4.7
	8	4.4	6.3
	12	4.7	6.8
44 (2 inch plate)	4	3.7	4.2
	8	4.7	5.5
	12	5.2	5.2
Mean Value (3 inch plate)	4	4.55	4.97
	8	5.30	5.90
	12	4.55	6.02
Mean Value (2 inch plate)	4	3.70	4.20
	8	3.45	4.35
	12	4.45	4.70
49 (3 inch plate)	4	2.6	3.3
	8	2.2	2.2
	12	2.2	2.8
50 (2 inch plate)	4	1.1	3.2
	8	0.5	1.1
	12	3.7	5.8

sponding to a load intensity of 12 psi was 0.0677 inches, therefore the prediction was 5 times 0.0677 = 0.338 inches. The mean value of the 2 inch model plate tests corresponding to a load intensity of 12 psi was 0.0432 inches, therefore the prediction from the smaller model tests was 7.5 times 0.0432 = 0.324 inches. The mean prediction was 0.331 inches.

The prototype test resulted in a settlement of 0.129 inches at a load intensity of 12 psi. Thus the magnitude of error was $\frac{.331 - .129}{.129} \times 100\% = 157\%$. The prototype settled less than predicted.

The fact that the prototype settled less than predicted in clay is reasonable. The basic consolidation expression, $T = \frac{c_v t}{H^2}$ is used in time-settlement predictions (53). t is the time of settlement, T is called the time factor and is constant for a particular degree of consolidation, H is the maximum distance within the compressible soil to a drainage face, and c_v is the coefficient of consolidation. Since the same soil is used for model and prototype, c_v will be the same for model and prototype systems. Thus $\frac{t_m}{H^2_m} = \frac{t}{H^2}$ for equal degrees of consolidation (equal T's). Therefore, $t_m = \frac{t}{\frac{H^2}{H_m}}$ and $t_m = t/n^2$ if similar systems exist, since $H/H_m = n$ for similar systems. The value of n with the 15 inch wide plate being the prototype and the 3 inch wide plate being the model is 5. Therefore $t_m = t/25$, and the prototype test should require a load duration 25 times longer to achieve an equal

degree of consolidation. Similarly, with the 2 inch wide plate, $t_m = t/56$, and the prototype test should require a load duration 56 times longer than the 2 inch model test.

The degree of consolidation which was reached in the prototype test was less than that reached in the model tests, since the model and prototype tests were conducted with the same time duration of load increments. The fact that the prototype test resulted in less settlement than was predicted from the model test is therefore seen to be due to the prototype test having achieved a lesser degree of consolidation than the model tests. The reason that this was not observed in the sand and loess tests was probably because the percent of settlement due to consolidation was much greater in the clay than in the sand and loess.

4. General

The experiments performed with membrane pressures approximating additional gravitational force resulted in prototype/model settlement ratios close to the theoretical value of 1.5. With no membrane pressure the settlement ratios were 1.19 for sand, 0.89 for loess and 1.22 for clay. Comparing the tests one sees that the larger plate settled more than the smaller plate in clay and sand, while the smaller plate settled more than the larger plate in loess. An examination of Terzaghi's size-relationship curves (Figure 1) shows a slope corresponding to the 2 model plate sizes which is negative for sand and

positive for clay, suggesting that different settlement phenomena occur in sand than in clay with small loaded areas. It has often been suggested that small plates in sand produce excessive shear strains, which supposedly explains the negative slope (57). However, it is proposed that the curves in Figure 1, although perhaps experimentally observable, are misleading. They imply that the comparison of settlement beneath different sized loaded areas should be 1.0. This is also implied in the interpretation of the curves, where, if the slope is negative, the explaination is that "excessive shear occurs in the small plate tests" (11, 57).

The standard of comparison for settlement-size relationships for similar soil-foundation systems should be n, the linear scale ratio. Thus in the model tests conducted in this study, n = 1.5, and 1.5 would be considered a true settlement ratio between the two models. Now the fact that without membrane pressure, ratios of 1.19, 0.89, and 1.22 were obtained has a new meaning. All 3 soils had ratios smaller than the "true" ratios. Therefore "excessive" settlement occurred in all 3 soils for the smaller plate (2") with respect to the larger model plate (3"). The reason for this consistently smaller ratio (although the ratio varies with the soil tested) can be seen in the analysis in section III D. The distorted model system (2" model) in which $\gamma_m = \gamma$, does not develop equal resisting stresses with those developed in the prototype system (in this case, the 3" model is the prototype).

Therefore it appears that excessive shear and excessive compression occurred for the model system in sand, loess, and clay, rather than just occurring in sand.

In section III F, it was suggested that the effect of distorted geometry on settlement could be investigated by an examination of the experimental data. The radii of curvature for all model plates were equal, being 3.25 inches. Since the 2 inch model plates were otherwise modeled to 1/1.5 times the linear dimensions of the 3 inch model plates, the relative radius of curvature of the 2 inch plates was 1.5 times that of the 3 inch plates. The prototype footing was designed with an "infinite" radius, since the plate was flat. Therefore the 2 inch model plates were closer to being geometrically similar to the prototype than were the 3 inch model plates.

The prediction errors from the test data are shown below:

2 inch model: sand prediction error - 14.3%
loess prediction error - 10.1%
clay prediction error - 151%

3 inch model: sand prediction error - 14.0%
loess prediction error - 13.3%
clay prediction error - 162%

The prediction errors do not show conclusively that the 2 inch model resulted in more accurate predictions, since only 2 of the 3 predictions were closer with the 2 inch model data. It does appear that, for the tests performed, the over-

all accuracy of the 2 inch model was slightly greater than that of the 3 inch model. This was reasonable since the 2 inch model was closer to being geometrically similar to the prototype. Furthermore, the relatively small differences in prediction accuracies from the two different sized models indicates that the effect of the distorted radii of curvature did not greatly affect the settlement.

B. Practical Applications

The use of the Model Settlement Apparatus data for settlement prediction will be examined for three possible cases:

Case I: One-soil system. The soil mass beneath the prototype foundation is one general soil type to a depth of at least twice the width of the foundation.

Case II: Two layered system, lower layer is more compressible than the upper layer.

Case III: Two layered system, lower layer is nearly rigid, upper layer is compressible.

In case I, Boussinesq or Westergaard equations may be used to determine theoretical vertical stress distribution and plotted as shown in Figure 60a. Model settlement tests are then conducted beneath the site of the proposed foundation. The model settlement data could be obtained from one hole, or average values could be taken from several holes spaced over the proposed foundation site.

Test procedure for all three cases:

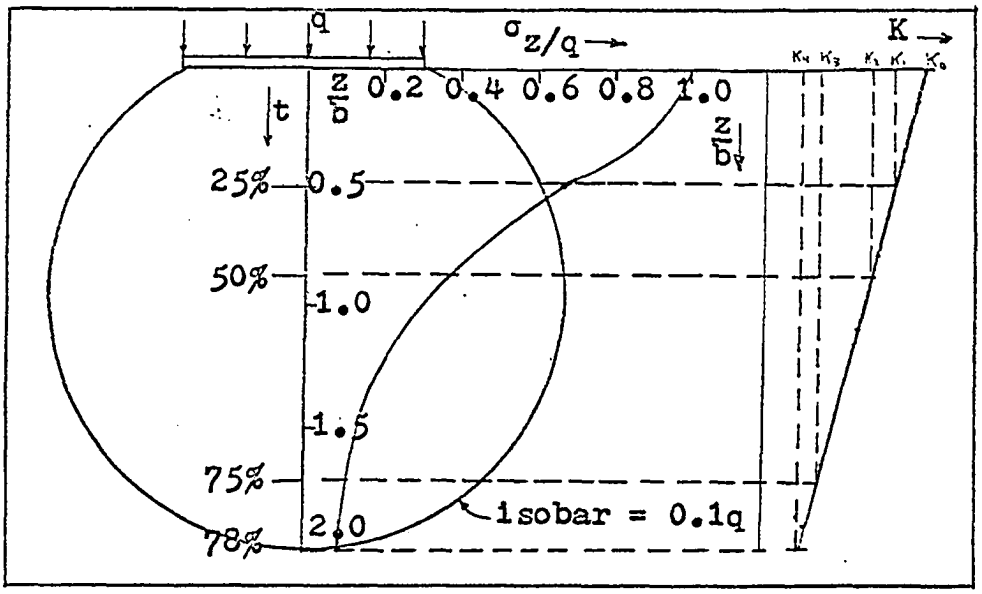

Figure 60a. One soil system, K decreases in depth

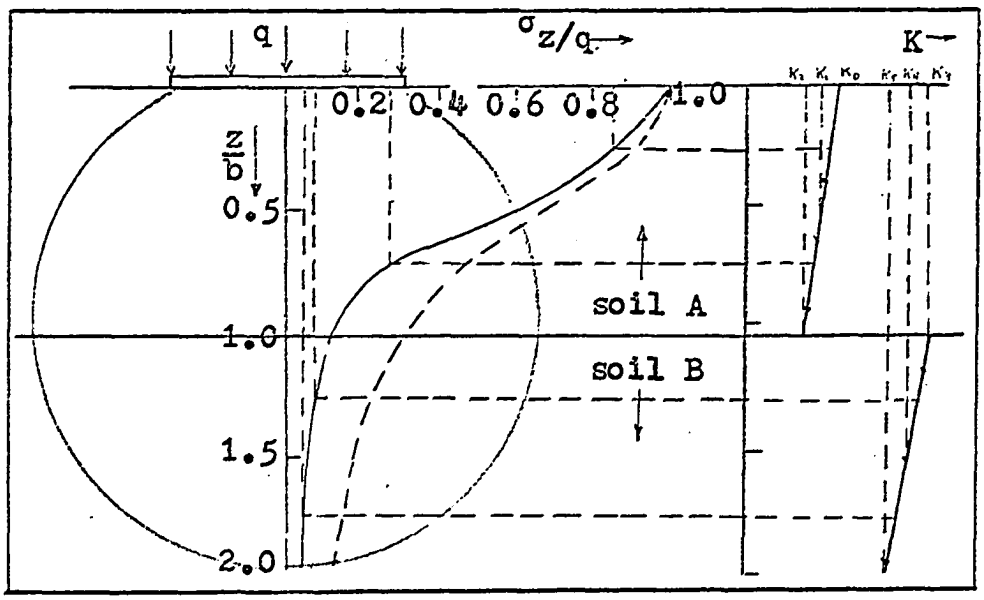

Figure 60b. Two layer system, lower layer more compressible

(1) The holes are drilled and boring logs are made showing depths to changes in soil type and other desired information.

(2) Each hole is reamed to produce a smooth cylindrical hole of the proper size for the Model Settlement Apparatus.

(3) Tests are conducted at chosen depths, starting from the test nearest the surface and testing downward. Arbitrary distances may be set between test depths as long as all soil layers are tested and no tests are performed at the interfaces between soil types.

(4) Maximum model load intensities for tests from the surface to a depth of 0.75 b (b = foundation width) should be 1.5q, where q = R/A. R is the prototype load in pounds, A is the prototype area in inches. Maximum model load intensities from depths of 0.75 b to 1.5 b should be 1.0q. Maximum load intensities below this depth should be 0.75 q.

(5) All test results should be recorded and K should be determined. K is the slope of the load-settlement curve and is equal to the change in load intensity divided by the corresponding change in settlement, and may be called a Compressibility Coefficient. Step (7) will explain a procedure if the load-settlement curve is non-linear.

(6) A stress distribution curve should next be constructed. If the system is a one-soil system, Boussinesq or Westergaard equations may be used. If the system is a layered system, which can be detected visually when drilling and from the K

values obtained in model testing, the various theories of Burmister (11) may be used to construct a modified stress distribution curve. Figures 60b and 60c show example K values that indicate a difference in soil type, and also modified stress distribution curves constructed after the K values have been determined. It is pointed out that K = 1/E, where Burmister calls E a "soil modulus" (11).

(7) If the slope of the load-settlement curve from the model test is not linear, an average value of K can be determined. Field test results in all soils have thus far shown linear curves until a stress intensity of at least 12 psi. The portion of the load-settlement curve considered for determining K will only be that portion between zero load intensity and σ_z at the corresponding depth. For example, a test conducted at a depth equivalent to 0.75 b in Figure 60b, corresponds to a vertical stress of 0.225 q. Therefore the portion of the model load-settlement curve of interest will be that up to 0.225 q.

(8) Plot K values versus depth as shown in Figures 60a, 60b, and 60c. Best-fit a straight line or a curved line through these test points as shown.

(9) Tabulate stress versus corresponding K values either at arbitrary depths such as are shown in the figures, or at depths corresponding to actual tests.

(10) Model settlements may now be determined. Divide K_i by σ_{zi} and the result is model settlement, y_{im}.

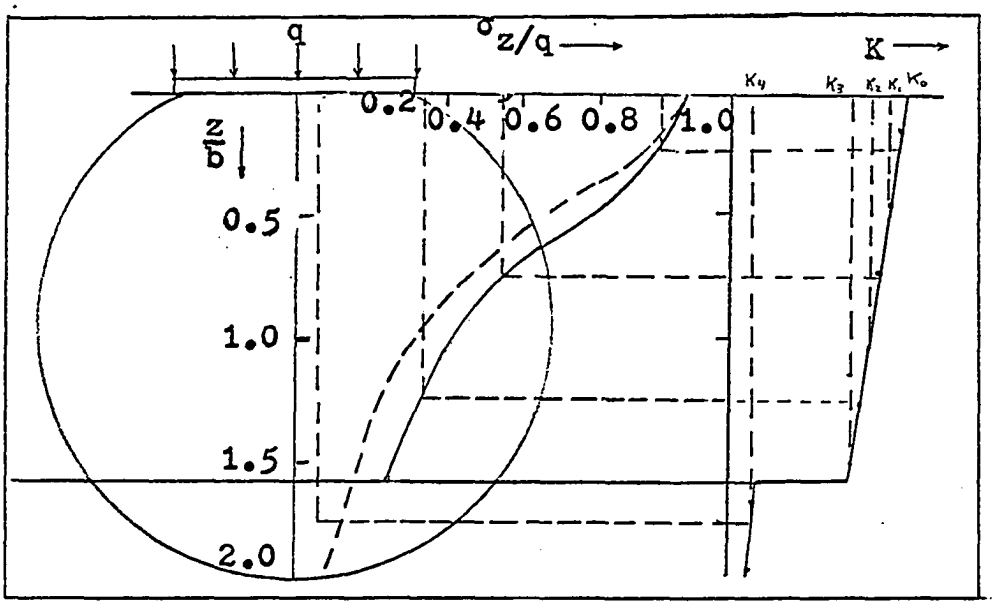

Figure 60c. Two layer system, lower layer nearly rigid

(11) Each model settlement must be multiplied by a corrected scale ratio, n', to determine its contribution to the prototype settlement. From static equilibrium, it is known that if a horizontal plate is passed at any depth below the loaded foundation, the soil at that depth must support the entire load, R. The area supporting this load at any depth can be calculated by dividing R by σ_{zi} at that depth. This area is assumed to be geometrically similar to the prototype foundation area, therefore the linear dimensions of this area are readily determinable. For example, if the prototype is a square foundation with dimensions of 200 inches by 200 inches, and R is 400,000 pounds, and if the vertical stress at some depth d, is 2 psi, then the area at this depth which supports the load is 400,000/2 = 200,000 square inches. The linear dimensions of this area are $\sqrt{200,000}$ = 448 inches by 448 inches. If the model plate dimensions were 4 inches by 4 inches, the original n would be 200/4 = 50. The modified n, n', is 448/4 = 112. It is this latter value on n which is used to determine the prototype settlement contribution within the tested zone. A test zone may be considered the depth midway between one test to midway between the next lower test.

Results of a hypothetical testing program are shown in Table 8. The results in the y column represent the predicted settlement contribution if the tested zone were 2b in depth. Since the tested zone will actually be less than this amount, a modification must be made. Every model test represents a

Table 8. Results of hypothetical testing program

Depth inches	K_i	σ_z, psi	$\sqrt{\sigma_z}$	S'_i inch x 10^{-3}	t_i	$S'_i t_i$ inch x 10^{-3}
60	100	8.0	2.83	448	0.15	67.2
120	90	6.0	2.45	349	0.15	52.3
180	80	5.0	2.23	283	0.15	42.5
240	70	4.5	2.12	235	0.15	35.3
300	60	4.0	2.00	190	0.15	28.5
350	50	3.6	1.90	150	0.15	22.5
400	40	3.3	1.82	115	0.15	17.2
						= 265.5

test within a homogeneous soil, since it has been specified that no test should be performed at a soil change interface. Therefore the information shown in Figure 60a can be used. The ratio z/b is determined, where z is the depth of the tested zone and b is the prototype width. This ratio is superimposed on the vertical axis in Figure 60a, and the percent settlement attributed to this depth is determined. For example, if z/b = 0.30, then from the figure, 15% of the settlement occurred within this depth. Therefore, one would multiply the results in column "S'_i" by 0.15. As long as z/b is equal or less than b/2, the percent of settlement contributed to the corresponding depth ratio (t) will be equal to approximately d/2b. When z/b is greater than b/2, t can be read directly from a graph such as that in Figure 60a. Thus for z/b = 0.50, t will be 0.50/2 = 0.25. The result of multiplying S'_i by t_i will be $S'_i t_i$. If the soil tested is clay, and the method of test is to test to

90% consolidation, this sum is multiplied by 1.1. The final prediction must be 4/3 times the corrected sum of settlement contributions, since it is assumed that 75% of the total settlement will occur within the pressure bulb shown in the figures (11).

A final equation may be derived to express the computation of the predicted settlement:

$$S'_i = K\sigma_{zi} n'_i$$

$$n'_i = \frac{\sqrt{R/\sigma_{zi}}}{b_m}$$

therefore, $S'_i = K\sigma_{zi}\frac{\sqrt{R/\sigma_{zi}}}{b_m} = \frac{K\sqrt{\sigma_{zi}R}}{b_m}$

and $S_{total} = \frac{4}{3}\frac{R}{b_m}\sum_{n=1}^{i} K_i\sqrt{\sigma_{zi}}\ t_i$. This equation would have to be multiplied by 1.1 if clay had been tested at 90% consolidation.

S_t also = 4/3 S'_i t_i.

From the results in Table 6, S_t = 4/3 times 2.65 inches, or 3.54 inches. This would be the predicted settlement, unless the consolidation correction were made, in which case the predicted settlement would be (1.1) 3.54 = 3.90 inches.

VII. SUMMARY AND CONCLUSIONS

A similitude analysis was performed in which distortions involved in model-prototype foundation settlement phenomena were isolated and analyzed. A means for removing or reducing the distortion caused by the soil weight not being modeled was proposed and analytically and experimentally investigated.

An instrument, the Model Settlement Apparatus, based on similitude principles and used within a bored hole to test soil at the sides of the hole, was designed, constructed, and tested. Simulated gravitational pressure (sgp) to reduce the distortion was applied separately from the application of model foundation loads. Based on results of actual usage and initial testing, a second instrument was designed, constructed and tested.

The following conclusions are based on experimental results:

1. The amount of distortion involved in the settlement phenomena due to size effects was significantly reduced in the sand, loess (silt), and clay tested when the sgp was applied. This substantiates the results of the similitude analysis and indicates that the distortion involved in the settlement phenomena may be significantly reduced by the method used.

2. The prototype footing settlement in sand and loess was in close agreement with predicted settlement values. The prediction of prototype footing settlement in clay was ex-

cessive. This excessive prediction for settlement in clay can be attributed to differences in degrees of consolidation occurring in the model and prototype systems.

3. Velocity measurements in clay were in close agreement with the design equation involving the Froude Number pi terms. Sgp did not significantly affect velocity of penetration (settlement) within the magnitudes of sgp employed.

VIII. SUGGESTIONS FOR FURTHER RESEARCH

The following areas for further research are recommended:

1. A testing program be initiated in which tests are performed at greater depths and with higher membrane pressures (greater n values). Tests should also be performed with longer time durations of load application.

2. Borings be made adjacent to actual documented foundations to determine agreement between predicted settlement and actual observed settlement.

3. Improved accessory equipment be assembled so that a constant load application may be regulated by means of a pressure regulator rather than by manipulation of a hand pump. This would improve the accuracy of settlement velocity measurements.

4. A testing program be initiated in which vertical and non-vertical holes be bored and tested in order to evaluate the effect of orientation of direction of load application on settlement magnitudes and settlement velocities in different soils.

IX. LITERATURE CITED

1. Aboshi, H. and Monden, H. Determination of the horizontal coefficient of consolidation of an alluvial clay. Australia-New Zealand Conference on Soil Mechanics and Foundation Engineering Proceedings 4: 159-164. 1964.

2. Akiyama, F. N. Shear strength properties of Western Iowa loess. Unpublished M.S. thesis. Ames, Iowa, Library, Iowa State University of Science and Technology. 1963.

3. American Society for Testing Materials. Procedures for testing soils. 4th edition. Philadelphia, Pa., author. 1964.

4. Bekker, M. G. Photographic method of determining the soil action beneath footings. Second International Conference on Soil Mechanics and Foundation Engineering Proceedings 3: 193-194. 1948.

5. Berezantzeu, V. G. and Yaroshenko, V. A. The bearing capacity of sands under deep foundations. Fourth International Conference on Soil Mechanics and Foundation Engineering Proceedings 1: 293. 1957.

6. Bergfelt, A. Loading tests on clay. Geotechnique 1: 15-31. 1956.

7. Bond, D. The use of model tests for the prediction of the settlement under foundations in dry sand. Unpublished Ph.D. thesis. London, England, Library, University of London. 1956.

8. Bridgman, P. W. Dimensional analysis. New Haven, Connecticut, Yale University Press. 1963.

9. Buckingham, E. On physically similar systems: illustrations of the use of dimensional equations. Physics Review 4: 345. 1914.

10. Bucky, P. B. and Fentress, A. L. Application of principles of simillitude to design of mine workings. American Institute of Mining and Metalurgical Engineers Technical Publication 529: 3-20. 1934.

11. Burmister, D. M. Prototype load-bearing tests for foundations of structures and pavements. American Society for Testing Materials Special Technical Publication 322: 98-119. 1963.

12. Davis, H. E. and Woodward, R. J. Some laboratory studies of factors pertaining to bearing capacity of soils. Highway Research Board Proceedings 29: 467-476. 1949.

13. Deaker, J. A. The mechanism of failure of sand foundations. Australia-New Zealand Conference on Soil Mechanics and Foundation Engineering 3: 87-92. 1960.

14. DeBeer, E. E. The scale effect on the phenomenon of progressive rupture in cohesionless soils. Sixth International Conference on Soil Mechanics and Foundation Engineering Proceedings 2: 13-17. 1965.

15. Feda, J. Research on the bearing capacity of loose soil. Fifth International Conference on Soil Mechanics and Foundation Engineering Proceedings 1: 635-642. 1961.

16. Ford, H. Advanced mechanics of materials. New York, New York, John Wiley and Sons, Inc. 1963.

17. Fox, N. S. Soil shear test device for use in bore holes. Unpublished M.S. thesis. Ames, Iowa, Library, Iowa State University of Science and Technology. 1966.

18. Fox, N. S., Lohnes, R. A., and Handy, R. L. Depth studies in Southwestern Iowa. IV. Shear strength. Iowa State University of Science and Technology Engineering Experiment Station Technical Report 2. 1966.

19. Gaynor, F. Concise dictionary of science: physics, mathematics, nucleonics, astronomy, chemistry. New York, New York, D. Van Nostrand, Inc. 1959.

20. Gilboy, G. Soil mechanics research. American Society of Civil Engineers Transactions 98: 218-240. 1933.

21. Golder, H. Q. The ultimate bearing pressure of rectangular footings. Institutional Civil Engineering Journal 17: 161-174. 1941.

22. Goodman, L. J., Hegedus, E. and Liston, R. A. Scaling considerations in plate sinkage tests. Unpublished mimeographed paper presented at Highway Research Board annual meeting, January 1966. Ames, Iowa, Department of Civil Engineering, Iowa State University of Science and Technology. 1966.

23. Hansen, J. B. General report. Fourth International Conference on Soil Mechanics and Foundation Engineering Proceedings 3: 138-139. 1957.

24. Holtz, W. G. and Gibbs, H. J. Consolidation testing and related properties of loessial soils. American Society of Testing Materials Symposium on Consolidation Testing of Soils 1: 9-26. 1951.

25. Horton, R. E. Erosional development of streams and their drainage basins. Geological Society of America Bulletin 56: 275-370. 1945.

26. Housel, W. S. A practical method for selection of foundations based on fundamental researchs in soil mechanics. Michigan University Engineering Bulletin 13. 1929.

27. Huntley, H. E. Dimensional analysis. London, England, Macdonald and Co., Ltd. 1958.

28. Jakobson, B. Isotropy in clays. Geotechnique 5: 23-28. 1955.

29. Jasiewicz, J. Applications of dimensional analysis methods to civil engineering problems. Civil Engineering and Public Works Review 4: 1125-1129. 1963.

30. Jumikis, A. R. Soil mechanics. Princeton, New Jersey, D. Van Nostrand Co., Inc. 1962.

31. Kogler, F. Discussion of "Soil mechanics research" by G. Gilboy. American Society of Civil Engineers Transactions 98: 299-301. 1951.

32. Kondner, R. L. and Krizek, R. J. Correlation of load bearing tests on soils. Highway Research Board Proceedings 41: 557-590. 1962.

33. Langhaar, H. L. Dimensional analysis and theory of models. New York, New York, John Wiley and Sons, Inc. 1951.

34. Lee, I. K. Elastic settlements of footings with a rough interface. Australia-New Zealand Conference on Soil Mechanics and Foundation Engineering Proceedings 4: 225-232. 1964.

35. Meldrum, H. R., Mogan, C. A., and Perfect, D. E. Soil survey, Story County, Iowa. U.S. Dept. of Garic. Soil Survey Series 9: 1-59. 1936.

36. Meyerhof, G. G. Influence of roughness of base and ground water conditions on the ultimate bearing capacity of foundations. Geotechnique 5: 227-242. 1955.

37. Meyerhof, G. G. An investigation of the bearing capacity of shallow footings on dry sand. Second International Conference on Soil Mechanics and Foundation Engineering Proceedings 1: 237-243. 1948.

38. Meyerhof, G. G. The ultimate bearing capacity of foundations. Geotechnique 2: 301-331. 1951.

39. Murphy, G. Similitude in engineering. New York, New York, The Ronald Press Co. 1950.

40. Olson, G. R. Direct shear and consolidation tests of undisturbed loess. Unpublished M.S. thesis. Ames, Iowa, Library, Iowa State University of Science and Technology. 1958.

41. Osterberg, J. O. Summary and evaluation of field data on soil bearing tests and laboratory soil tests. American Society of Civil Engineers Technical Progress Report 4. 1947.

42. Osterberg, J. O. Symposium on load tests of bearing capacity of soils. American Society of Testing Materials Special Technical Publication 79: 1-5. 1948.

43. Peynircioglu, H. Tests on bearing capacity of shallow foundations on horizontal top surfaces of sand fills and the behavior of soils under such foundations. Second International Conference on Soil Mechanics and Foundation Engineering Proceedings 3: 194-205. 1948.

44. Rayleigh, L. The principle of similitude. Nature 1: 95. 1915.

45. Roberts, J. E. Small-scale footing studies: a review of the literature. Massachusetts Institute of Technology Publication 108. 1961.

46. Rocha, M. and Folque, J. Some results of settlement observations in actual structures and in models. Laboratorio Nacional Engenhiria Civil (Lisbon, Portugal) Publication 36. 1953.

47. Schmertmann, J. H. Stability of cuts in soft clays: discussion. American Society of Civil Engineers Proceedings 90: 1. 1964.

48. Selig, E. T. and McKee, E. E. Static and dynamic behavior of small footings. American Society of Civil Engineers Proceedings 87: 29-47. 1961.

49. Skempton, A. W. An investigation of the bearing capacity of a soft clay soil. Institution of Civil Engineers Journal 7: 307-321. 1942.

50. Sowers, G. F. Discussion. Fourth International Conference on Soil Mechanics and Foundation Engineering Proceedings 3: 152-153. 1957.

51. Spangler, M. G. Soil engineering. 2nd edition. Scranton, Pa., International Textbook Co. 1960.

52. Stowe, W. W., Handy, R. L., and Fero, J. P. Model evaluation of soil factors affecting rigid pavement pumping. Iowa State University of Science and Technology Soil Research Laboratory Publication 64-9. 1964.

53. Taylor, D. W. Fundamentals of soil mechanics. New York, New York, John Wiley and Sons, Inc. 1948.

54. Tcheng, Y. Foundations superficielles en mileau scratifie. Fourth International Conference on Soil Mechanics and Foundation Engineering Proceedings 1: 449-452. 1957.

55. Terzaghi, K. Relation between soil mechanics and foundation engineering. Presidential address. First International Conference on Soil Mechanics and Foundation Engineering Proceedings 3: 17. 1936.

56. Terzaghi, K. Theoretical soil mechanics. New York, New York, John Wiley and Sons, Inc. 1943.

57. Terzaghi, K. and Peck, R. B. Soil mechanics in engineering practice. New York, New York, John Wiley and Sons, Inc. 1948.

58. Timoshenko, S. and Goodier, J. N. Theory of elasticity. New York, New York, McGraw-Hill Book Co., Inc. 1951.

59. Vesic, A. S., Banks, D. C., and Woodard, J. M. An experimental study of dynamic bearing capacity of footings on sand. Sixth International Conference on Soil Mechanics and Foundation Engineering Proceedings 2: 209-213. 1965.

60. Yoder, E. J. Principles of pavement design. New York, New York, John Wiley and Sons, Inc. 1964.

X. ACKNOWLEDGEMENTS

The author expresses his sincere appreciation to Dr. R. L. Handy, Professor of Civil Engineering in charge of soil engineering, for his timely suggestions and guidance during all phases of the investigation.

Appreciation is also extended to Dr. Turgut Demirel, Mr. Glen Ferguson, and Mr. Charles Easton, for their technical advice and suggestions.

The valuable assistance given by Mr. Keith Anderson during the field testing phase of the investigation is gratefully acknowledged.

The work performed by the Engineering Shop in constructing the first apparatus and the Instrument Shop in constructing a portion of the second apparatus is sincerely appreciated.